NTATION PAGE

Form Approved
OMB No. 0704-0188

1. AGENCY USE ONLY (Leave blank)	2. REPORT DATE	3. REPORT TYPE AND DATES COVERED
	10 May 93	Final Report--1 July - 30 Nov 92

4. TITLE AND SUBTITLE
Pulse Response Based Control for Minimum Time Maneuver of Flexible Spacecraft

5. FUNDING NUMBERS
Grant Number
AFOSR-90-0297

6. AUTHOR(S)
Jeffrey K. Bennighof

7. PERFORMING ORGANIZATION NAME(S) AND ADDRESS(ES)
The University of Texas at Austin
Center for Aeromechanics Research
Austin, TX 78712-1085

8. PERFORMING ORGANIZATION REPORT NUMBER
AEOSR-TR 93 0239

9. SPONSORING/MONITORING AGENCY NAME(S) AND ADDRESS(ES)
Air Force Office of Scientific Research
Building 410
Bolling AFB, DC 20332

10. SPONSORING/MONITORING AGENCY REPORT NUMBER

11. SUPPLEMENTARY NOTES

12a. DISTRIBUTION/AVAILABILITY STATEMENT
Approved for public release,
distribution unlimited

13. ABSTRACT (Maximum 200 words)

The pulse response based control method for minimum time maneuver of flexible spacecraft is described. This method makes it possible to obtain minimum time control profiles for linear systems solely on the basis of measured response to pulses in control inputs and gross inertial properties of the system, such as total mass or total mass moment of inertia. The accuracy with which the final state of the system can be specified is shown to be related to the observability of the system with the given outputs. A special algorithm is developed for solving the numerical optimization problem arising in this approach. For maneuver problems, nonlinear behavior is handled by explicitly modeling the deviation from linear behavior in those few modes in which it is significant. A feedback control scheme to complement pulse response based control, which is stable in the presence of nonlinear rotational stiffening effects and input bounds, is presented. Also, a near minimum time method which requires virtually no real time computation is described. Numerical examples illustrate the method and its features and extensions.

14. SUBJECT TERMS	15. NUMBER OF PAGES
Minimum time control, maneuver of flexible spacecraft, slewing of flexible spacecraft, control-structure interaction	98
	16. PRICE CODE

17. SECURITY CLASSIFICATION OF REPORT	18. SECURITY CLASSIFICATION OF THIS PAGE	19. SECURITY CLASSIFICATION OF ABSTRACT	20. LIMITATION OF ABSTRACT
UNCLASSIFIED	UNCLASSIFIED	UNCLASSIFIED	UL

Pulse Response Based Control for Minimum Time Maneuver of Flexible Spacecraft

Jeffrey K. Bennighof
Principal Investigator

Department of Aerospace Engineering and Engineering Mechanics
The University of Texas at Austin
Austin, Texas

Supported by the Air Force
Office of Scientific Research
Grant Number AFOSR-90-0297

May 10, 1993

Abstract

The pulse response based control method for minimum time maneuver of flexible spacecraft is described. This method makes it possible to obtain minimum time control profiles for linear systems solely on the basis of measured response to pulses in control inputs and gross inertial properties of the system, such as total mass or total mass moment of inertia. The accuracy with which the final state of the system can be specified is shown to be related to the observability of the system with the given outputs. A special algorithm is developed for solving the numerical optimization problem arising in this approach. For maneuver problems, nonlinear behavior is handled by explicitly modeling the deviation from linear behavior in those few modes in which it is significant. A feedback control scheme to complement pulse response based control, which is stable in the presence of nonlinear rotational stiffening effects and input bounds, is presented. Also, a near minimum time method which requires virtually no real time computation is described. Numerical examples illustrate the method and its features and extensions.

This report also presents an exact solution of a minimum time control problem for a distributed parameter system, obtained using a traveling wave formulation.

Contents

List of Figures

Chapter 1

Introduction

In the minimum time maneuver of flexible spacecraft, bounded control inputs are used to accomplish a given change in rigid body modal states as quickly as possible, with minimal residual energy in flexible modes at the end of the maneuver. Since 1980 or so, a number of different approaches have been taken to address these problems.

Turner and Junkins[1] represent flexible motion in terms of several assumed modes, and minimize a quadratic performance index with a single-actuator control, with specified final states and final time. A continuation method is used to obtain a solution of the nonlinear two-point boundary value problem that results when kinematic nonlinearity is present in the formulation. Turner and Chun extend this approach for the case in which a number of actuators are distributed throughout the structure.[2] Meirovitch and Quinn[3] develop a perturbation approach in which the nonlinear rigid body maneuver is taken as a zero order problem and the small motions, including flexible motions and small rigid body motions, are treated as a first order perturbation, for nonlinear maneuvers of flexible spacecraft. The rigid body maneuver problem is solved using an inverse dynamics approach where the required zero order feedforward control torques are obtained from the nonlinear rigid body equations of motion. The first order, linear vibration problem with time varying coefficients is solved independently using feedback control. Chun, Turner and Juang obtain a frequency-shaped open-loop control for the rigid body modes, using a continuation method to handle nonlinearity, and then design a feedback control for the flexible motion by linearizing the flexible response about several points in the open-loop rigid-body trajectory.[4] In a later paper, they replace the solution of the open-loop problem for the rigid body modes with a programmed-motion/inverse dynamics approach, where the trajectories of the rigid body modes are simply specified as smooth functions

and the required control torques are obtained from the nonlinear rigid body equations of motion.[5] Meirovitch and Sharony[6] use the perturbation approach and use a minimum time (bang-bang) control to handle the rigid body problem, and a linear quadratic regulator with integral feedback and prescribed convergence rate to drive the flexible motion to zero at the end of the maneuver. Bounds on control inputs are only considered in the design of the rigid body portion of the control, so, as in all of the work mentioned thus far, a true minimum time control problem for the flexible maneuver is not solved. True minimum time control is investigated by Ben-Asher, Burns and Cliff,[7] in which the flexible behavior is modeled in terms of a small number of assumed modes, and switching times for the bang-bang control of this model are found for both linear and nonlinear problems using a parameter optimization approach. More recently, Junkins, Rahman and Bang have pursued an approach in which near minimum time maneuver is achieved by smoothing the bang-bang control profile for minimum time maneuver of a rigid spacecraft having the same inertial properties, and then designing a stable feedback control to suppress any vibration that is excited by the smoothed profile.[8]

The difficulty of these problems is due largely to several issues which are all related to modeling the flexible behavior of the spacecraft. First, there is the difficulty of obtaining an accurate model, i.e., system identification and realization. All but the last of the methods referred to above require an accurate modal or state space model of the spacecraft, which is usually difficult to obtain for structures with high modal density. Verification of the model is difficult because of the need to compensate for gravitational and atmospheric effects if testing is done on the earth's surface, or because of the limited amount of test hardware available if testing is done in orbit. If properties are time-varying, the model must be updated after any significant change in properties. Second, since the systems to be controlled are distributed parameter systems, they typically require high order models for representing all significant behavior. This greatly increases computational requirements associated with control, particularly if a nonlinear two point boundary problem must be solved. Third, a finite order model is guaranteed to have a bang-bang minimum time control, for which only the switching times must be determined, whereas the minimum time control for the distributed parameter system being modeled is not ordinarily bang-bang,[9] which means that a control profile in which control inputs are not always equal to their bounds should be found. This means that the optimal control profile for the spacecraft is qualitatively quite different from the bang-bang

minimum time control of its finite order model.

These considerations point to the need for a minimum time maneuver method which does not rely on an explicit modal or state space model of the spacecraft. The approach of Junkins *et al.*[8] does not use any model of flexible behavior, but instead modifies a bang-bang minimum time control profile for a rigid spacecraft, by smoothing it to reduce excitation of vibration, and by adding to it a Lyapunov-stable feedback component for vibration suppression. The resulting control profiles approximate minimum time control for a flexible spacecraft, at least in some sense. However, the fact that this approach accomodates flexible behavior in such a generic manner raises the question of whether flexible response can be handled more effectively by taking flexible behavior into account earlier in the process of obtaining control profiles, yet without introducing the difficulties often associated with obtaining an accurate model. Another important question is whether real time computational requirements can be low enough with such an approach that implementation in a minimum time context is feasible.

The approach that is taken in this work is to obtain control profiles for minimum time maneuver as directly as possible from measured input-output relationships. More specifically, square pulses are applied in control inputs and the sensor outputs resulting from the response to these pulses are saved in a pulse response (Hankel) matrix. Then a control profile that will result in desired sensor outputs at the end of a maneuver is found. The control profile is piecewise continuous in time, so it is a train of square pulses of the type used to generate the pulse response matrix. It is not bang-bang, but is instead a profile that can be expected to approach the exact solution of the minimum time maneuver problem as the pulse width decreases. The sensor outputs resulting from the control profile are available from the pulse response matrix by simple convolution, if behavior is linear. The representation of the elastic behavior is without modal truncation of the type that is typical in modal methods, because an infinity of modes can contribute to the pulse response data.

For rapid large-angle maneuver, nonlinear effects can become significant. Nonlinear behavior cannot be represented using the simple convolution mentioned above, so the approach taken is to explicitly account for the deviation from the linear behavior that the pulse response data represents. It turns out that the number of modes that must be known to account for this deviation is very small, so identification requirements are low even for nonlinear problems. As an additional capability, a feedback component of the control is introduced to handle deviations from the response expected

from pulse response data that are due to noise or disturbances. This feedback control could also be used to compensate for deviations resulting from unmodeled nonlinear behavior.

This report is organized as follows. The second chapter presents the first known exact solution of a minimum time control problem for a structure, and it is found that the minimum time control profiles are not bang-bang, and they are not smooth. This exact solution provides some direction for the work summarized in later chapters, and a test case for evaluating minimum time and near minimum time maneuver methods. It also provides a certain midpoint condition for minimum time rest to rest control of distributed systems which is useful in the fifth chapter.

The third chapter presents the basic pulse response based control method for minimum time control of structures. In this chapter, the method is applied to linear problems. An efficient algorithm is developed for solving the numerical optimization problem that is encountered in this method. The effect of measurement noise is investigated. The method is applied to the problem of the second chapter for which the exact solution is known, and to the problem of extremely rapid rest to rest translation of a flexible beam, without any information about the beam besides its total mass and its pulse response data.

In the fourth chapter, the method is extended to nonlinear maneuver problems, where the nonlinearity is associated with rotational stiffening. The algorithm of the preceding chapter is modified to handle these nonlinear problems, and the method is applied to the extremely rapid rotation of a beam using two transverse force inputs at the ends. It is found in this chapter that the model order required for representing this type of nonlinear behavior can be expected to be extremely low.

The fifth chapter addresses some important practical implementation issues. The first of these is that of minimizing the amount of real time computation that must be done, and a near minimum time method that requires virtually no real time computation is developed. The second issue is that of developing a feedback control component which is stable in spite of nonlinear rotational stiffening effects and bounds on the control inputs. These two capabilities are demonstrated on a structure consisting of a rigid hub with four flexible appendages, with a torque actuator on the hub and force actuators at the ends of two of the appendages. It is found that the near minimum time control method performs very well, and the feedback component can easily handle deviations from linear response due to centrifugal effects for this structure, even for large-angle maneuver that is

much more rapid than could be addressed using other methods.

The final chapter contains conclusions and a summary of the entire project. The material in the second, third, fourth and fifth chapters is essentially covered in a number of papers that are in various stages of archival journal review and publication.[9–12] These papers have also appeared in unrefereed conference proceedings.

Chapter 2

Exact Minimum Time Control of a Distributed System Using a Traveling Wave Formulation

2.1 Introduction

In recent years, considerable interest in minimum-time control of distributed parameter systems has been motivated by the need to execute maneuvers of flexible spacecraft as quickly as possible. The "bang-bang" principle for minimum-time control of time-invariant finite-dimensional linear systems was presented by LaSalle in 1960.[13] It asserts that if a minimum-time control exists for a given system, then there exists a bang-bang optimal control in which the control inputs are almost always at a vertex of the polyhedron defined by the input bounds. The bang-bang principle has been extended to distributed parameter systems by Egorov,[14] Fattorini,[15] and Friedman,[16] among others. More directly applicable to the structure control problem is the work of Balakrishnan,[17] in which he examined the case in which the state and the control are in different Hilbert spaces. He proved that if the infinitesimal generator of the problem generates a compact semigroup, which is ordinarily the case in structure problems, the minimum-time control need not be bang-bang. However, it is a weak limit of an approximating sequence of bang-bang controls.

In practical applications, flexible spacecraft are usually modeled as finite-dimensional systems by using a truncated set of natural modes of vibration as a basis for the response. The use of a finite-dimensional model suggests bang-bang control as an approximation of the minimum-time control. A distributed parameter model is seldom available, and even including a large number of modes is costly because they are difficult to identify accurately, and because of the increased

complexity of the switching for bang-bang control. Some investigators have used the heuristic approach of "frequency-shaping" or "smoothing" to reduce the excitation of uncontrolled higher modes during a maneuver.[4,5,18] Another approach to the problem of rapid maneuver has been to use a perturbation approach in which the minimum-time control of the rigid-body mode or modes constitutes the zero-order problem, and suppression of the resulting flexible motion constitutes a first-order perturbation.[3,6,19] This approach does not result in minimum-time control subject to bounds on all inputs; for example, Ref. 6 only considers the use of one bounded input in the solution of the minimum-time zero-order problem, and bounds on all inputs are ignored in the solution of the first-order perturbation problem.

Exact control of distributed systems is addressed in Ref. 20 and in the many references cited therein. In this chapter, the solution of a minimum-time control problem for exact rest-to-rest translation of a simple distributed system using two bounded inputs is presented. A traveling wave formulation permits the consideration of the motion of this system without approximation. Traveling wave formulations have been used for vibration suppression and isolation in structure control problems.[21] To the authors' knowledge, the solution presented in this chapter is the only solution that has been obtained for exact minimum-time control of a distributed system by means of a finite number of bounded inputs.

The second section of this chapter presents a traveling wave formulation of the minimum-time control problem. In the third section, the solution is obtained for the case in which the control task can be carried out quickly enough that reflections of waves at the ends of the system need not be considered. The fourth section presents the solution for the general case in which reflections are considered, and a result for minimum time control of general undamped structures which will be important in the fifth chapter. The final section of the chapter contains a discussion of the solution and some conclusions.

2.2 Traveling Wave Formulation of the Problem

The minimum-time control problem for carrying out a rest-to-rest translation of a distributed system by means of two discrete, bounded control inputs is formulated in this section in terms of wave profiles traveling through the system. A one-dimensional second-order system is chosen for

its simplicity, and its response is governed by the partial differential equation

$$-\frac{\partial}{\partial x}\left(s(x)\frac{\partial u(x,t)}{\partial x}\right)+m(x)\frac{\partial^2 u(x,t)}{\partial t^2}=f(x,t), \qquad x\in(0,L), \tag{2.1}$$

in which $u(x,t)$ is the displacement as a function of x and t. This equation governs the motion of rods in axial vibration, shafts in torsional vibration, and strings in transverse vibration.[22] The terms $s(x)$ and $m(x)$ represent distributed stiffness and mass, and $f(x,t)$ is a distributed force or torque per unit length. In this chapter, a uniform system is considered, so that s and m are constant. Additionally, there is no internal excitation, so that $f(x,t)$ is zero.

For a uniform system without internal excitation, Eq. (2.1) admits the traveling wave solution

$$u(x,t)=U_+(x-ct)+U_-(x+ct), \tag{2.2}$$

in which $U_+(x-ct)$ and $U_-(x+ct)$ represent wave profiles moving in the positive and negative x directions, respectively, with the wave speed $c=\sqrt{s/m}$. If the displacement and velocity profiles $u(x,t)$ and $\dot{u}(x,t)$ are given for some time t, the wave profiles can be determined from them to within an arbitrary constant. Differentiation of Eq. (2.2) with respect to t and x yields

$$\dot{u}(x,t)=-cU_+^*(x-ct)+cU_-^*(x+ct) \tag{2.3a}$$

$$u'(x,t)=U_+^*(x-ct)+U_-^*(x+ct), \tag{2.3b}$$

where U^* denotes differentiation of U with respect to its argument. At a given time $\hat{t}$, the wave profiles can be obtained by making use of Eqs. (2.3) and integrating with respect to x, so that

$$U_+(x-c\hat{t})=\frac{1}{2}\int_0^x\left[u'(\xi,\hat{t})-\frac{1}{c}\dot{u}(\xi,\hat{t})\right]d\xi+C_1, \tag{2.4a}$$

$$U_-(x+c\hat{t})=\frac{1}{2}\int_0^x\left[u'(\xi,\hat{t})+\frac{1}{c}\dot{u}(\xi,\hat{t})\right]d\xi+C_2. \tag{2.4b}$$

Note that the constants C_1 and C_2 are not independent; one of them can be eliminated by considering Eq. (2.2), while the other remains arbitrary.

If the system is controlled by means of control inputs at the ends, the boundary conditions are

$$-s\frac{\partial u(x,t)}{\partial x}\bigg|_{x=0}=F_1(t), \qquad s\frac{\partial u(x,t)}{\partial x}\bigg|_{x=L}=F_2(t). \tag{2.5}$$

In this chapter, the control inputs are taken to be Lebesgue measurable in $[0,T]$, where T is the final time. In terms of wave profiles, the boundary condition at the left end can be written

$$F_1(t)=-s\frac{\partial}{\partial x}\left\{U_+(x-ct)+U_-(x+ct)\right\}\bigg|_{x=0}. \tag{2.6}$$

It will prove convenient to partition $F_1(t)$ into one component that generates right-going waves, $F_{1G}(t)$, and one that absorbs left-going waves, $F_{1A}(t)$, so that $F_1(t) = F_{1G}(t) + F_{1A}(t)$. The two components are then given by

$$F_{1G}(t) = -s\frac{\partial}{\partial x}(U_+(x-ct))\Big|_{x=0}, \tag{2.7a}$$

$$F_{1A}(t) = -s\frac{\partial}{\partial x}(U_-(x+ct))\Big|_{x=0}. \tag{2.7b}$$

The control input at the right end can be partitioned similarly. Note that if a control input is zero, this does not imply that its two components are zero; for example, if $F_1(t) = 0$, left-going waves that reach the left end result in $F_{1G}(t) = -F_{1A}(t) \neq 0$, and are reflected as right-going waves. If control inputs are employed in interior locations, they can generate and absorb wave profiles traveling in both directions. In general, in executing a given control task, the control inputs must generate and absorb traveling wave profiles that effect a change in the state of the system.

In order to express the response of the system explicitly in terms of the control inputs, note first that

$$\frac{\partial}{\partial x}(U_+(x-ct)) = \frac{-1}{c}\frac{\partial}{\partial t}(U_+(x-ct)). \tag{2.8}$$

The wave-generating component of $F_1(t)$, given in Eq. (2.7), can then be rewritten as

$$F_{1G}(t) = \frac{s}{c}\frac{\partial}{\partial t}(U_+(x-ct))\Big|_{x=0}. \tag{2.9}$$

Integrating both sides with respect to t and substituting $c = \sqrt{s/m}$ gives

$$U_+(x-ct)\Big|_{x=0} = \frac{1}{\sqrt{sm}}\int_0^t F_{1G}(\tau)\,d\tau + U_+(0-ct)\Big|_{t=0}, \tag{2.10}$$

where the constant of integration $U_+(0)$ can be arbitrarily taken to be the displacement of the left end at the initial time. This equation explicitly gives the dependence of the right-traveling wave profile on the generating component of the left control input and the initial conditions. Similarly, the left-traveling profile is determined by the generating component of the right control input as

$$U_-(x+ct)\Big|_{x=L} = \frac{1}{\sqrt{sm}}\int_0^t F_{2G}(\tau)\,d\tau + U_-(L+ct)\Big|_{t=0} + C, \tag{2.11}$$

where C must be chosen so that initial conditions are satisfied. Since the absorbing components of the control inputs are determined by the arriving wave profiles, the response of the system at a

time $t > 0$ can be found from the displacement and velocity of the system at $t = 0$ and the history of the control inputs for $t > 0$.

If the control inputs are to execute a change in position for the system, so that it goes from rest to rest as quickly as possible, initial and final conditions must be specified for the associated optimal control problem. The initial conditions can be taken to be

$$u(x,0) = 0, \quad \dot{u}(x,0) = 0, \qquad x \in (0,L), \tag{2.12}$$

so that the final conditions are

$$u(x,T) = u_0, \quad \dot{u}(x,T) = 0, \qquad x \in (0,L). \tag{2.13}$$

The initial and final conditions impose certain necessary conditions on the generating and absorbing components of the control inputs. From Eqs. (2.4), the final conditions require that both $U_+(x-ct)$ and $U_-(x+ct)$ must be constant over the length of the system at the final time T. Therefore, for a fixed value of x, each wave profile must be constant over a certain time interval. The right-traveling wave profile must be constant over the time interval $T - L/c < t < T$ at $x = 0$, where L/c is the time required for waves to travel the length of the system, and the left-traveling profile must be constant over the same time interval at $x = L$. From the boundary conditions the requirement that

$$F_{iG}(t) = 0, \qquad i = 1,2, \qquad T - L/c < t < T \tag{2.14}$$

is obtained. Eq. (2.14) defines an absorbing control interval at the end of the control history during which the control inputs can only be allowed to absorb arriving wave profiles. Similarly, the initial conditions require the absorbing components of the control inputs to satisfy

$$F_{iA}(t) = 0, \qquad i = 1,2, \qquad 0 < t < L/c, \tag{2.15}$$

which defines a generating control interval. The requirement that waves must be allowed to travel the length of the system between the end of wave profile generation and the end of the control history, and before absorption can begin at the beginning of the control history, limits how quickly the control task can be executed.

From the initial conditions of Eq. (2.12), the wave profiles are found from Eqs. (2.10) and (2.11) to be given by

$$U_+(x-ct)\Big|_{x=0} = \frac{1}{\sqrt{sm}} \int_0^t F_{1G}(\tau)\, d\tau, \tag{2.16a}$$

$$U_-(x+ct)\Big|_{x=L} = \frac{1}{\sqrt{sm}} \int_0^t F_{2G}(\tau)\, d\tau. \tag{2.16b}$$

From Eqs. (2.4) and the final conditions, Eq. (2.13), the wave profiles must satisfy

$$U_+(x-cT) = C, \quad U_-(x+cT) = u_0 - C, \qquad x \in (0, L) \tag{2.17}$$

for some constant C. Because both $F_{1G}(t)$ and $F_{2G}(t)$ must be zero over the absorbing control interval $T - L/c < t < T$, Eqs. (2.16) and (2.17) yield the requirement that

$$u_0 = \frac{1}{\sqrt{sm}} \int_0^{T-L/c} (F_{1G}(\tau) + F_{2G}(\tau))\, d\tau. \tag{2.18}$$

From this result it is evident that the control task cannot be executed in less time than the wave travel time L/c, regardless of the bounds on control inputs. This is in agreement with conclusions reached in Ref. 23.

In the following sections, the time required for carrying out a rest-to-rest translation is minimized subject to the constraints

$$|F_i(t)| \leq B \qquad \text{a.e. in } [0, T], \tag{2.19}$$

where B is a bound on the control inputs. In the next section, the problem is solved for the case in which no reflections at the ends occur, and the following section addresses the case in which reflections at the ends must be considered.

2.3 Minimum Time Control Without Reflections

If the ratio of the input bound B to the required final displacement u_0 is sufficiently large, wave profiles can be generated quickly enough by the control inputs that the control task can be accomplished without reflections at the ends of the system. Over the time interval $0 < t < L/c$, Eq. (2.15) requires that $F_{iA}(t) = 0$, so that $F_{iG}(t) = F_i(t)$ over this time interval. Suppose that the upper limit on the integral in Eq. (2.18) lies in the interval $0 < (T - L/c) < L/c$. Then the time interval T is obviously minimized by maximizing the control inputs, so that $F_{1G}(t) = F_{2G}(t) = B$ for $0 < t < T - L/c$. Carrying out the integration and solving for the minimal control interval gives

$$T_{min} = \frac{u_0\sqrt{sm}}{2B} + \frac{L}{c}. \tag{2.20}$$

which is valid for $T_{min} < 2L/c$ or, equivalently, $B/u_0 > s/2L$. As the input bound approaches infinity, the first term approaches zero, but the constant term remains.

The minimum-time control is found by recalling that the absorbing component of a control input is determined by the arriving wave profile, which is determined by the generating component of the other control input at a time L/c earlier. Making appropriate substitutions in Eq. (2.7) results in

$$\begin{aligned} F_{1A}(t) &= -s\frac{\partial}{\partial x}\{U_-(x+ct)\}\Big|_{x=0} \\ &= -s\frac{\partial}{\partial x}\{U_-(x+c(t-\frac{L}{c}))\}\Big|_{x=L} \\ &= -F_{2G}(t-\frac{L}{c}), \end{aligned} \tag{2.21}$$

and a similar result for $F_{2A}(t)$. With these and the fact that $F_{iG}(t)$ is equal to the input bound over $0 < t < T - L/c$ and zero over $T - L/c < t < T$, the minimum-time control is obtained as

$$F_i(t) = \begin{cases} B, & t \in (0, T - L/c), \\ 0, & t \in (T - L/c, L/c), \\ -B, & t \in (L/c, T). \end{cases} \tag{2.22}$$

Figure 2.1 shows the minimum-time control for several values of B. Note that there is a time interval over which the control inputs must be zero for synchronization with the traveling wave profiles, so that the control is characterized as "bang-off-bang".

In Fig. 2.2, the displacement of the system is plotted at several times during the minimum-time control history for the case $B = 5u_0 s/L$, which is shown in Fig. 2.1. At the beginning of the control history, the control inputs move the ends halfway to the desired final position as quickly as possible, and this action sends wavefronts into the system from both ends. The wavefronts cross in the middle, and add so that the displacement at the center, between the separating wavefronts, is equal to the desired final displacement. When the wavefronts reach the ends, the control inputs absorb them perfectly and leave the system at rest at the desired final position.

In the next section, the optimal control problem is solved for the more general case in which reflections at the ends of the system must be taken into account.

2.4 Minimum Time Control for the General Case

The minimum-time control problem for the general case, in which reflections at the ends of the system must be taken into account, is solved in several steps. First, it is shown that for any control

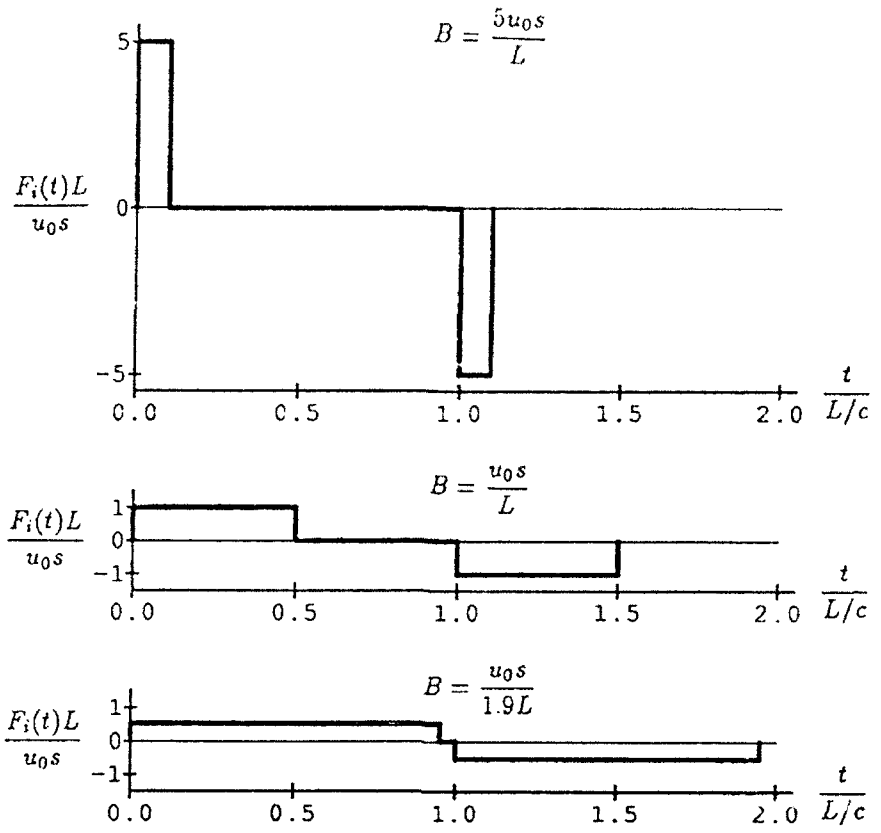

Figure 2.1: Minimum time control histories for three values of B

that satisfies the input bounds and the final conditions, with the specified initial conditions, a control that possesses a certain anti-symmetry property in time also satisfies the input bounds and the final conditions. This means that there is no loss of optimality in requiring the control to possess this anti-symmetry property. It should be noted that similar results for minimum-time control of a finite-dimensional system were obtained in Ref. 24, using a different approach. Second, it is shown that an anti-symmetric control satisfies the final conditions with the given initial conditions if and only if it satisfies a certain condition at the midpoint of the control history. The midpoint condition turns out to be applicable to minimum time control of a very large class of structures using ideal bounded inputs, and will be used in the fifth chapter in the development of a near minimum time control method. Finally, the minimum-time control satisfying this midpoint condition with the given initial conditions is obtained for the first half of the control history, and it is extended anti-symmetrically into the second half of the control history to yield a minimum-time control for the system.

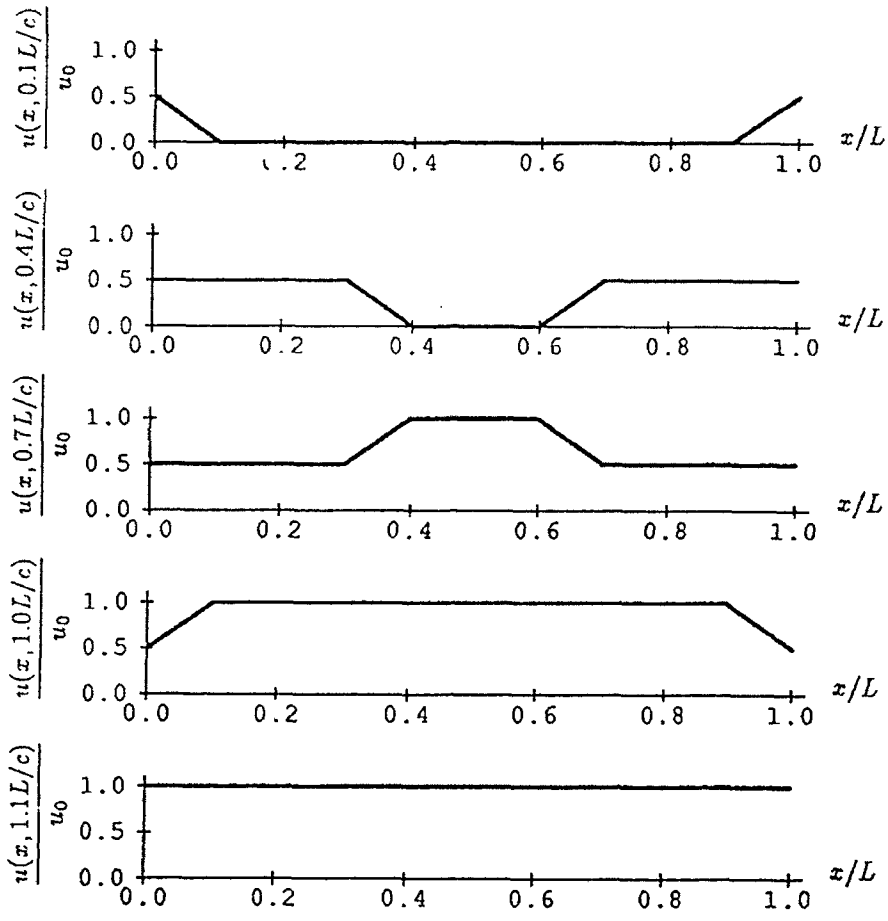

Figure 2.2: Displacement profile at several times for the case $B = 5u_0 s/L$

For any control $F_i(t)$, $t \in [0,T]$ satisfying the input bounds, it is clear by inspection that the control

$$F_i^{as}(t) = \frac{F_i(t) - F_i(T-t)}{2}, \qquad t \in [0,T], \tag{2.23}$$

which is anti-symmetric in time about $t = T/2$, must also satisfy the input bounds. It remains to be shown that if $F_i(t)$ drives the system from the origin to the prescribed final state, $F_i^{as}(t)$ does as well. The natural modes of vibration constitute an orthonormal basis for representing the system response, and they include a rigid-body mode:

$$\phi_0(x) = \frac{1}{\sqrt{mL}}, \tag{2.24}$$

and the flexible modes:

$$\phi_j(x) = \sqrt{\frac{2}{mL}} \cos\frac{j\pi x}{L}, \qquad j = 1,2,\ldots \tag{2.25}$$

The modes satisfy the orthogonality relations

$$\int_0^L \phi_j(x)\phi_k(x)\,dx = \delta_{jk}, \quad \int_0^L s\phi_j'(x)\phi_k'(x)\,dx = \lambda_j\delta_{jk}, \qquad j,k = 0,1,\ldots, \tag{2.26}$$

where δ_{jk} is the Kronecker delta and

$$\lambda_j = \omega_j^2 = \frac{(j\pi)^2 s}{mL^2}, \qquad j = 0,1,\ldots \tag{2.27}$$

is the jth eigenvalue and the square of the jth natural frequency. Inserting the modal representation

$$u(x,t) = \sum_{j=0}^{\infty} \phi_j(x)q_j(t) \tag{2.28}$$

in the partial differential equation of motion for the system, multiplying by $\phi_k(x)$, integrating over the system domain, and exploiting the orthogonality relations results in the modal equations of motion

$$\ddot{q}_0(t) = \frac{1}{\sqrt{mL}}Q_0(t) \tag{2.29}$$

and

$$\ddot{q}_j(t) + \lambda_j q_j(t) = \sqrt{\frac{2}{mL}}Q_j(t), \qquad j = 1,2,\ldots \tag{2.30}$$

where $Q_j(t)$ is proportional to the jth modal force, and is given by

$$Q_j(t) = [F_1(t) + (-1)^j F_2(t)], \qquad j = 0,1,\ldots \tag{2.31}$$

The initial and final conditions for a rest-to-rest translation, given in Eqs. (2.12) and (2.13), require that the flexible modal displacements and velocities must be zero at the beginning and end of the control interval:

$$q_j(0) = \dot{q}_j(0) = q_j(T) = \dot{q}_j(T) = 0, \qquad j = 1,2,\ldots \tag{2.32}$$

The initial and final conditions for the rigid-body mode are

$$q_0(0) = \dot{q}_0(0) = \dot{q}_0(T) = 0, \qquad q_0(T) = u_0\sqrt{mL}. \tag{2.33}$$

For the flexible modes of the system, for any control $F_1(t)$ that satisfies the initial and final conditions of Eqs. (2.32), the following convolution integrals must be satisfied for modal displacements:

$$\int_0^T Q_j(\tau)\sin\omega_j(T-\tau)\,d\tau = 0, \qquad j = 1,2,\ldots \tag{2.34}$$

and modal velocities:

$$\int_0^T Q_j(\tau)\cos\omega_j(T-\tau)\,d\tau = 0, \qquad j = 1,2,\ldots \tag{2.35}$$

Using angle addition formulas in Eqs. (2.34) and (2.35), and multiplying the first of these by $\sin\omega_j T$ and the second by $\cos\omega_j T$ and adding yields

$$\int_0^T Q_j(\tau)\cos\omega_j\tau\,d\tau = 0. \tag{2.36}$$

Similarly, multiplying the first by $(-\cos\omega_j T)$ and the second by $\sin\omega_j T$ and adding yields

$$\int_0^T Q_j(\tau)\sin\omega_j\tau\,d\tau = 0. \tag{2.37}$$

Using an appropriate change of variable in these two equations and subtracting them from Eqs. (2.34) and (2.35) results in

$$\int_0^T \left[\frac{Q_j(\tau) - Q_j(T-\tau)}{2}\right]\sin\omega_j(T-\tau)\,d\tau = 0 \tag{2.38}$$

and

$$\int_0^T \left[\frac{Q_j(\tau) - Q_j(T-\tau)}{2}\right]\cos\omega_j(T-\tau)\,d\tau = 0. \tag{2.39}$$

These two equations show that if a control $F_i(t)$ satisfies the final conditions in the flexible modes, with zero initial conditions, then the anti-symmetric control constructed from $F_i(t)$ also satisfies the initial and final conditions in all flexible modes. It is straightforward to show, using a similar approach, that if the control $F_i(t)$ satisfies the specified initial and final conditions for the rigid-body mode, the anti-symmetric control $F_i^{as}(t)$ also satisfies the initial and final conditions for the rigid-body mode. Hence, for any optimal control there exists an anti-symmetric control that is also optimal, so a restriction to anti-symmetric controls results in no loss of optimality.

For an antisymmetric control that satisfies initial and final conditions, final flexible mode displacements must be zero, so the convolution integrals of Eqs. (2.34) must be satisfied. Splitting these integrals into two halves in time and recalling the antisymmetry property of the control results in

$$\int_0^{T/2} Q_j^{as}(\tau)\sin\omega_j(T-\tau)\,d\tau - \int_{T/2}^T Q_j^{as}(T-\tau)\sin\omega_j(T-\tau)\,d\tau = 0,\ j = 1,2,\ldots \tag{2.40}$$

Using a change of variable in the second integral so that its limits match those of the first integral, and combining the two integrals gives the result

$$2\cos\omega_j T/2 \int_0^{T/2} Q_j^{as}(\tau)\sin\omega_j(T/2-\tau)\,d\tau = 0,\ j = 1,2,\ldots, \tag{2.41}$$

which indicates that, if $\cos\omega_j T/2 \neq 0$, the flexible modal displacements at the midpoint of the control interval must be zero. If $\cos\omega_j T/2 = 0$, similar steps can be taken with the final modal velocities to obtain

$$2\sin\omega_j T/2 \int_0^{T/2} Q_j^{as}(\tau)\sin\omega_j(T/2-\tau)\,d\tau = 0,\ j = 1,2,\ldots, \tag{2.42}$$

which will then require the flexible modal displacements at the midpoint of the control interval to be zero. It is straightforward to show that when the antisymmetric control $F_i^{as}(t)$ is applied to the system, the rigid-body mode displacement at the midpoint of the control interval is equal to one-half of the final rigid-body mode displacement. Hence, a necessary condition for an antisymmetric control to satisfy the final conditions with the given initial conditions is that it must result in a system displacement at the midpoint of the control interval given by

$$u(x,T/2) = u_0/2, \qquad x \in (0,L). \tag{2.43}$$

It can be easily shown that this is a sufficient condition for satisfying the final conditions as well. Therefore, a minimum-time control that drives the system from zero initial conditions to the system displacement given in the above midpoint condition, with the velocity unspecified, can be extended anti-symmetrically in time to yield a minimum-time control for the original problem.

The results obtained thus far in this section are applicable to minimum time rest to rest control of a large class of structures which possess one or more rigid body modes and an infinity of flexible modes, whose responses are governed by equations in the form of Eqs. (2.29) and (2.30) respectively. This fact will be exploited in the development of a near minimum time control method in the fifth chapter.

The midpoint condition, Eq. (2.43), requires the partial derivative of the displacement with respect to x to vanish over the length of the system at the midpoint of the control time interval. From the second of Eqs. (2.3), the traveling wave profiles must satisfy the equation

$$U_+^*(x - cT/2) + U_-^*(x + cT/2) = 0, \qquad x \in (0,L). \tag{2.44}$$

This can be related to the control inputs by using the boundary conditions with an appropriate time shift. For example, the derivative of the right-traveling wave profile at the time T and a location x can be expressed in terms of $F_{1G}(t)$ using the first of Eqs. (2.7) and a time shift of x/c as

$$U_+^*(x - cT/2) = U_+^*(0 - c(T/2 - x/c)) = -\frac{1}{s}F_{1G}(T/2 - x/c), \tag{2.45}$$

and the left-traveling wave profile can be handled similarly. Using these results in Eq. (2.44) and multiplying by s results in the equation

$$F_{1G}(T/2 - x/c) = F_{2G}(T/2 - (L - x)/c), \qquad x \in (0, L). \tag{2.46}$$

Upon introducing the variable $\xi = (L - 2x)/2c$, this becomes

$$F_{1G}(T/2 - L/2c - \xi) = F_{2G}(T/2 - L/2c + \xi), \qquad \xi \in (-L/2c, L/2c), \tag{2.47}$$

which is a necessary and sufficient condition for the system displacement to be constant at the midpoint of the control history. The midpoint condition will then be satisfied if the displacement is additionally required to be equal to $u_0/2$ at $t = T/2$ for some $x \in (0, L)$ that can be chosen arbitrarily. Choosing the location $x = L/2$ for convenience, and expressing wave profiles in terms of the generating components of the control inputs, results in the requirement:

$$\begin{aligned} u(L/2, T/2) &= U_+(L/2 - cT/2) + U_-(L/2 + cT/2) \\ &= U_+(0 - c(T/2 - L/2c)) + U_-(L + c(T/2 - L/2c)) \\ &= \frac{1}{\sqrt{sm}}\int_0^{T/2 - L/2c} F_{1G}(\tau) + F_{2G}(\tau)\, d\tau = \frac{u_0}{2}. \end{aligned} \tag{2.48}$$

From the last line above, it is clear that the control time interval will be minimized by maximizing $F_{1G}(t)$ and $F_{2G}(t)$, subject to the constraint of Eq. (2.47). This result is similar to the case considered in the previous section. However, because of nonzero reflections at the ends, the generating components of control inputs are not simply equal to the applied control inputs as they were in the previous section. Instead, the generating component of a control input can be written $F_{iG}(t) = F_i(t) - F_{iA}(t)$, where the absorbing component is determined by the generating component at the other end at a time L/c earlier. If $F_{1G}(t)$ and $F_{2G}(t)$ are maximized by setting $F_1(t) = F_2(t) = B$, the result will be

$$F_{iG}(t) = nB \quad \text{for} \quad (n - 1)L/c < t < nL/c, \qquad n = 1, 2, \ldots \tag{2.49}$$

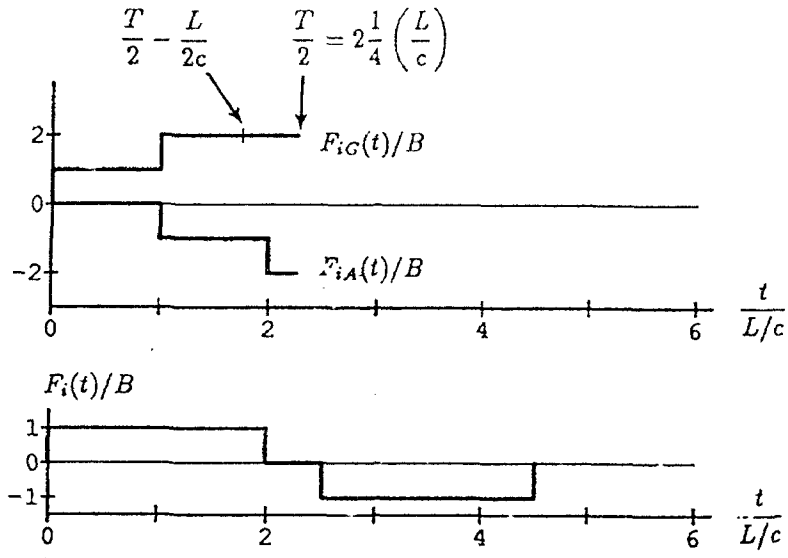

Figure 2.3: Generating and absorbing components of control inputs, and control history for a case where $(n-1/2)L/c < T/2 - L/2c < nL/c$

so that the maximized generating component of each control input will become a piecewise constant "stairstep" function of time. By inspection, $F_{1G}(t)$ and $F_{2G}(t)$ are maximized for all $t \in (0, T/2)$ subject to Eq. (2.47) if they are simply maximized up to $T/2 - L/2c$, and then extended for $t \in (T/2 - L/2c, T/2)$ to satisfy Eq. (2.47), which requires them to be extended symmetrically in time around $t = T/2 - L/2c$.

If the time $T/2 - L/2c$ happens to fall between $(n-1/2)L/c$ and nL/c, where n is an integer, the generating components of the control inputs will remain constant until $T/2$ to satisfy Eq. (2.47), as illustrated in Fig. 2.3. On the other hand, if $T/2 - L/2c$ falls between nL/c and $(n+1/2)L/c$, the generating components will have to decrease by an amount B at a certain time before $T/2$, as shown in Fig. 2.4. The control inputs are given by $F_i(t) = F_{iG}(t) + F_{iA}(t)$, where the absorbing component is determined by the arriving wave profile and is equal to the negative of the other end's generating component L/c earlier. When this is considered, the control inputs are found to be

$$F_i(t) = \begin{cases} B, & \text{for } 0 < t < nL/c; \\ 0, & \text{for } nL/c < t < T/2; \end{cases} \tag{2.50}$$

for the case in which $(n - 1/2)L/c \leq T/2 - L/2c \leq nL/c$, and

$$F_i(t) = \begin{cases} B, & \text{for } 0 < t < T - (n+1)L/c; \\ 0, & \text{for } T - (n+1)L/c < t < T/2; \end{cases} \tag{2.51}$$

for the case in which $nL/c \leq T/2 - L/2c \leq (n+1/2)L/c$. When these control inputs are extended in time so that they satisfy $F_i(T-t) = -F_i(t)$, the minimum-time control for rest-to-rest translation

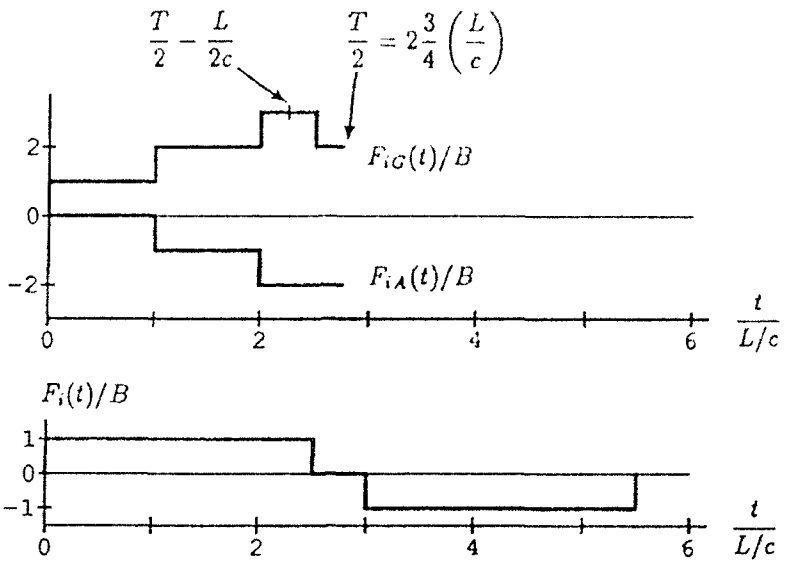

Figure 2.4: Generating and absorbing components of control inputs, and control history for a case where $nL/c < T/2 - L/2c < (n + 1/2)L/c$

of the system is obtained. Again, as in the previous section, the control can be described as "bang-off-bang", where the "off" period in the center of the control history is required for proper synchronization with the wave profiles traveling through the system.

To relate these control histories to the distance translated and the time required, the displacement of a point in the system at the time $T/2$ can be evaluated. From Eqs. (2.48) and (2.49), the displacement at the center of the system is given by

$$\begin{aligned} u(\frac{L}{2}, \frac{T}{2}) = \frac{u_0}{2} &= \frac{2}{\sqrt{sm}}\left[B\frac{L}{c} + 2B\frac{L}{c} + \cdots + nB\left\{\frac{T}{2} - \frac{L}{2c} - (n-1)\frac{L}{c}\right\}\right] \\ &= \frac{2}{\sqrt{sm}}\left[B\frac{L}{c}\frac{n(n-1)}{2} + nB\left\{\frac{T}{2} - \left(n - \frac{1}{2}\right)\frac{L}{c}\right\}\right] \\ &= \frac{BL}{s}(-n^2) + \frac{nBT}{\sqrt{sm}}. \end{aligned} \tag{2.52}$$

This is only valid if the term in braces in the equations above, which represents the amount of time before $t = T/2 - L/2c$ that $F_{iG}(t) = nB$, is between zero and L/c. Satisfying this requirement will identify the appropriate value of n. Solving for T in the equation above gives the minimum time required to complete the control task:

$$T_{min} = \frac{u_0\sqrt{sm}}{2nB} + n\frac{L}{c}. \tag{2.53}$$

The required time interval can be nondimensionalized by dividing it by the time required for waves to travel the length of the system, which is a lower bound on the time required regardless of the

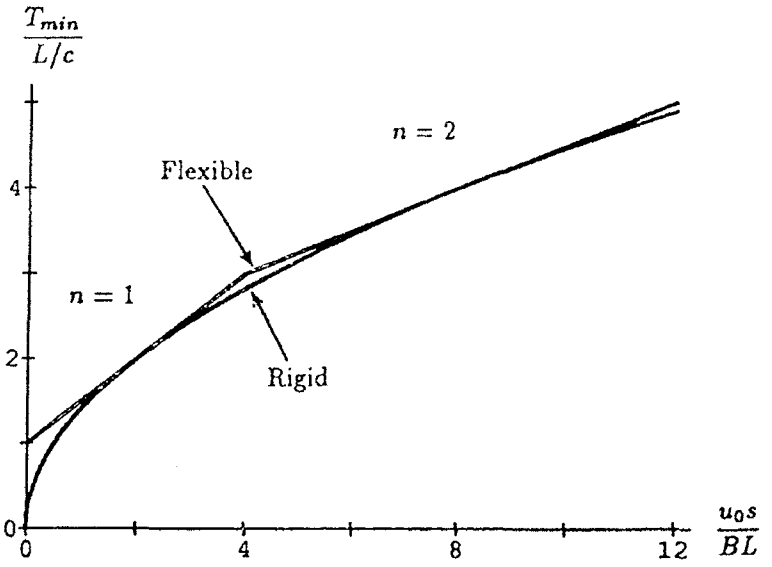

Figure 2.5: Time required for control of flexible and rigid systems

bounds on the control inputs. This gives

$$\frac{T_{min}}{L/c} = \frac{u_0 s}{2nBL} + n. \tag{2.54}$$

From this, n must satisfy the inequalities

$$2n(n-1) \leq \frac{u_0 s}{BL} \leq 2n(n+1). \tag{2.55}$$

The normalized time required to execute a rest-to-rest translation of the flexible system is plotted against the nondimensional quantity $u_0 s/BL$ in Fig. 2.5. Note that the solution for large input bounds obtained in the previous section is a special case of the results obtained here. For comparison, the time required to execute the same task on a rigid system having the same mass is also plotted in the same figure. The solution of the minimum-time control problem for the comparable rigid system is bang-bang, and the time required is $T_{min} = \sqrt{2u_0 mL/B}$. Although the wave speed c and the stiffness s are not meaningful for a rigid system, it is convenient for comparison to divide the time required for translation of the rigid system by L/c, which yields

$$\frac{T_{min}}{L/c} = \sqrt{\frac{2u_0 s}{BL}} \tag{2.56}$$

for the rigid system.

When the two curves are plotted on the same graph, it is seen that the time required for translation of the flexible system bounds the time required for translation of the rigid system from

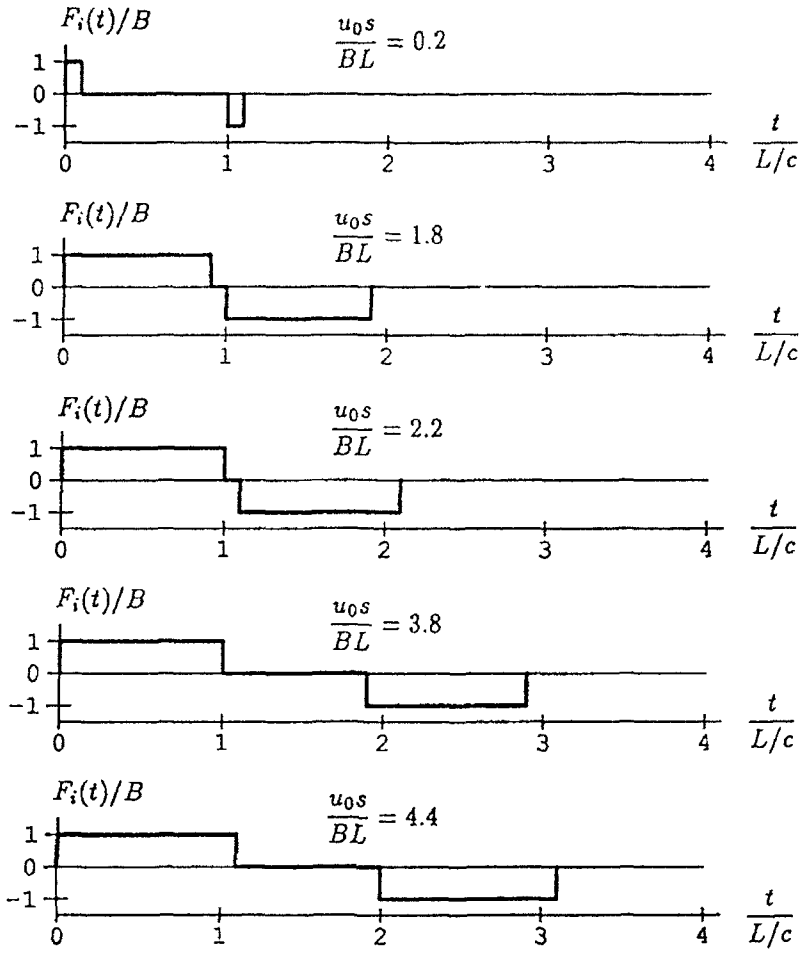

Figure 2.6: Minimum time control histories for several values of u_0

above, and that the two curves are tangent at discrete points. For more insight into this, consider increasing the distance translated, u_0, from zero while all other parameters are held constant. Figure 2.6 shows the "bang-off-bang" control histories that result from doing this. For values of u_0 less than $2BL/s$, the second "bang" begins at $t = L/c$. As u_0 increases from zero, the "bangs" become wider, narrowing the "off" time interval. When u_0 reaches $2BL/s$, the "bangs" meet, and the minimum-time control history for the flexible system duplicates that for a rigid system having the same mass. This corresponds to the first tangent point on the plot in Fig. 2.5. As u_0 increases beyond $2BL/s$, the two "bangs" remain of length L/c in time, but begin to separate, so that an "off" interval is reestablished. The length of the "off" interval increases until it reaches L/c and u_0 reaches $4BL/s$. At this point, the length of the "bang" intervals begins to increase from L/c, so that the "off" interval is narrowed again. When u_0 reaches $8BL/s$, the control history

again becomes "bang-bang" and the second point of tangency between the two curves in Fig. 2.5 is reached. This pattern is repeated as u_0 continues to increase, and tangent points occur whenever $u_0 s/BL$ is equal to twice the square of an integer.

For large values of $u_0 s/BL$, the time required for translating a comparable rigid system is a good approximation of the time required for executing a rest-to-rest translation of the flexible system. The greatest difference between the two is seen when $u_0 s/BL$ is less than one, which corresponds to small translations with large bounds on the control inputs.

2.5 Conclusions

The minimum-time control problem associated with exact rest-to-rest translation of a simple distributed system by means of two bounded inputs has been solved using a traveling wave formulation of the problem. The minimum-time control has been found to be "bang-off-bang", where two time intervals over which the control inputs operate at their limits are separated by a period of control inactivity.

It is interesting to compare the solution obtained here with solutions of minimum-time problems for truncated modal models of the system. If no flexible modes are included in the model, the minimum-time control is bang-bang with only one switching, and the time required is given by the lower curve in Fig. 2.5. As flexible modes are added to the model, the number of switchings in the control history will increase, and the time required for control will increase monotonically, approaching an upper bound equal to the time required for exact control of the distributed system. The control history will continue to be bang-bang, of course, but it will approximate the "off" interval in the exact solution with an interval around the midpoint of the control history that contains increasingly rapid switching as more modes are controlled. The exact solution for the distributed system is much simpler than the solution for a high-order modal model of the system, and the complex switching in the control for the model can be attributed entirely to the modal truncation in the model. It should be noted that the fact that the control inputs are "off" when they are not operating at their limits can be traced to the non-dispersive nature of the particular system studied here, and the requirement of synchronization with wave profiles. For more general structures, the exact minimum-time control can be expected to be operating at the input bounds over much of the control history, but should not be expected to be zero over the remainder. From

the exact solution obtained in this chapter, it is evident that bang-bang minimum-time control for a truncated model may not be a good approximation of the exact solution. Observing that the exact solution obtained here is not "smooth", a "smoothed" bang-bang control may not approximate the exact solution any better.

Chapter 3

Pulse Response Based Control of Linear Systems

3.1 Introduction

As mentioned in the first chapter, most methods that have been developed for rapid maneuver of flexible spacecraft rely on modal or state space models which represent flexible behavior explicitly. Accurate system identification is therefore a prerequisite for these methods. This presents difficulties associated with testing large flexible spacecraft, either on earth or in orbit. Truncation of the model is inevitable, and this raises the issues of whether unmodeled dynamics will be significant in the response of the system, and of the bang-bang minimum time control profile for the truncated model being qualitatively quite different from the minimum time control profile for the flexible system.

This chapter presents a new approach to minimum time control of flexible spacecraft which is not subject to the difficulties mentioned above. The flexible behavior of the spacecraft is represented in terms of measured response to pulses in control inputs, rather than in terms of an explicit model. A minimum time control profile is obtained which results in prescribed outputs at the end of the control task, according to convolution of the pulse response data. The main advantage of this approach is that measurements of pulse response can be obtained much more easily and directly than the explicit model data required for conventional approaches. There is no modal truncation because all modes excited by the control inputs participate in the pulse response data, assuming that the system is observable. This chapter addresses application of Pulse Response Based Control to linear problems, while the following two chapters address application to nonlinear maneuver

problems.

In the second section of this chapter, the Pulse Response Based Control (PRBC) method is presented. The third section presents an efficient numerical algorithm for implementing PRBC. The effect of measurement noise on the accuracy of the final state of the system is investigated in the fourth section. In the fifth section, a numerical example is presented. The final section contains a brief summary for the chapter.

3.2 Pulse Response Based Control

Suppose a linear dynamic system is controlled by a single input $u(t)$, with no other excitations, and its response is measured in terms of m outputs that constitute a vector $y(t)$. If the system is initially at rest and a square pulse in $u(t)$, of unit amplitude and duration Δt, is applied, and the outputs $y(t)$ are sampled every Δt for a total time $n\Delta t$, an $m \times n$ pulse response matrix H is obtained, of the form

$$\begin{aligned} H &\equiv [\, y(n\Delta t) \quad y((n-1)\Delta t) \quad \cdots \quad y(\Delta t)\,] \\ &= [\, h_1 \quad h_2 \quad \cdots \quad h_n\,], \end{aligned} \tag{3.1}$$

where the order of the output vectors is reversed for use in a convolution sum. Note that the matrix H is a Hankel matrix. Suppose the system is initially at rest and a control profile $u(t)$ that is constant over each time step Δt between $t = 0$ and $t = n\Delta t$ is applied to the system, so that the control input is equal to u_i over the ith time step. Then the output vector at $n\Delta t$ can be found by convolution, because of the linearity of the system. Each value u_i is multiplied by a vector in the pulse response matrix H, so that the output vector is given by

$$y(n\Delta t) = \sum_{i=1}^{n} h_i u_i = H u, \tag{3.2}$$

where $u = [\, u_1 \quad u_2 \quad \cdots \quad u_n\,]^T$. Note that this control profile is piecewise constant, and not a series of spike-like impulses. Obviously, other types of pulses (e.g., triangular) could be used to obtain other types of control profiles (e.g., piecewise linear).

If there are p inputs, the scalar entries u_i in the vector u are replaced by the subvectors $u_i = [\, u_{1,i} \quad \cdots \quad u_{p,i}\,]^T$, and the vectors h_i must be replaced by $m \times p$ submatrices H_i. The pulse response matrix H is then filled by applying pulses in one control input at a time, and sampling the

outputs resulting from each pulse every Δt over an interval of length $n\Delta t$. The outputs resulting from a pulse in the first control input will fill the first vector of each submatrix H_i in H, and each of the other $p-1$ columns in a submatrix H_i will be obtained from response to a pulse in another control input.

If a control task that consists of driving the system from rest at $t = 0$ to a desired state at a time $t_f = n\Delta t$ is successfully accomplished by a piecewise constant control profile of the type described above, the set of linear equations

$$\boldsymbol{y}(t_f) = H\boldsymbol{u} \tag{3.3}$$

must be satisfied by the control profile $\boldsymbol{u}$, where the vector $\boldsymbol{y}(t_f)$ contains outputs consistent with the desired final state of the system. Also, if there is no excitation of the system after t_f, the equations

$$\boldsymbol{y}(t_f + j\Delta t) = [\, H_{1-j} \quad H_{2-j} \quad \cdots \quad H_{n-j}\,]\,\boldsymbol{u} \tag{3.4}$$

must be satisfied, where the time-shifted submatrix H_{k-j} contains outputs measured $(n-k+1)+j$ *time steps after applying test pulses in control inputs*, and where the outputs $\boldsymbol{y}(t_f + j\Delta t)$ must be consistent with the desired state of the system at t_f, with free response after t_f.

These observations suggest the following approach for minimum time control problems: Find the smallest integer number of time steps n such that there exists a control history vector $\boldsymbol{u} \equiv [\boldsymbol{u}_1^T \quad \cdots \quad \boldsymbol{u}_n^T]^T$ satisfying the equations

$$\overline{H}\boldsymbol{u} = \overline{\boldsymbol{y}}_f \tag{3.5}$$

and the input bounds, typically of the form

$$B_j^l \le u_{j,i} \le B_j^u, \quad j = 1, \ldots, p;\ i = 1, \ldots, n, \tag{3.6}$$

in which B_j^l and B_j^u are lower and upper bounds for the jth control input. The vector $\overline{\boldsymbol{y}}_f$ contains outputs at t_f and at l time steps afterward:

$$\overline{\boldsymbol{y}}_f \equiv \left\{ \begin{array}{c} \boldsymbol{y}(t_f) \\ \boldsymbol{y}(t_f + \Delta t) \\ \vdots \\ \boldsymbol{y}(t_f + l\Delta t) \end{array} \right\}, \tag{3.7}$$

and the matrix $\overline{H}$ is given by

$$\overline{H} \equiv \begin{bmatrix} H_1 & H_2 & \cdots & H_n \\ H_0 & H_1 & \cdots & H_{n-1} \\ \vdots & \vdots & & \vdots \\ H_{1-l} & H_{2-l} & \cdots & H_{n-l} \end{bmatrix}. \tag{3.8}$$

Satisfaction of Eqs. (3.5) is a necessary but not sufficient condition for accomplishing the control task exactly. An important question is how precisely the final state of the system is specified by these equations. If the system is of finite order with state equations in the standard form

$$\dot{\boldsymbol{x}} = A\boldsymbol{x} + B\boldsymbol{u}, \tag{3.9}$$

where $\boldsymbol{x}$ is the state vector and A and B are constant, and the outputs are related to the states by the equation $\boldsymbol{y} = C\boldsymbol{x}$, then the vector $\overline{\boldsymbol{y}}_f$ is given by

$$\overline{\boldsymbol{y}}_f = \begin{bmatrix} C \\ C\Phi \\ \vdots \\ C\Phi^l \end{bmatrix} \boldsymbol{x}(t_f), \tag{3.10}$$

where $\Phi \equiv e^{A\Delta t}$ is the state transition matrix for the time step Δt. It is apparent from this that if a finite-order system is observable by means of the outputs in $\boldsymbol{y}$, then the final state can be specified exactly by this approach. In general, if there are s states and the rank of $\overline{H}$ is r, then the final state $\boldsymbol{x}(t_f)$ is confined to a subspace of order $s - r$.

Flexible spacecraft are distributed parameter systems of infinite order. However, practical considerations ordinarily require finite-order representation for control, typically using a truncated modal model. The PRBC approach outlined above, on the other hand, can be used on linear distributed parameter systems without any explicit modeling. In addition, because all modes can participate in the pulse response measurements, there is no modal truncation in the system representation used by PRBC. By specifying the outputs at the final time t_f and at l time steps afterward, PRBC places a finite set of constraints on the final state, as modal methods do when the final states of a finite number of modes are specified. An important difference between the two is that there is no assumption of finite-order dynamics for the system in PRBC.

If actuators do not respond instantaneously to control commands, but instead exhibit linear response behavior, the actuator dynamics can be considered part of the system dynamics. Square pulses in control commands, rather than in the actual forces or moments applied to the system,

are used to obtain pulse response data, and the vector $\boldsymbol{u}$ represents command profiles rather than force or moment profiles.

The outputs in $\boldsymbol{y}$ will typically include measurements of response quantities that are most critical to the performance of the spacecraft. Therefore, specifying these outputs will have the natural effect of specifying the final states of modes that are most important to performance, without explicit consideration of which modes are most important. In comparison with the conventional modal approach, which requires explicit identification of modes from response measurements and explicit modeling of response in these modes, PRBC is a more direct approach.

Ordinarily the inertial properties of spacecraft are known with a high level of accuracy, especially in comparison with modal properties. If this is the case, it is straightforward to determine the response of a structure in its rigid body modes to pulses in the control inputs, so that the desired rigid body mode states at the final time t_f can be included in the vector of specified outputs $\overline{\boldsymbol{y}}_f$. Of course, if pulse responses are known accurately for any flexible modes, their final modal states can also be included in $\overline{\boldsymbol{y}}_f$.

The matrix $\overline{H}$ is obtained by simply collecting measurements of pulse response, and it will not necessarily be of full rank. This can lead to numerical difficulties in the solution of the optimization problem, because the equality constraints will not be linearly independent if $\overline{H}$ is rank deficient. This problem can be easily handled by finding the singular value decomposition of $\overline{H}$, so that

$$\overline{H} = U\Sigma V^T, \tag{3.11}$$

where U and V are square orthogonal matrices containing the left and right singular vectors of $\overline{H}$, and Σ is a rectangular matrix consisting of a diagonal square submatrix containing singular values of $\overline{H}$, with null columns appended on the right to make the matrices conformal. If a tolerance ϵ is chosen so that singular values less than ϵ are taken to indicate rank-deficiency, then the matrices $\tilde{U}$, $\tilde{\Sigma}$ and $\tilde{V}$ can be obtained from U, Σ and V by retaining only the columns associated with singular values greater than ϵ. A maximal set of linearly independent equality constraints that agree with the original, possibly dependent, equality constraints can be written as

$$\tilde{V}^T\boldsymbol{u} = \tilde{\Sigma}^{-1}\tilde{U}^T\overline{\boldsymbol{y}}_f. \tag{3.12}$$

Even if the original equality constraints are linearly independent, this step can improve numerical conditioning because of the orthogonality of the columns of $\tilde{V}$.

It is worth noting that since the matrix $\overline{H}$ is a generalized Hankel matrix, the maximum rank of $\overline{H}$ that can be obtained by adding rows corresponding to outputs at additional time steps is equal to the maximum order of a system model that can be realized from the outputs in y.[25]

3.3 An Algorithm for the Optimization Problem

The Pulse Response Based Control method addresses the minimum time control problem by finding the minimum number of time steps for which a control profile exists satisfying the equality constraints of Eq. (3.5) and the input bounds. The resulting numerical optimization problem is therefore an integer programming problem. In this section, an algorithm is presented for solving this integer programming problem using standard linear programming methods.

Before the problem is solved for a given control task and time step size Δt, the number of time steps for which outputs must be specified in $\overline{y}_f$, in order to adequately specify the desired final state of the system, is not known. If this and the minimum time required for control, t_f, were known in advance, a piecewise constant approximation of the minimum time control profile could be obtained by simply finding a vector u satisfying the equality constraints and the input bounds, with a number of time steps n in the control profile such that $n\Delta t \geq t_f$. To verify that n is a minimal number of time steps, it is only necessary to show that no feasible solution exists with $n-1$ time steps.

However, both t_f and the number of time steps for which outputs must be specified are not known in advance. Perhaps the most straightforward approach to the problem is to begin by including only the final rigid body mode states and the outputs at the final time in $\overline{y}_f$, and incrementing the number of time steps in the control history until a feasible solution u can be found. Then the desired outputs for $t_f + \Delta t$ can be added to $\overline{y}_f$, and the number of time steps n can be increased again until a feasible solution is found. When including outputs for more time steps in $\overline{y}_f$ no longer causes the number of time steps in the control history or the control profile u to change, it can be concluded that a control profile which achieves the desired final state in a minimal number of time steps has been found. The disadvantage of this approach is its computational expense. If the control profile is to be accurate, the time step Δt must be small. This implies that there will be a large number of unknowns in the vector u, so that investigating

existence of feasible solutions will be costly, especially if it must be done for many values of n.

The number of values of n for which existence of feasible solutions is investigated can be reduced by getting an inexpensive estimate of t_f with a larger time step size and therefore fewer unknowns in the vector $\boldsymbol{u}$. Once pulse response data for pulses of width Δt has been obtained in a matrix $H^{\Delta t}$, it is straightforward to obtain a pulse response matrix for pulses of width $q\Delta t$, where q is an integer:

$$H^{q\Delta t} \equiv [\, H_1^{q\Delta t} \quad H_2^{q\Delta t} \quad \cdots] = \left[\sum_{i=1}^{q} H_i^{\Delta t} \quad \sum_{i=q+1}^{2q} H_i^{\Delta t} \quad \cdots \right]. \tag{3.13}$$

Then each entry in a corresponding $\boldsymbol{u}$ vector gives the value of a control input over a time interval of length $q\Delta t$. The approach taken in the algorithm presented here is to recursively generate pulse response matrices $H^{2\Delta t}$, $H^{4\Delta t}$, $H^{8\Delta t}$, etc., by adding consecutive pairs of submatrices H_i for one step size to obtain submatrices for a step size twice as large. Then the minimum time problem is solved first with the largest step size, and this gives a starting point for solving the problem with a step size half as large. The problem is solved with successively smaller step sizes until the original time step size Δt is reached.

There must be a criterion for determining when the control problem has been solved accurately enough to change to a smaller step size or to ultimately consider the problem solved. As an indicator of how accurately a given control profile causes the system to reach the desired final state, using only information available from pulse response data, the outputs for several time steps after the end of the control history, for which outputs have not been specified, are obtained by convolution. This is done for the first time, for reference, with the first minimum time control profile found, for which only the final rigid body mode states are specified and the largest time step size ΔT_0 is used. A vector $(\overline{\boldsymbol{e}}_{unsp.})_0$ is defined as

$$(\overline{\boldsymbol{e}}_{unsp.})_0 \equiv \left\{ \begin{array}{c} \boldsymbol{e}(t_f) \\ \boldsymbol{e}(t_f + \Delta T_0) \\ \vdots \\ \boldsymbol{e}(t_f + k\Delta T_0) \end{array} \right\}, \tag{3.14}$$

where each vector $\boldsymbol{e}$ is the error in the output vector $\boldsymbol{y}$, k is an integer, and t_f is the final time obtained for this profile. For each new control profile obtained in the algorithm, a vector

$$\overline{\boldsymbol{e}}_{unsp.} \equiv \left\{ \begin{array}{c} \boldsymbol{e}(t_{unsp.}) \\ \boldsymbol{e}(t_{unsp.} + \Delta T_0) \\ \vdots \\ \boldsymbol{e}(t_{unsp.} + k\Delta T_0) \end{array} \right\} \tag{3.15}$$

is obtained, where $t_{unsp.} = t_{last} + \Delta T_0$, where t_{last} is the last time step for which outputs have been specified for the current profile. The ratio of norms of these two vectors

$$R \equiv \frac{\|\bar{e}_{unsp.}\|_2}{\|(\bar{e}_{unsp.})_0\|_2} \tag{3.16}$$

is used as an indicator of how accurately the desired final state has been achieved. In principle, if the control task is accomplished exactly, there will be no error in outputs at any time after the end of the control history. In implementation of the algorithm, allowable values for R must be specified for each change in time step size and for final termination of the computation.

The following is an outline of the algorithm for solving the numerical optimization problem encountered in PRBC:

1. Obtain pulse response matrix H for time step Δt, from measurements of the system response. Also, given the system's inertial properties, calculate the matrix of pulse response in rigid body mode states H_R, for which the number of rows will be equal to the number of specified rigid body mode states.

2. From these matrices $H^{\Delta t}$ and $H_R^{\Delta t}$, obtain $H^{2\Delta t}$, $H^{4\Delta t}$, etc., and $H_R^{2\Delta t}$, $H_R^{4\Delta t}$, etc., as described earlier. Set ΔT equal to the largest time step size for which these matrices are generated.

3. First, solve the problem for the time step size ΔT considering only rigid body mode states.

   (a) Choose a number of time steps $n \geq t_{f_{RIGID}}/\Delta T$, where $t_{f_{RIGID}}$ is the minimum time interval in which the desired change in rigid body mode states can be accomplished with a set of p ideal control inputs having the given input bounds. If actuator dynamics are significant, n should be increased accordingly, but it is assumed for simplicity that n is chosen so that it is not possible to achieve the final rigid body mode states with fewer than n time steps.

   (b) Choose an initial guess u_0 appropriate for the control task at hand. For example, a bang-bang profile is likely to be a suitable choice for a rest-to-rest maneuver. With the desired final rigid body mode states in the vector y_R, obtain the error resulting from the initial guess as $e = y_R - H_R u_0$. Solve an auxiliary problem to determine whether a

feasible solution exists with n time steps, by minimizing $J = w$, subject to the equality constraints

$$[\,H_R^{\Delta T} \quad e\,]\left\{\begin{matrix} u \\ w \end{matrix}\right\} = y_R, \tag{3.17}$$

the input bounds, and the inequality $w \geq 0$, where w is an artificial variable. The upper-bounded simplex method[26] is appropriate since the unknowns are subject to both upper and lower bounds. If J cannot be driven to zero, the number of time steps must be increased. If $J = 0$, a control profile achieving the desired final rigid body mode states has been found. This profile will be modified over the course of the algorithm until the final solution is obtained. The norm of the error in unspecified outputs at the final time $n\Delta T$ and at several later time steps is calculated for comparison later in the algorithm.

4. Solve minimum time problems with outputs specified for an increasing number of time steps at the end of the control profile.

   (a) So that outputs can be specified at the final time, set

$$\overline{H} = \begin{bmatrix} H_R^{\Delta T} \\ H^{\Delta T} \end{bmatrix}.$$

   Find a control profile resulting in the desired rigid body mode states and outputs at the final time, if one exists, by computing $e = \overline{y}_f - \overline{H}u$, where $\overline{y}_f$ now contains both the final rigid body mode states and the outputs at the final time, and solving an auxiliary problem as in 3. (b) above. Note that e is nonzero only in entries corresponding to newly applied constraints. Also, in the implementation of the simplex method, after each iteration it is only possible for these new constraints to be violated, since the equation analogous to Eq. (3.17) will always be satisfied, with monotonically decreasing values of w.

   In general, outputs will be specified at the first time step of length ΔT at the end of the control history for which outputs have not yet been specified. Then the matrix $\overline{H}$ will take the form

$$\overline{H} = \begin{bmatrix} H_{R1}^{\Delta T} & \cdots & H_{Rn}^{\Delta T} \\ H_1^{\Delta T} & \cdots & H_n^{\Delta T} \\ H_0^{\Delta T} & \cdots & H_{n-1}^{\Delta T} \\ \vdots & \cdots & \vdots \end{bmatrix},$$

with a new row added each time outputs are specified for an additional time step. Similarly, a new subvector of outputs will be appended to $\overline{y}_f$ each time outputs are specified for another time step.

(b) If $J = w$ for the auxiliary problem cannot be driven to zero, the number of time steps n must be increased by one. If $J = 0$, compute unspecified outputs at time steps at the end of the control profile, and check whether the ratio R is less than a value specified by the user for the current step size. If not, specify outputs for another time step, find a feasible control profile, and check again. If so, decrease the time step size by half.

5. To continue with a time step of half the size, set $\Delta T = \Delta T/2$ and $n = 2n$. The current control profile $\boldsymbol{u}$ is converted for the smaller step size by inserting, after the subvector for each time step, a duplicate copy of that subvector. Converting $\boldsymbol{u}$ for the smaller step size doubles the number of entries in $\boldsymbol{u}$ that are not equal to one of the bounds, so half of these which are closest to bounds are made equal to bounds while the rest are retained as basic variables. The equation $\overline{H}\boldsymbol{u} = \overline{y}_f$ is then solved for the basic variables. If any of these are found to violate a bound a small auxiliary problem, involving only those variables which were not equal to bounds upon changing to a smaller step size, is solved to obtain a basic feasible solution.

When the time step size has been halved, the existence of a control profile satisfying the same set of equality constraints and the input bounds, and having fewer time steps than the new value of n, must be investigated. Frequently the final time can be reduced due to the ability to resolve the control profile more accurately with a smaller time step. The existence of a feasible control profile having $n - 1$ time steps is investigated by determining whether the control inputs for the first time step can be driven to zero in a feasible solution. For each positive (negative) entry $u_{j,1}$ in $\boldsymbol{u}_1$, the lower (upper) bound is reset to zero, and a coefficient c_j is set to (minus) one. Then the objective function $J = \sum_{j=1}^{p} c_j u_{j,1}$ is minimized subject to the equality constraints and the input bounds. If $J = 0$, a control profile with $n - 1$ steps has been found, and the existence of a control profile with one fewer time step is investigated. When $J \neq 0$, a minimal number of time steps has been found for which a feasible control profile with the time step size ΔT exists. At this point, the number of time steps for which

outputs are specified is again increased, starting with the time $t_f + \Delta T$, since outputs have already been specified for t_f, $t_f + 2\Delta T$, $t_f + 4\Delta T$, etc. This continues until the ratio R decreases below the value specified for the current step size. Then the time step size is halved again.

Sampling for the ratio of output error norms R should be done each time with the largest step size ΔT_0 that is used at first, so that even though the step size is halved repeatedly, the length of time over which the system response is monitored in R remains consistent.

6. When the time step size Δt is reached, the minimum time control profile can be approximated with the maximum accuracy permitted by the pulse response data. The number of time steps for which outputs are specified is increased until the ratio R decreases below the value specified for the final result. At this point, the final time should have stopped increasing with the specification of additional outputs, since the desired final state of the system should be obtained very accurately. Since the control inputs are required by the simplex method to be equal to bounds for as many entries in $\boldsymbol{u}$ as possible, the control profile can usually be improved, in terms of the control effort expended and the smoothness of the profile, by minimizing the quadratic objective function $J = \boldsymbol{u}^T\boldsymbol{u}$ subject to the equality constraints $\overline{H}\boldsymbol{u} = \overline{y}_f$ and the input bounds, with the same number of time steps.

The algorithm is demonstrated in the numerical example section of this chapter.

3.4 Effect of Measurement Noise

Noise in the pulse response measurements will result in inaccuracy in the H matrix, and this will lead to error in the predicted outputs at the end of the control task. This section examines the relationship between measurement noise and error in the predicted outputs at the end of the control history.

For a single input system, the predicted outputs at $t_f = n\Delta t$ are given by

$$\hat{y}(n\Delta t) = \hat{H}\boldsymbol{u} = \sum_{i=1}^{n} \hat{h}_i u_i, \tag{3.18}$$

if $\hat{H}$ contains pulse response measurements that are subject to noise. An error vector can be defined

as

$$\boldsymbol{e}_i = \hat{\boldsymbol{h}}_i - \boldsymbol{h}_i, \tag{3.19}$$

where $\boldsymbol{h}_i$ is a measurement vector without noise. The expected outer product between two error vectors is

$$E[\boldsymbol{e}_i \boldsymbol{e}_j^T] = K_e \delta_{ij} \tag{3.20}$$

if the error in measurements is zero-mean and uncorrelated in time, where K_e is the error vector covariance matrix and δ_{ij} is the Kronecker delta. In the limit as Δt approaches zero, the pulse response of the distributed system is proportional to Δt, because the impulse associated with a pulse of unit amplitude and duration Δt is proportional to Δt. If measurement hardware is selected appropriately for the signal levels encountered, the mean square error can be expected to be proportional to the mean square signal in the pulse response measurements. This will make K_e proportional to $(\Delta t)^2$, or $1/n^2$ if $t_f = n\Delta t$ is held constant.

The mean or expected value of $\hat{\boldsymbol{y}}(n\Delta t)$ is given by

$$\boldsymbol{\mu}_y \equiv E[\hat{\boldsymbol{y}}(n\Delta t)] = \sum_{i=1}^{n} E[\hat{\boldsymbol{h}}_i]u_i = H\boldsymbol{u} = \boldsymbol{y}(n\Delta t), \tag{3.21}$$

if $\boldsymbol{e}_i$ is zero-mean. The covariance matrix for $\hat{\boldsymbol{y}}(n\Delta t)$ is

$$\begin{aligned} K_y &\equiv E[\left(\hat{\boldsymbol{y}}(n\Delta t) - \boldsymbol{\mu}_y\right)\left(\hat{\boldsymbol{y}}(n\Delta t) - \boldsymbol{\mu}_y\right)^T] \\ &= E[\sum_{i=1}^{n} \boldsymbol{e}_i u_i \sum_{j=1}^{n} \boldsymbol{e}_j^T u_j] \\ &= \sum_{i=1}^{n}\sum_{j=1}^{n} u_i u_j K_e \delta_{ij} \leq nB^2 K_e, \end{aligned} \tag{3.22}$$

where B is an input bound. Since K_e is proportional to $1/n^2$, K_y is proportional to $1/n$. This result reflects the averaging of error that takes place in the convolution sum in the PRBC method.

It should be pointed out that the effect of error can be reduced by the usual approach of obtaining multiple sets of measurements and averaging the results. For PRBC, as it has been described here, this would require generating H repeatedly and averaging the different versions obtained. It is straightforward to show that when this is done, the error covariance matrix K_e is inversely proportional to the number of samples averaged. It should be mentioned that there is a vast literature on adaptive filtering and identification techniques that would be applicable for obtaining and continually refining H in a practical setting.

A final consideration for this section is that if the pulse response measurements are corrupted by noise, a control history $\boldsymbol{u}$ that drives the system to the desired final state will not satisfy the equations $\hat{\overline{H}}\boldsymbol{u} = \overline{y}_f$, where $\hat{\overline{H}}$ contains noisy data. For this reason, it may be advisable, for example, to replace the equality constraints in the algorithm of the preceding section with pairs of inequality constraints that require the predicted outputs to be within some tolerance of the desired outputs, where this tolerance would be based on measurement noise statistics.

3.5 Numerical Examples

In this section, the results of implementing PRBC on two simple distributed parameter systems are presented. The first system is the second-order system of the last chapter, so the exact solution of the minimum time control problem is known. The second system is a beam in translation, for which the exact solution is not known.

Second-Order System

For this system, the responses to pulses in the control inputs, with zero initial conditions, must be obtained so that PRBC can be implemented. Square pulses are applied, in the form

$$F_i(t) = \begin{cases} 1, & \text{for } 0 < t < \Delta t; \\ 0, & \text{for } t > \Delta t; \end{cases} \qquad i = 1, 2. \tag{3.23}$$

where it can reasonably be assumed that Δt is less than L/c, which is the time required for a wave to travel the length of the system, and one half of the period of the first flexible mode of the system. For determining the response of the system to these pulses, it is convenient to use the traveling wave representation of the last chapter, which is exact. For zero initial conditions, the wave profiles can be taken to be zero over a certain range of their arguments:

$$U_+(\xi) = U_-(\xi) = 0, \qquad 0 < \xi < L. \tag{3.24}$$

For response to a pulse in $F_1(t)$, the right end of the system is free, so its boundary condition becomes

$$s\frac{\partial u(x,t)}{\partial x}\bigg|_{x=L} = 0. \tag{3.25}$$

Inserting the traveling wave representation in this boundary condition results in

$$\frac{s}{c}\frac{\partial}{\partial t}(-U_+(x-ct) + U_-(x+ct))\bigg|_{x=L} = 0. \tag{3.26}$$

Integrating with respect to time gives the result

$$U_-(L+ct) = U_+(L-ct), \qquad t > 0, \tag{3.27}$$

which can be written

$$U_-(\xi) = U_+(2L-\xi), \qquad \xi > L. \tag{3.28}$$

From this and the initial values of the wave profiles, it can be observed that

$$U_-(\xi) = 0, \qquad 0 < \xi < 2L. \tag{3.29}$$

Using a similar approach on the left end boundary condition gives the result

$$\frac{s}{c}\frac{\partial}{\partial t}(U_+(x-ct) - U_-(x+ct))\Big|_{x=0} = F_1(t), \tag{3.30}$$

which yields, upon integration,

$$U_+(-ct) = U_-(ct) + \frac{c}{s}\int_0^t F_1(\tau)\,d\tau, \qquad t > 0. \tag{3.31}$$

Making the change of variable $\xi = -ct$, the wave profile $U_+(\xi)$ is found for all relevant values of its argument to be

$$U_+(\xi) = \begin{cases} 0, & \text{for } L > \xi > 0; \\ -\dfrac{\xi}{s}, & \text{for } 0 > \xi > -c\Delta t; \\ \dfrac{c\Delta t}{s}, & \text{for } c\Delta t > \xi > -2L; \\ U_+(2L+\xi) + \dfrac{c\Delta t}{s}, & \text{for } \xi < -2L; \end{cases} \tag{3.32}$$

and $U_-(\xi)$ is given in terms of $U_+(\xi)$ in Eq. (3.28), so that the wave profiles appearing in the traveling wave representation of the system displacement are now known. The system velocity is given in terms of the wave profiles as

$$\dot{u}(x,t) = -cU_+^*(x-ct) + cU_-^*(x+ct), \tag{3.33}$$

where asterisks denote differentiation of wave profiles with respect to their arguments. Pulse response measurements that would be obtained by displacement or velocity sensors at arbitrary locations are now available. The system response to a pulse in $F_2(t)$ can be obtained in a similar manner.

For this system, the response in the rigid body mode is equivalent to the motion of the mass center, which is governed by the equation

$$mL\ddot{u}_G = F_1(t) + F_2(t), \qquad t > 0, \tag{3.34}$$

where u_G is the displacement of the mass center. The displacement and velocity of the mass center in the response of the system to a pulse in either control input are therefore given by

$$u_G(t) = \frac{(2t - \Delta t)\Delta t}{2mL} \quad \text{for } t \geq \Delta t \tag{3.35}$$

and

$$\dot{u}_G(t) = \frac{\Delta t}{mL} \quad \text{for } t \geq \Delta t. \tag{3.36}$$

Because the control profiles for the exact solution of the minimum time control problem are piecewise constant, they can be obtained by the PRBC approach if the intervals in the control history over which the control inputs are constant are divisible by the time step Δt. For this reason, the results of this example will be presented by simply telling how many time steps at the end of the control history must have outputs specified in order for the exact solution to be obtained. The rigid body mode states at t_f are specified in all cases, and the other outputs that are specified are simply the displacement and velocity at locations $x = 0^+$ and $x = L^-$, which are infinitesimal distances from the ends of the system, at t_f, $t_f + \Delta t$, $t_f + 2\Delta t$, etc. The time step Δt, which is the duration of the pulses in control inputs and the sampling interval for measurements, is taken to be $0.1L/c$.

Table 3.1 shows the number of time steps for which the displacement and velocity at the ends of the system must be specified to obtain the exact solution of the minimum time problem. The minimum value of t_f is varied by changing the input bounds according to the result from the last chapter

$$B = \frac{u_0\sqrt{sm}}{2n(t_f - nL/c)}, \tag{3.37}$$

where $nL/c \leq t_f \leq (n+1)L/c$. Values of zero in the table indicate that specification of only the rigid body mode states at the end of the control task was sufficient to obtain the exact solution of the minimum time problem using PRBC. This is the case whenever the exact solution happens to be bang-bang, which is true when t_f is equal to an even multiple of L/c. As the number of time steps for which outputs are specified is increased for a given value of B, the residual energy at the

Table 3.1: Number of time steps for which outputs must be specified to obtain exact solution

$\frac{t_f c}{L}$	No. of Δt's	$\frac{t_f c}{L}$	No. of Δt's	$\frac{t_f c}{L}$	No. of Δt's	$\frac{t_f c}{L}$	No. of Δt's	$\frac{t_f c}{L}$	No. of Δt's	$\frac{t_f c}{L}$	No. of Δt's
1.1	2	2.1	0	3.1	2	4.1	1	5.1	2	6.1	1
1.2	8	2.2	1	3.2	7	4.2	1	5.2	7	6.2	2
1.3	6	2.3	6	3.3	7	4.3	8	5.3	6	6.3	8
1.4	5	2.4	6	3.4	5	4.4	8	5.4	6	6.4	6
1.5	4	2.5	6	3.5	5	4.5	6	5.5	4	6.5	6
1.6	4	2.6	4	3.6	3	4.6	4	5.6	3	6.6	6
1.7	1	2.7	3	3.7	3	4.7	3	5.7	2	6.7	3
1.8	1	2.8	2	3.8	2	4.8	2	5.8	1	6.8	2
1.9	0	2.9	2	3.9	1	4.9	2	5.9	1	6.9	2
2.0	0	3.0	1	4.0	0	5.0	1	6.0	0	7.0	1

end of the control task, obtained through simulation, typically decreases slowly until outputs are specified for the number of time steps given in Table 3.1, at which point it suddenly decreases by at least several orders of magnitude. The final control history that is obtained agrees with the exact one extremely well, although typically not to full machine precision. For all of the cases reported in the table, the residual energy at t_f is less than 0.01% of the maximum amount of energy in the system over the control history. Of course, once enough measurements are specified to obtain the exact solution, any additional specified measurements that are consistent with the desired final state of the system will also be satisfied.

These results demonstrate that PRBC can obtain the exact solution of a minimum time control problem, if that exact solution can be represented in terms of the type of pulses used to generate pulse response measurements. Of course, it is unusual to be able to represent the exact solution exactly in terms of these pulses, so the best that can be hoped for is that PRBC will be able to produce the most accurate solution available with a given time step size, in terms of achieving a minimal final time with minimal error in the state of the system at the end of the control history, which can be measured in terms of residual energy. The next example will address how well PRBC can achieve this.

Fourth-Order System

In this example, PRBC is used to solve the minimum time control problem for transverse rest-to-rest translation of a slender beam using bounded force inputs at its two ends. Although PRBC,

as presented in this chapter, is intended for any structure that exhibits linear behavior, a uniform beam is used for this example because the infinity of modes are known. This means that modal truncation effects can be virtually eliminated in simulation.

The motion of the beam is governed by the equation[22]

$$EI\frac{\partial^4 v(x,t)}{\partial x^4} + m\frac{\partial^2 v(x,t)}{\partial t^2} = 0, \quad -L/2 < x < L/2, \tag{3.38}$$

in which $v(x,t)$ is the transverse displacement, EI is the flexural rigidity, m is the mass per unit length, and the length of the beam is L. For this problem it is convenient to locate the origin at the center of the beam. Shear deformation and rotatory inertia are neglected. There is no moment applied at the ends of the beam, and the beam is controlled by transverse force inputs at its ends, so the boundary conditions are

$$EI\frac{\partial^2 v(x,t)}{\partial x^2}\bigg|_{x=\pm L/2} = 0, \quad EI\frac{\partial^3 v(x,t)}{\partial x^3}\bigg|_{x=-L/2} = F_1(t), \quad EI\frac{\partial^3 v(x,t)}{\partial x^3}\bigg|_{x=L/2} = -F_2(t). \tag{3.39}$$

The control task consists of translating the beam a distance v_0 as quickly as possible, with no residual vibration at the end of the control task. Hence the initial and final conditions are

$$v(x,0) = \dot{v}(x,0) = \dot{v}(x,t_f) = 0, \quad v(x,t_f) = v_0, \qquad -L/2 < x < L/2. \tag{3.40}$$

For this example, it is assumed that there are displacement and velocity sensors at the ends of the beam. Because of the symmetry of the system and the control task, it is sufficient to consider outputs from only one end of the beam. For the same reason, the force inputs are taken to be equal, i.e.,

$$F(t) \equiv F_1(t) = F_2(t). \tag{3.41}$$

The force inputs are taken to be nonideal, with their dynamic behavior governed by the first-order ordinary differential equation

$$\dot{F}(t) + aF(t) = u(t) \tag{3.42}$$

in which $u(t)$ is the force command, and $1/a$ is the time constant for the actuators' response. A piecewise constant approximation of the minimum time profile in $u(t)$ is to be obtained using PRBC, with $u(t)$ subject to the bounds $|u(t)| \leq B$.

A modal simulation is used to generate pulse response data for the system, with modal truncation effects reduced to a negligible level by including as many as one hundred symmetric modes

in the model. The natural modes of vibration form an orthonormal basis for the response of the system, so the displacement $v(x,t)$ can be represented in terms of the eigenfunctions $\phi_r(x)$ and the modal displacements $\eta_r(t)$ as $v(x,t) = \sum_{r=0}^{\infty} \phi_r(x)\eta_r(t)$. Because of symmetry, the antisymmetric modes need not be included in the analysis. The mass normalized symmetric rigid body and flexible modes are

$$\phi_0(x) = \frac{1}{\sqrt{mL}}, \quad \phi_r(x) = \sqrt{\frac{2}{mL}} \left[\frac{\cosh\frac{\beta_r L}{2}\cos\beta_r x + \cos\frac{\beta_r L}{2}\cosh\beta_r x}{\left[\cosh^2\frac{\beta_r L}{2} + \cos^2\frac{\beta_r L}{2}\right]^{1/2}} \right], \; r = 1,2,\ldots \qquad (3.43)$$

where the β_r's are from those roots of the characteristic equation $\cos\beta_r L \cosh\beta_r L = 1$ that are associated with the symmetric eigenfunctions. The pulse response matrix H is generated in simulation by exploiting the orthogonality properties of the modes to obtain modal equations of motion, solving for modal responses to actuator forces resulting from a square pulse in $u(t)$, and adding up the modal contributions to the outputs.

The statement of the minimum time problem is complete when the bound B on the control inputs is specified. For this example, this bound is chosen based on the time $(t_f)_{RIGID}$ that would be required to carry out the desired translation on a rigid bar having the same mass, with ideal inputs. The relationship between $(t_f)_{RIGID}$ and the ratio B/v_0 is expressed in the equation

$$\frac{B}{v_0} = \frac{2mL}{(t_f)^2_{RIGID}}. \qquad (3.44)$$

If the bang-bang minimum time solution for the rigid system is applied to the flexible system, the residual energy at the end of the control history will depend upon how $(t_f)_{RIGID}$ compares to the period of the first flexible mode T. For this example, the ratio B/v_0 is chosen so that $(t_f)_{RIGID}$ is equal to $T/4$, which indicates that a bang-bang control profile would result in a very large amount of residual vibration. Recall that the minimum time for control of a uniform second-order one-dimensional system with *unbounded* inputs at its two ends is equal to one half of the period of the first flexible mode. The minimum time problem to be solved, then, is for extremely rapid control of the beam.

If the final rigid body displacement is specified in $\overline{y}_f$, it will be obtained exactly, and the accuracy of the final state of the system can be measured in terms of the residual energy at the

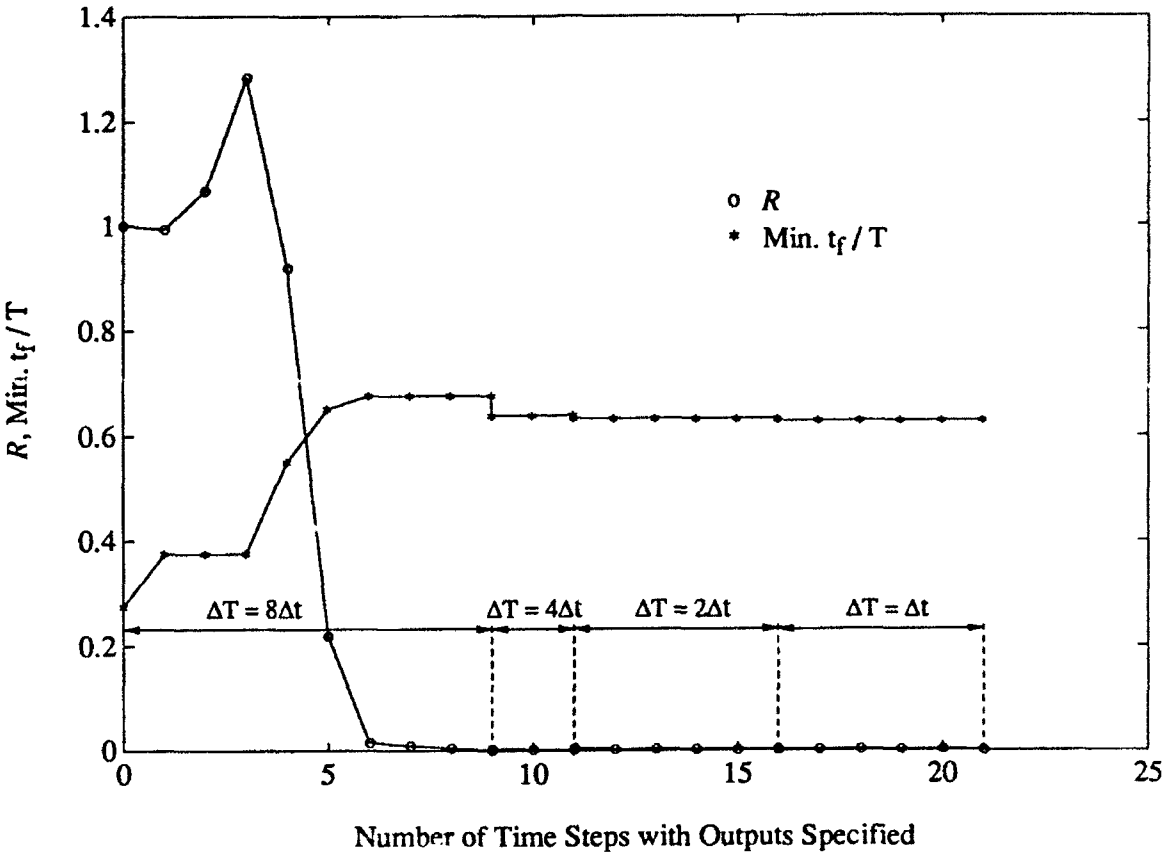

Figure 3.1: Ratio of output error norms R and final time t_f, as outputs are specified for increasing numbers of time steps

end of the control task, which is given by the modal sum

$$E_{res} = \frac{1}{2}\sum_{r=0}^{\infty}(\dot{\eta}_r^2(t_f) + \lambda_r \eta_r^2(t_f)), \tag{3.45}$$

where $\lambda_r = \omega_r^2$ is an eigenvalue and the square of a natural frequency. In the results presented here, the residual energy is scaled by the maximum energy in the corresponding rigid system in its minimum time control, which occurs at mid-"maneuver" and is given by

$$E_{m-m} = \frac{2mLv_0^2}{(t_f)_{RIGID}^2}. \tag{3.46}$$

Residual energy is not ordinarily calculated in PRBC because of the absence of a model, but it is calculated for this example and presented as a measure of success in eliminating residual vibration.

For this example, the time constant for the force inputs is set equal to one percent of the first period T. Pulse response data is generated by modal simulation for a time step size Δt equal to one eightieth of $(t_f)_{RIGID}$, and then H matrices for pulses of width $2\Delta t$, $4\Delta t$, and $8\Delta t$ are obtained

as described earlier in the section on the algorithm. The vector $\overline{y}_f$ initially contains only the displacement and velocity in the translational rigid body mode, and then contains the transverse displacement and velocity at one end of the beam at t_f and later time steps. Figure 3.1 shows how the ratio of output error norms R decreases, and how t_f increases as the number of time steps for which outputs are specified increases. The number of time steps for which outputs are specified is increased until $R \leq 0.002$, at which point the time step size is decreased from $8\Delta t$ to $4\Delta t$. For this example, the time step size is halved whenever R is reduced to 0.002 with the current step size, and the algorithm is terminated when this value is reached with the step size Δt. In all cases, R is obtained using outputs from five time steps spaced $8\Delta t$ apart.

The time required for control, t_f, increases from its initial value, which is slightly greater than $(t_f)_{RIGID}$, to a value which is somewhat higher than the final value obtained, while the time step size is $8\Delta t$. Each time the time step size is halved, there is a reduction in t_f due to the improved resolution of the control profile. The final value of t_f is equal to $0.628125T$, which is about two and one-half times $(t_f)_{RIGID}$, so there are about two hundred time steps in the final control profile, and about two hundred unknowns when the time step size Δt is used.

Figure 3.2 shows the residual energy in the system at the end of the control history as a function of the number of time steps for which outputs are specified. The minimum time control for achieving the desired final rigid body mode states results in residual energy more than four times as great as the kinetic energy in the corresponding rigid system at mid-maneuver. Initially, as outputs are specified for time steps at the end of the control task, the residual energy increases. This is because the number of specified outputs is not yet large enough to ensure that the control profile drives the system close to the desired final state. This is evident from Fig. 3.1, in the values of R and t_f. However, once outputs have been specified for six time steps, the residual energy and R drop close to zero, and t_f levels off at the largest value encountered in the calculations. Once outputs have been specified for eight time steps, the residual energy is driven to less than 0.1% of the mid-maneuver energy, and stays at approximately that level for the rest of the calculations. This means that the main benefit resulting from continuing the computation with smaller time steps is a reduction in t_f, since the desired final state is already obtained very accurately in this early approximation of the minimum time control profile.

It is particularly interesting to note that, even though a very large number of modes is used

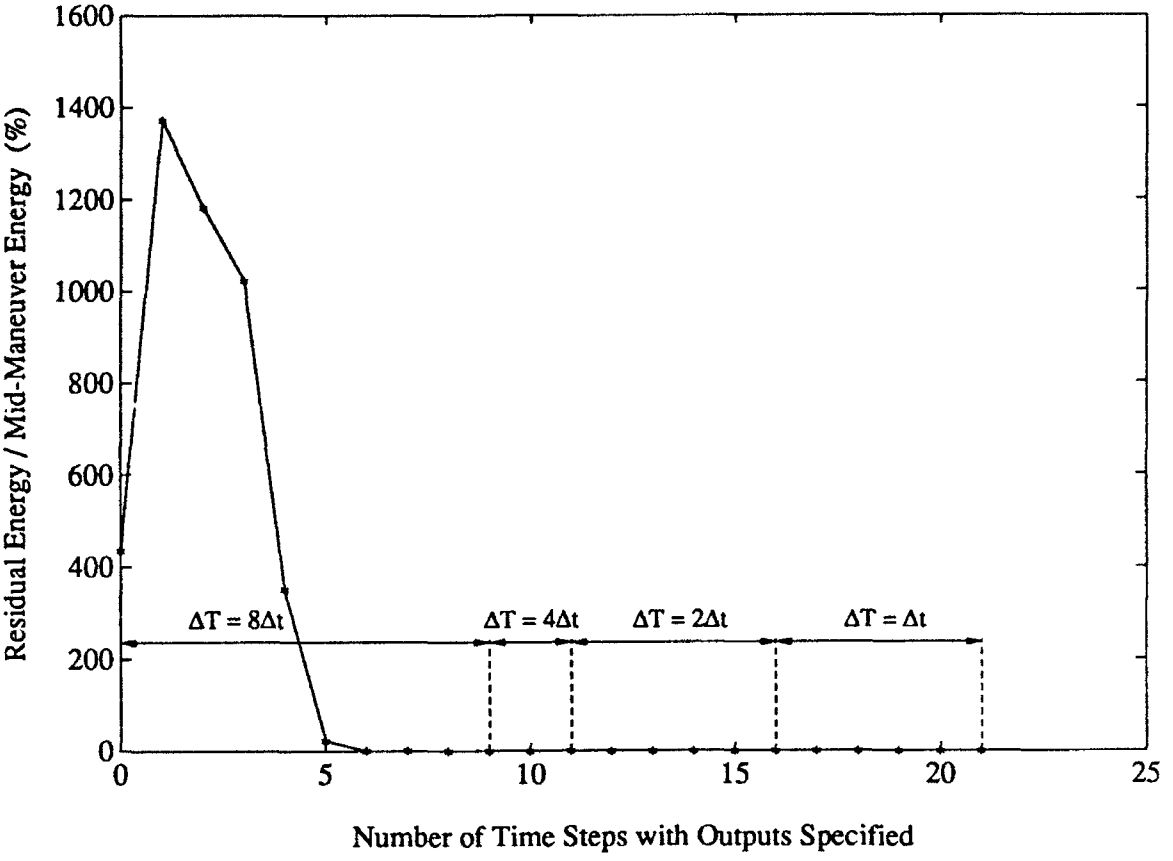

Figure 3.2: Residual energy as outputs are specified for increasing numbers of time steps

to model this system, specifying outputs for only eight time steps at the end of the control profile effectively specifies the final state very precisely, at least for this example system.

Figure 3.3 shows the final profiles obtained for the command $u(t)$ and the actuator force $F(t)$. It is obvious that these profiles are not small perturbations of the bang-bang minimum time control for the corresponding rigid system. The PRBC approach is therefore not subject to the inherent limitations of a perturbation approach on the rapidity of the control relative to the flexibility of the system. The profiles are not smooth, but the residual energy is negligible. This is consistent with the exact minimum time solution for the second-order system, and points out an important difference between PRBC and the more conventional modal approach. When the response in a finite number of modes is considered, it is often helpful to smooth the control profile to reduce unwanted excitation of higher modes. However, since there is no modal truncation in the representation of the system dynamics in PRBC, this artificial smoothing is unnecessary. A final observation related to the control profile is that if there is a finite time constant characterizing the actuator dynamics,

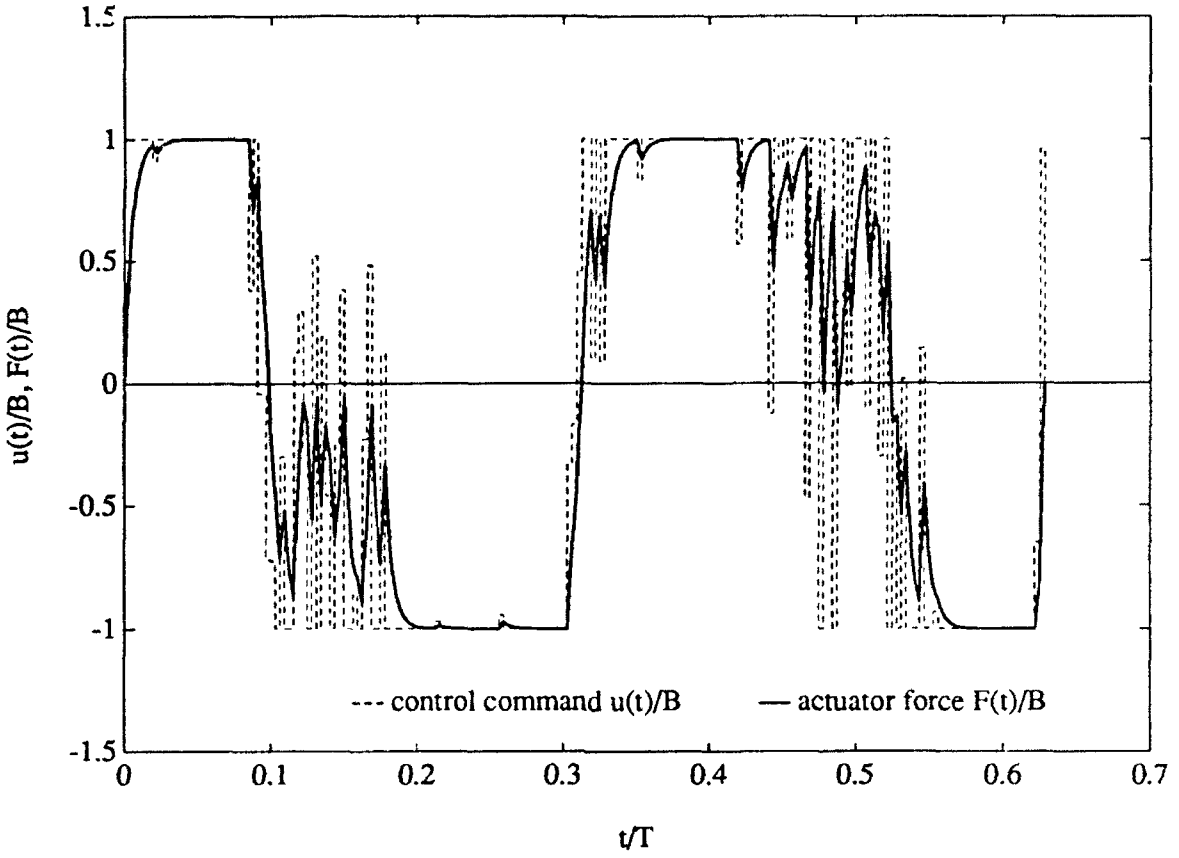

Figure 3.3: Control command and actuator force profiles in minimum time control

there is little to be gained by using a time step size that is much smaller than the time constant.

Figure 3.4 shows plots of the deflected shape of the beam at intervals of $0.375(t_f)_{RIGID}$. For this problem, in which the distance translated is small relative to the input force available, for minimum time control the actuators must initially move the ends of the beam well past their final position and excite quite a bit of flexible response. However, this flexible response is eliminated by the time the control task is completed.

Table 3.2 shows how much computation time was spent approximating the minimum time control profile with each time step size ΔT, on a Sun SPARCstation 2. The number of unknowns in the control history given in the table is for the final result obtained with each time step size. From the table it is evident that in the computation done with the largest time step size, the algorithm uses only a small fraction of the total computation time to obtain a reasonably accurate approximation of t_f and the minimum time control profiles for the control task, as is evident from Figs. 3.1 and 3.2. Once these results have been obtained, the amount of computation that must

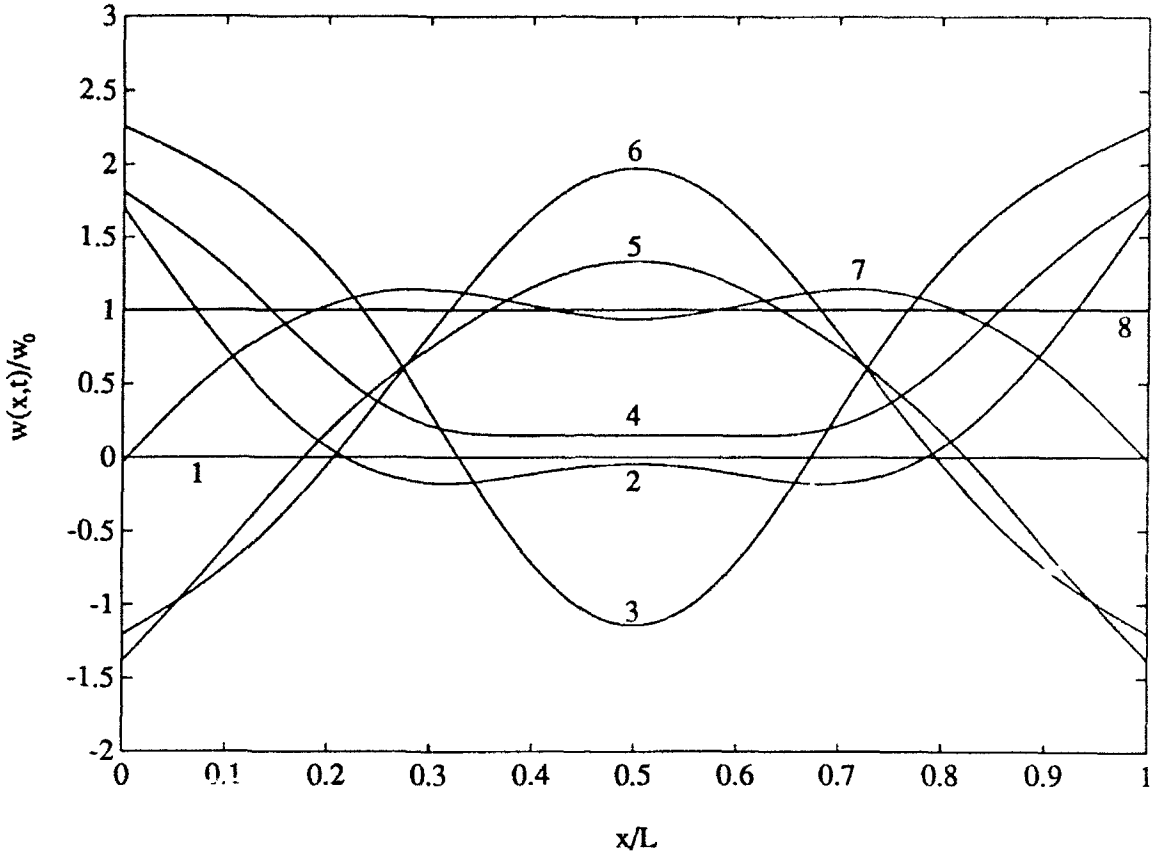

Figure 3.4: Deflected shape of the beam at various times during control history

be done with smaller time steps and more unknowns is quite modest. If the existence of feasible control profiles with final times ranging from $(t_f)_{RIGID}$ to the minimum t_f for the flexible problem were to be investigated with the time step size Δt, much more computation would be required. The total computation time is less than twenty-five seconds on the Sun SPARCstation 2, which is not a particularly fast machine for floating-point computation compared to other workstations that are currently available.

A minimum norm control profile with the same final time t_f can be obtained if desired. For this problem, solving the associated quadratic programming problem requires about seventy-five seconds of additional computation time, and results in a control profile that does not differ substantially from the one shown in Fig. 3.3.

The quality of the results obtained using the PRBC algorithm is evident from the fact that it is evident that no control history with the time step size Δt that satisfies the equality constraints on $\overline{y}_f$ exists with fewer time steps. Also, the time step is small enough that the control profile is

Table 3.2: CPU time for each time step size

Time step size ΔT	Number of steps in control history	CPU time* (seconds)
$8\Delta t$	27	3.15
$4\Delta t$	51	1.84
$2\Delta t$	101	5.05
Δt	201	14.49
Total CPU time		24.53

*CPU time for Sun SPARCstation 2.

divided into over two hundred time steps, and Δt is less than one third as long as the time constant for the control inputs. Finally, the residual energy in the system is extremely small, and the desired final rigid body displacement is obtained exactly, so the desired final state is indeed obtained quite accurately.

It is true that, although there is no modal truncation or explicit truncation of a system model in the PRBC approach, there is truncation in the sense that the pulse response matrix is of finite order, and a finite number of outputs are specified at the final time and afterward. However, it is evident from the numerical results presented here that convergence in residual energy to an extremely low level occurs quite quickly as outputs for additional time steps are specified, so this truncation is not likely to be of much practical significance.

The results presented for this example are obtained by PRBC without an explicit model of the system, since the only information that is used in finding the control profile is the pulse response data and the total mass of the system. In spite of this, a very accurate approximate solution of the minimum time problem is obtained, with far less computation than would be required by any other method which takes many modes into consideration. The solution obtained is for extremely rapid control, with a considerable amount of excitation and subsequent elimination of flexible response. Although the PRBC method is intended for systems for which an accurate model is not available, the example presented here demonstrates that it also provides an economical means for studying minimum time control of distributed systems whose properties are known accurately.

3.6 Conclusions

In this chapter, a powerful new method for solving minimum time control problems for flexible structures is presented. The pulse response based control method does not require an explicit model of the dynamic system to be controlled. Instead, it uses readily obtained measurements of response to pulses in control inputs to obtain minimum time control profiles. Since all modes contribute to the pulse response measurements, there is no modal truncation in the representation of the system dynamics. Actuator dynamics are automatically taken into account as part of the system dynamics in this approach, if the test pulses are applied in commands to the control inputs rather than in actual control forces or moments. The precision with which the final state of the system can be specified using pulse response based control is only limited by the observability of the system with the given set of outputs. The effect of measurement noise on the accuracy of the results obtained is shown to decrease as the pulse width decreases, due to the averaging of error that takes place in the convolution sum used in pulse response based control. The control profile obtained using pulse response based control is not bang-bang, which is appropriate since the exact minimum time control profile for the distributed parameter system is not ordinarily bang-bang. A special algorithm is developed for implementing pulse response based control, in which pulse response data for several larger pulse widths, or time step sizes, is synthesized from the original pulse response measurement data. Then approximations of the minimum time solution are obtained first with the largest time step size, and then with decreasing time step sizes until the pulse width used to obtain the original pulse response data is reached. Two numerical examples demonstrate the effectiveness of the pulse response based control method and the efficiency of the algorithm. In the first, it is found that the exact solution of the minimum time problem of the last chapter can be easily obtained using pulse response based control, with outputs specified for a small number of time steps at the end of the control task. For the second example, the algorithm uses a modest amount of computation to obtain an approximation of the minimum time control profile with a very small time step size, and establishes that the number of time steps is minimal. The desired final state of the system is obtained accurately, so it can be concluded that an excellent approximation of the minimum time solution is economically obtained.

Chapter 4

Pulse Response Based Maneuver of Flexible Spacecraft

4.1 Introduction

In the rapid maneuver of flexible spacecraft, nonlinear effects associated with rotational stiffening can become significant. The first chapter reviews a number of approaches that have been taken to address these problems. In general, the objective of these approaches is to obtain a good approximation of minimum time maneuver profiles without the computational cost associated with solving the nonlinear two point boundary value problem arising from a straightforward application of optimal control theory. Most of these approaches rely on an explicit modal or assumed mode model of the structure for the design of the control.

In this chapter the pulse response based control method developed in the last chapter is extended so that the nonlinear behavior associated with large angle rotation in maneuver problems can be handled. This requires explicit modeling of those flexible modes in which the deviation from the linear behavior represented in pulse response measurements due to nonlinear behavior is significant, which is ordinarily a very small number of modes. There is still no modal truncation or explicit modeling required in the representation of linear behavior, so the method has substantial advantages over previous methods. The amount of computation required for nonlinear problems is close to the amount required for linear problems. In the second section of this chapter, the extension of the pulse response based control method to nonlinear problems is presented. The third section gives a numerical example. The final section contains a brief summary.

4.2 Pulse Response Based Control for Maneuver Problems

The pulse response based control method developed in the last chapter can be used on distributed parameter systems whose behavior is linear. However, for rapid large angle maneuver problems, nonlinear behavior arising from rotation must be taken into account. Since the pulse response measurements essentially represent a linearization about the state of the system when the pulses are applied, nonlinear behavior will result in a deviation from this linearization. The basic approach for dealing with the nonlinearity is to use the pulse response measurements to obtain an initial approximation of the minimum time control profile and the minimum time trajectory for the system, and then to correct the pulse response measurements so that they represent a linearization about the trajectory, at least in those modes that exhibit significant nonlinear behavior. Then the minimum time problem can be solved again with the corrected pulse response measurements. If the new minimum time trajectory differs significantly from the one obtained based on the original pulse response measurements, the measurements can be corrected again so a more accurate control profile can be found. In this section, the procedure for correcting the pulse response measurements so that they represent a linearization about a given trajectory is presented.

For a deformable body which can undergo large rigid body displacements and small elastic deformations, the instantaneous position vector of any point on the body is given by

$$\boldsymbol{R} = \boldsymbol{R}_O + \boldsymbol{r} + \boldsymbol{d}, \tag{4.1}$$

where $\boldsymbol{R}_O$ locates the origin of a reference frame and is expressed in terms of an inertial frame, $\boldsymbol{r}$ is the position vector from this origin to the point in the undeformed position, and $\boldsymbol{d}$ is the elastic displacement. If the vectors $\boldsymbol{r}$ and $\boldsymbol{d}$ are expressed in terms of a frame that rotates with angular velocity $\boldsymbol{\omega}$, the kinetic energy of the system is given by

$$\begin{aligned} T \;=\; & \frac{1}{2}M\dot{\boldsymbol{R}}_O \cdot \dot{\boldsymbol{R}}_O + \frac{1}{2}\int_M \dot{\boldsymbol{d}} \cdot \dot{\boldsymbol{d}}\, dm + \frac{1}{2}\int_M [\boldsymbol{\omega} \times (\boldsymbol{r}+\boldsymbol{d})] \cdot [\boldsymbol{\omega} \times (\boldsymbol{r}+\boldsymbol{d})]\, dm + \\ & \dot{\boldsymbol{R}}_O \cdot \boldsymbol{\omega} \times \int_M (\boldsymbol{r}+\boldsymbol{d})\, dm + \dot{\boldsymbol{R}}_O \cdot \int_M \dot{\boldsymbol{d}}\, dm + \boldsymbol{\omega} \cdot \int_M (\boldsymbol{r}+\boldsymbol{d}) \times \dot{\boldsymbol{d}}\, dm, \end{aligned} \tag{4.2}$$

where M is the total mass of the structure. It is advantageous to use a floating reference frame for the flexible structure to simplify the equations of motion. Using the Tisserand frame,[27] which is subject to the constraints

$$\int_M (\boldsymbol{r}+\boldsymbol{d})\, dm = 0, \qquad \int_M (\boldsymbol{r}+\boldsymbol{d}) \times \dot{\boldsymbol{d}}\, dm = 0, \tag{4.3}$$

the expression for the kinetic energy becomes, after some manipulation,

$$T = \frac{1}{2}M\dot{\boldsymbol{R}}_G \cdot \dot{\boldsymbol{R}}_G + \frac{1}{2}\boldsymbol{\omega}\cdot\boldsymbol{\omega}\int_M (\boldsymbol{r}+\boldsymbol{d})\cdot(\boldsymbol{r}+\boldsymbol{d})\,dm - \frac{1}{2}\int_M [\boldsymbol{\omega}\cdot(\boldsymbol{r}+\boldsymbol{d})]^2\,dm + \frac{1}{2}\int_M \dot{\boldsymbol{d}}\cdot\dot{\boldsymbol{d}}\,dm + \boldsymbol{\omega}\cdot\int_M \boldsymbol{d}\times\dot{\boldsymbol{d}}\,dm. \tag{4.4}$$

The origin of the reference frame is now located at the instantaneous center of mass of the structure, which has $\boldsymbol{R}_G$ as its position vector.

In this paper, PRBC is applied to an example problem in which a uniform Bernoulli-Euler beam is to be rotated through a large angle in minimum time. For this beam, the transverse elastic displacement is represented as $v(x,t)$, and the vectors $\boldsymbol{r}$, $\boldsymbol{\omega}$ and $\boldsymbol{d}$ are written in terms of unit vectors $\boldsymbol{i}$, $\boldsymbol{j}$ and $\boldsymbol{k}$ as $\boldsymbol{r} = x\boldsymbol{i}$, $\boldsymbol{\omega} = \dot{\theta}\boldsymbol{k}$ and

$$\boldsymbol{d}(x,t) = v(x,t)\boldsymbol{j} - \frac{1}{2}\int_0^x v'(\xi,t)^2\,d\xi\,\boldsymbol{i}, \tag{4.5}$$

where only up to quadratic terms in $v(x,t)$ and its derivatives are retained. The kinetic and potential energies for the system become

$$T = \frac{1}{2}mL\dot{\boldsymbol{R}}_G\cdot\dot{\boldsymbol{R}}_G + \frac{1}{2}\int_{-L/2}^{L/2} m\left[(x\dot{\theta})^2 + (v\dot{\theta})^2 + \dot{v}^2 - \left(\frac{(L/2)^2 - x^2}{2}\right)\dot{\theta}^2 v'^2\right]dx$$

and

$$V = \frac{1}{2}\int_{-L/2}^{L/2} EIv''^2\,dx, \tag{4.6}$$

where m is the mass per unit length, EI is the flexural rigidity, and L is the length of the beam. The beam is controlled by transverse force inputs at its ends, so the non-conservative virtual work, linearized in $v(x,t)$ and its derivatives, is

$$\delta W_{nc} = (F_1+F_2)\boldsymbol{j}\cdot\delta\boldsymbol{R}_G + F_1\delta v(L/2,t) + F_2\delta v(-L/2,t) + (F_1 - F_2)\frac{L}{2}\delta\theta. \tag{4.7}$$

Applying the extended Hamilton's principle results in ordinary differential equations for translational and rotational motion and a partial differential equation governing the flexible response. For a rotational maneuver the translational equations of motion can be ignored and the control inputs are related by

$$F_1(t) = -F_2(t) \equiv u(t). \tag{4.8}$$

Due to the choice of the Tisserand frame the equation governing the rotation angle θ is uncoupled from the flexible motion and is given by

$$\frac{mL^3}{12}\ddot{\theta} = Lu. \tag{4.9}$$

Once the minimum time control problem associated with a given H matrix has been solved for a control profile $u(t)$, this equation can be integrated to obtain $\dot{\theta}(t)$, which appears in the equation governing the flexible response and must be used to correct the pulse response measurements. The flexible response is governed by the partial differential equation

$$m\ddot{v} - \frac{m\dot{\theta}^2}{2}\left[(\frac{L^2}{4} - x^2)v'\right]' + EIv'''' - m\dot{\theta}^2 v = 0 \tag{4.10}$$

with boundary conditions

$$EIv''\Big|_{x=\pm L/2} = 0, \quad EIv'''\Big|_{x=\pm L/2} = -u(t). \tag{4.11}$$

The terms involving $\dot{\theta}^2$ in Eq. (4.10) represent the nonlinear effects. The control inputs are subject to the bounds $|u(t)| \leq B$ and the control task is to carry out a rotational maneuver in minimum time, with no residual energy at the end of the task. Hence the initial and final conditions become

$$\theta(0) = \dot{\theta}(0) = \dot{\theta}(t_f) = 0, \quad \theta(t_f) = \theta_0, \tag{4.12}$$

and

$$v(x,0) = \dot{v}(x,0) = v(x,t_f) = \dot{v}(x,t_f) = 0, \quad -L/2 < x < L/2. \tag{4.13}$$

The modes of a free-free uniform beam can be used to discretize the partial differential equation governing the flexible motion. The symmetric modes need not be considered due to the anti-symmetric nature of the problem. The mass-normalized anti-symmetric flexible modes are given by

$$\phi_r(x) = \sqrt{\frac{2}{mL}}\left[\frac{\sinh\frac{\beta_r L}{2}\sin\beta_r x + \sin\frac{\beta_r L}{2}\sinh\beta_r x}{\left[\sinh^2\frac{\beta_r L}{2} - \sin^2\frac{\beta_r L}{2}\right]^{1/2}}\right], \quad r = 1,2,\ldots \tag{4.14}$$

where the β_r's are roots of the characteristic equation $\cos\beta_r L\cosh\beta_r L = 1$ associated with the anti-symmetric modes. The displacement $v(x,t)$ can now be written as

$$v(x,t) = \sum_{r=1}^{\infty}\phi_r(x)\eta_r(t). \tag{4.15}$$

Note that the choice of the Tisserand reference frame makes the flexible displacement $v(x,t)$ orthogonal to rigid body motion due to Eqs. (4.3).

For nonlinear systems the matrix H contains measurements of the system response to pulse inputs and represents the response linearized about the state of the system when the pulses are

applied. In order for H to represent response linearized about a maneuver trajectory, it must be modified to account for nonlinear effects. This modification can be approximated by considering the nonlinear response of a finite number of modes. Modal equations of motion are obtained by inserting the representation of Eq. (4.15) in the partial differential equation of motion and exploiting the orthogonality properties of the modes. The modal equations of motion are given by

$$\ddot{\eta}_r + \omega_r^2 \eta_r - \dot{\theta}^2 \eta_r + \dot{\theta}^2 \sum_{s=1}^{p} k_{rs} \eta_s = 2u\phi_r(L/2), \quad r = 1, \ldots, p, \tag{4.16}$$

where p is the number of modes used to model the nonlinear effects, and the geometric stiffness coefficients k_{rs} are given by

$$k_{rs} = \frac{1}{2} \int_{-L/2}^{L/2} m(\frac{L^2}{4} - x^2) \phi_r' \phi_s' \, dx. \tag{4.17}$$

Using the partial state vector $\boldsymbol{x} = [\eta_1 \ \ldots \ \eta_p \ \dot{\eta}_1 \ \ldots \ \dot{\eta}_p]^T$, which does not include rigid body mode states because the linear equation of motion for the rigid body mode remains valid, state equations can be written as

$$\dot{\boldsymbol{x}} = (A_1 + \dot{\theta}^2 A_2)\boldsymbol{x} + Bu \tag{4.18}$$

in which

$$A_1 \equiv \begin{bmatrix} 0 & I \\ -\mathrm{diag}(\omega_r^2) & 0 \end{bmatrix}, \ A_2 \equiv \begin{bmatrix} 0 & 0 \\ I - K & 0 \end{bmatrix}, \tag{4.19}$$

where K contains the geometric stiffness coefficients k_{rs}, and

$$B \equiv [\mathbf{0}^T \quad 2\phi_1(L/2) \quad \cdots \quad 2\phi_p(L/2)]^T. \tag{4.20}$$

If the control input is piecewise constant, the solution of Eq. (4.18) is given by

$$\begin{aligned} \boldsymbol{x}(i\Delta t) &= \Phi\left(i\Delta t, (i-1)\Delta t\right) \boldsymbol{x}\left((i-1)\Delta t\right) + \Gamma\left(i\Delta t, (i-1)\Delta t\right) u_i \\ &= \Phi_i \boldsymbol{x}_{i-1} + \Gamma_i u_i, \end{aligned} \tag{4.21}$$

where the state transition matrix Φ and the input matrix Γ have the usual definitions. From the state equations, it is evident that Φ and Γ depend on the angular velocity $\dot{\theta}$, which varies slowly so that these matrices can be approximated by taking $\dot{\theta}$ to be equal to $\dot{\theta}((i-1)\Delta t)$ over the ith time step. In fact, it is convenient to parametrize them in terms of $\dot{\theta}$ so that

$$\Phi_i \approx \Phi\left(\dot{\theta}((i-1)\Delta t)\right), \quad \Gamma_i \approx \Gamma\left(\dot{\theta}((i-1)\Delta t)\right). \tag{4.22}$$

Denoting the contribution to the output vector $\boldsymbol{y}$ from the first p anti-symmetric flexible modes by $\boldsymbol{y}_p = C\boldsymbol{x}$, the linear relationship between the the last time step's control input u_n and $y_p(n\Delta t)$ is obtained using

$$\boldsymbol{x}_n = \Phi_n \boldsymbol{x}_{n-1} + \Gamma_n u_n, \tag{4.23}$$

so that

$$\boldsymbol{y}_p(n\Delta t) = C(\Phi_n \boldsymbol{x}_{n-1} + \Gamma_n u_n). \tag{4.24}$$

A vector $\boldsymbol{h}_n^{NL}$ which represents a linearization about the trajectory in the lowest p modes, and which will be multiplied by u_n in the convolution sum, is available from

$$\boldsymbol{h}_n^{NL} = \boldsymbol{h}_n^{L} + C(\Gamma_n - \Gamma^L), \tag{4.25}$$

where $\boldsymbol{h}_n^L$ is from the original pulse response measurements, and Γ^L is the input matrix evaluated with the angular velocity equal to that of the system when pulses in control inputs were applied to generate pulse response measurements. Since

$$\boldsymbol{x}_{n-1} = \Phi_{n-1} \boldsymbol{x}_{n-2} + \Gamma_{n-1} u_{n-1}, \tag{4.26}$$

the vector $\boldsymbol{h}_{n-1}^{NL}$ is given by

$$\boldsymbol{h}_{n-1}^{NL} = \boldsymbol{h}_{n-1}^{L} + C(\Phi_n \Gamma_{n-1} - \Phi^L \Gamma^L), \tag{4.27}$$

where Φ^L is the state transition matrix evaluated with the angular velocity equal to that of the system when pulses in control inputs were applied. In general, the vector $\boldsymbol{h}_{n-i}^{NL}$ is given by

$$\boldsymbol{h}_{n-i}^{NL} = \boldsymbol{h}_{n-i}^{L} + C\left(\left(\prod_{j=0}^{i-1} \Phi_{n-j}\right)\Gamma_{n-i} - (\Phi^L)^i \Gamma^L\right). \tag{4.28}$$

Generalization of these results for the multi-input case, in which u_i is replaced with $\boldsymbol{u}_i$ and the vector $\boldsymbol{h}_{n-i}^{NL}$ is replaced with the submatrix H_{n-i}^{NL}, is straightforward.

The algorithm described in the last chapter can be used to solve the minimum time problem of a nonlinear system by correcting the H matrix as the algorithm proceeds. The H matrix can be corrected whenever the algorithm switches from a larger time step to a smaller time step, using the last control profile obtained with the larger time step. The angular velocity history used to make this correction can be expected to approach the true angular velocity profile as the size of the time step is reduced. The effectiveness of making the nonlinear correction is illustrated in the numerical example presented in the next section.

4.3 Numerical Example

In this section, the solution of the problem described in the preceding section, which is the minimum time maneuver of a slender beam through a large angle by means of transverse force inputs at the ends of the beam, is obtained using pulse response based control. The exact solution of this minimum time control problem is unknown. A ninety degree rotation is to be executed in this example. The results obtained here are valid for uniform beams of various lengths and cross-sectional properties, as long as their deformation does not violate the Bernoulli-Euler assumptions.

The bounds for the control inputs are of the form $|u(t)| \leq B$. The ratio of the input bound to the angle of rotation, B/θ_0, is chosen based on the time that would be required to carry out the desired maneuver on a rigid system with the same inertial properties. For the rigid system, the minimum time control is bang-bang, so the final time $(t_f)_{RIGID}$ can be related to the ratio B/θ_0 by considering the angle at mid-maneuver, which must be

$$\frac{\theta_0}{2} = \frac{1}{2}\frac{BL}{mL^3/12}\left(\frac{(t_f)_{RIGID}}{2}\right)^2. \tag{4.29}$$

If the bang-bang minimum time solution for the rigid system is applied to the flexible system, the residual energy at the end of the control history will depend on how small $(t_f)_{RIGID}$ is compared to the natural periods of the system. For this example, a time scale characterizing the dynamics of the system is taken to be the period T of the lowest (symmetric) flexible mode. The ratio B/θ_0 is chosen so that $(t_f)_{RIGID}$ is equal to $T/2$, which indicates that the bang-bang control profile for the rigid system would result in a very large amount of residual vibration. Note that the minimum time for control of a uniform second-order one-dimensional system with *unbounded* inputs at its two ends is equal to one half of the period of the first flexible mode.[9] The minimum time problem to be solved, then, is for extremely rapid control of the beam.

The state transition matrix of the system whose state equations appear in Eq. (4.18) can be obtained using Kinariwala's procedure.[28] If $\dot{\theta}^2 A_2$ can be regarded as a perturbation of A_1, then the state transition matrix can be approximated as

$$\Phi(t+\Delta t, t) \approx \Phi_1(t+\Delta t, t) + \dot{\theta}^2(t)\Phi_2(t+\Delta t, t), \tag{4.30}$$

where $\Phi_1 = e^{A_1 \Delta t}$, and Φ_2 can be obtained using

$$\Phi_2(t+\Delta t, t) = \int_t^{t+\Delta t} \Phi_1(t+\Delta t, \tau) A_2 \Phi_1(\tau, t)\, d\tau. \tag{4.31}$$

If the control input is piecewise constant the solution of Eq. (4.18) can be approximated by

$$\boldsymbol{x}(t+\Delta t) \approx (\Phi_1 + \dot{\theta}^2\Phi_2)\boldsymbol{x}(t) + (\Gamma_1 + \dot{\theta}^2\Gamma_2)\boldsymbol{u}, \tag{4.32}$$

where the matrices Γ_1 and Γ_2 are available from

$$\Gamma_1 = \int_t^{t+\Delta t} \Phi_1(\tau,t)B\,d\tau, \quad \Gamma_2 = \int_t^{t+\Delta t} \Phi_2(\tau,t)B\,d\tau. \tag{4.33}$$

The accuracy of the final state of the system is measured in terms of the residual energy at the end of the control task, given by the modal sum

$$E_{res} = \frac{1}{2}\frac{mL^3}{12}\dot{\theta}^2 + \frac{1}{2}\sum_{r=1}^{\infty}(\dot{\eta}_r^2(t_f) + \lambda_r\eta_r^2(t_f)), \tag{4.34}$$

which is scaled against the maximum energy in the corresponding rigid system in its minimum time control, which occurs at mid-maneuver and is given by

$$E_{m-m} = \frac{1}{2}\frac{mL^3}{12}\left(\frac{2\theta_0}{(t_f)_{RIGID}}\right)^2. \tag{4.35}$$

The vector of specified outputs $\overline{y}_f$ contains the final rotational rigid body modal states in all cases, so there will be no error in these states. This means that the first term in the residual energy will always be zero. Also, $\overline{y}_f$ contains displacement and velocity at one end of the beam at various numbers of time steps at the end of the control task, so that displacement and velocity sensors are taken to be located at one end of the beam. Because only anti-symmetric modes are excited by the anti-symmetric control, only one end of the beam needs to be considered.

The pulse response matrix H of the system is generated about the state $\dot{\theta}(t) = 0$, by means of a modal simulation in which as many as one hundred anti-symmetric modes are included in Eq. (4.15) so that the effects of modal truncation will be negligible. An approximate solution of

Table 4.1: CPU time for each time step size

Time step size ΔT	Number of steps in control history	CPU time* (seconds)
$8\Delta t$	22	0.37
$4\Delta t$	46	29.32
$2\Delta t$	83	56.01
Δt	164	87.16
Total CPU time		172.86

*CPU time for Sun SPARCstation 2.

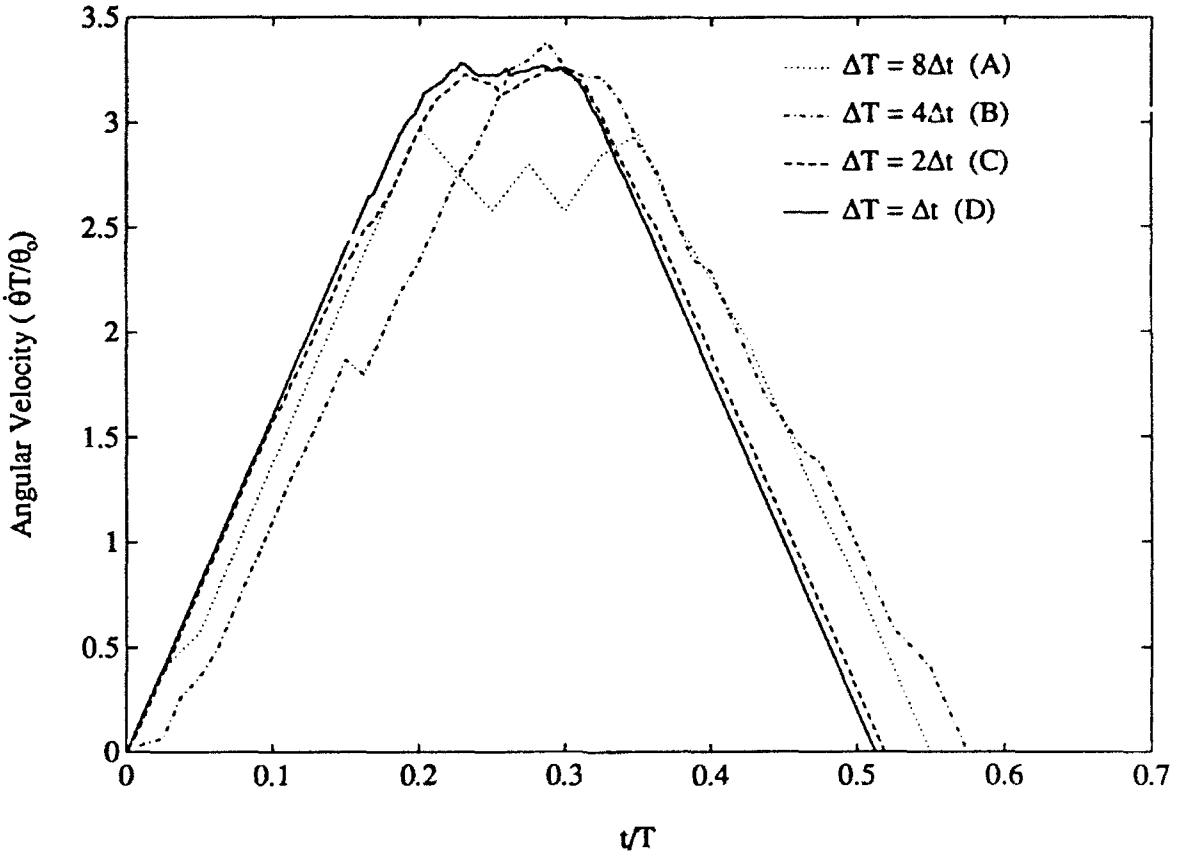

Figure 4.1: Angular velocity profiles for nonlinear correction

the linear problem associated with this pulse response matrix is obtained using a time step size of $\Delta t_1 = 8\,\Delta t$, where $\Delta t = (t_f)_{RIGID}/160$ is the smallest time step used. This is done by using the algorithm of the preceding chapter and specifying outputs for time steps at the end of the control profile until the ratio of unspecified outputs R, defined in the preceding chapter, decreases to less than twenty percent. The control profile obtained is then used to compute the angular velocity history using Eq. (4.9). This angular velocity history is shown in Fig. 4.1 as trajectory A. This trajectory is used to calculate Φ_i and Γ_i matrices from Eq. (4.22), which are used to correct individual columns of $H^{4\Delta t}$ using Eq. (4.28). The number of modes in which nonlinear behavior is considered to make this correction can be chosen arbitrarily, but for the plots of this example, nonlinear behavior is considered in the first two anti-symmetric flexible modes. The minimum time problem associated with the corrected H matrix is now solved approximately using a time step size of $4\,\Delta t$, with additional outputs specified until R is less than twenty percent of the value allowed at the termination of computation with $\Delta T = 8\,\Delta t$, so that the norm of unspecified outputs is less

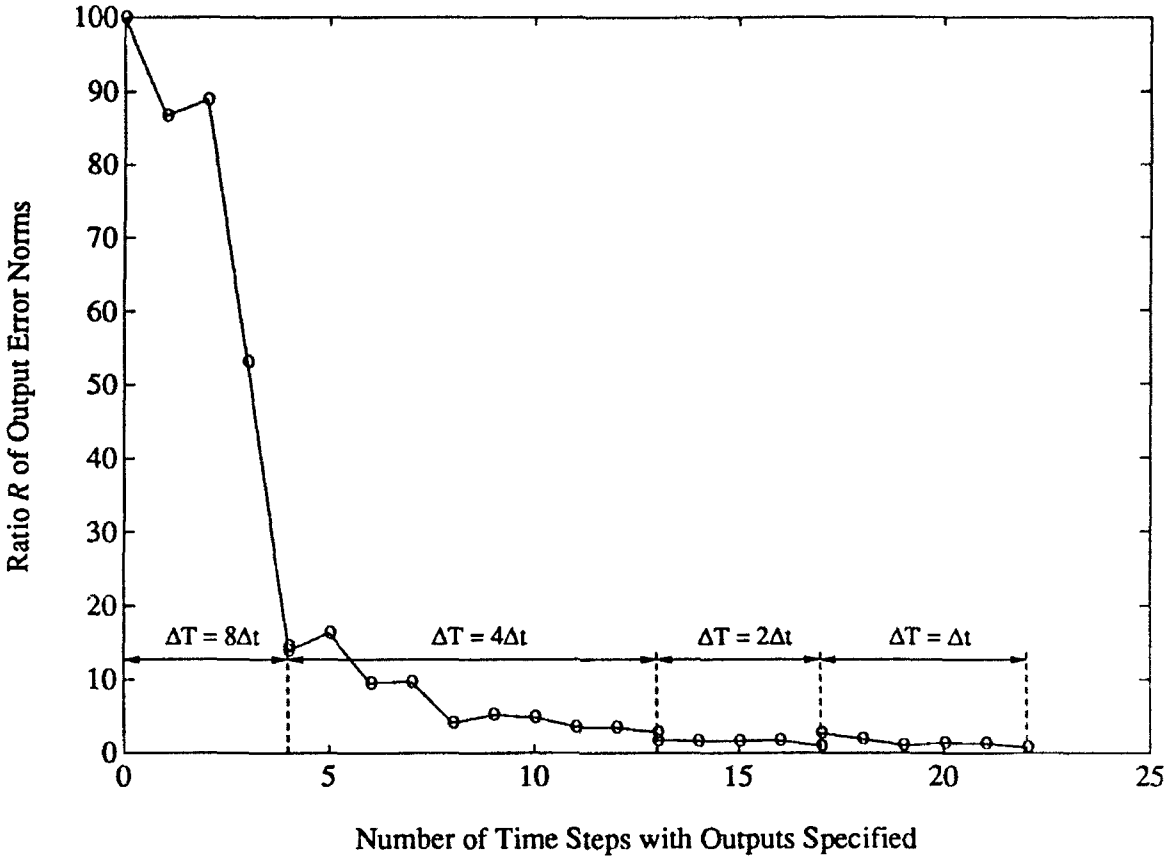

Figure 4.2: Variation of R

than four percent of its original bang-bang value. The resulting angular velocity profile is shown in Fig. 4.1 as trajectory B. It can be seen that there is a significant difference between trajectories A and B. The $H^{2\Delta t}$ matrix is then corrected so that the pulse response measurements now represent linearization about trajectory B, and the minimum time maneuver problem is solved with a time step size of $2\,\Delta t$. Finally, the matrix $H^{\Delta t}$ is corrected and the minimum time problem is solved for the last time. For each of these last two solutions, R is simply driven to less than one percent. The trajectories C and D obtained as a result of the last two corrections are nearly identical and hence, trajectory D can be taken to be a good approximation of the minimum time trajectory. The minimum time of control is found to be $t_f = 0.5125\ T$ with outputs specified for 22 time steps after t_f.

Table 4.1 shows how much computation time is spent approximating the minimum time control profile with each time step size. The number of unknowns in the control history given in the table is for the final result obtained with each time step size. The total computation time is less than

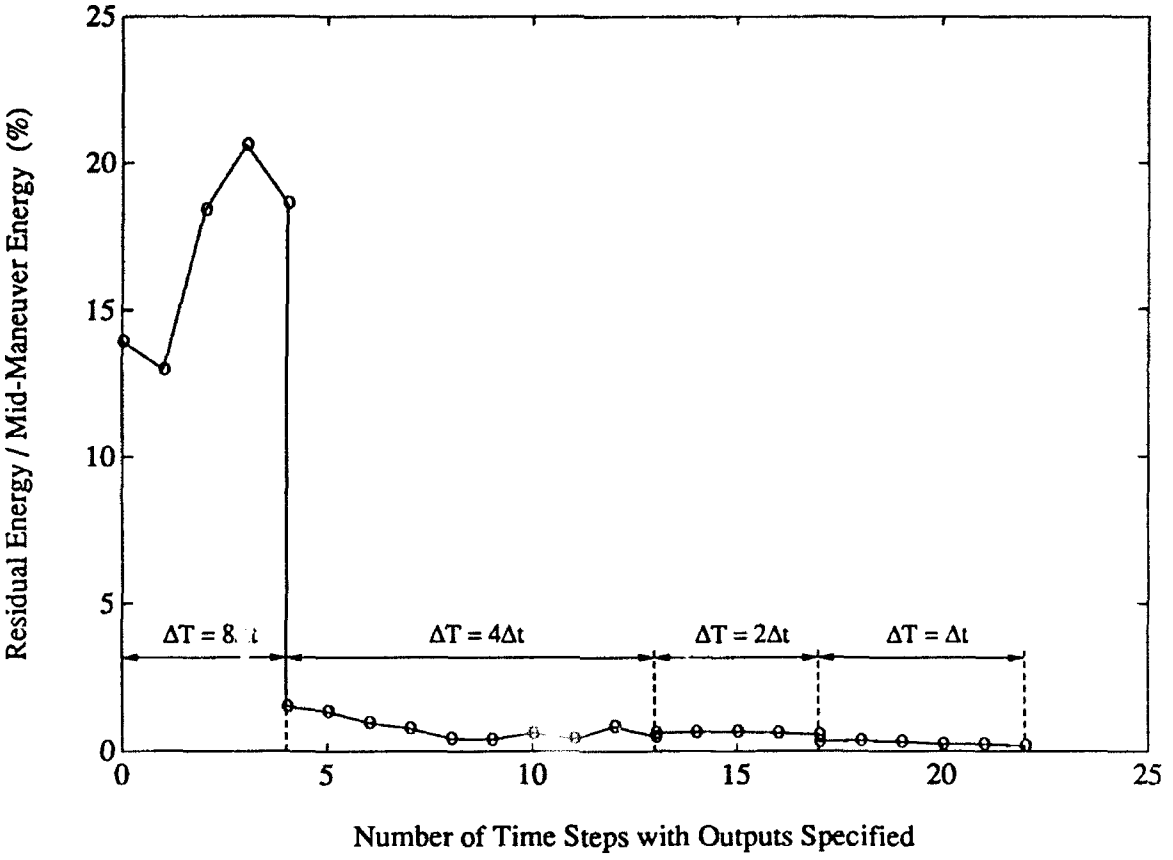

Figure 4.3: Residual energy variation

three minutes on a Sun SPARCstation 2.

It is interesting to examine convergence as the number of specified outputs increases, in terms of both R, the ratio of norms of error in unspecified outputs, and the residual energy in the nonlinear system at the end of the control history. Figure 4.2 shows how R varies over the course of the algorithm. Two points are plotted for the same number of specified outputs every time the time step size is halved. The first value of R is obtained with an H matrix that has not yet been corrected to account for linearization about a new trajectory, and the second value is obtained with a corrected H matrix. Figure 4.3 shows how the residual energy decreases over the course of the computation. Before the H matrix is corrected the first time, specifying additional outputs is not effective in reducing residual energy. After the first correction, though, the correspondence between R and the residual energy at the end of the maneuver is much better. The residual energy for the nonlinear system is ultimately driven to less than 0.2% of the mid-maneuver energy for bang-bang control of an inertially identical rigid system for this case in which nonlinear behavior in two modes

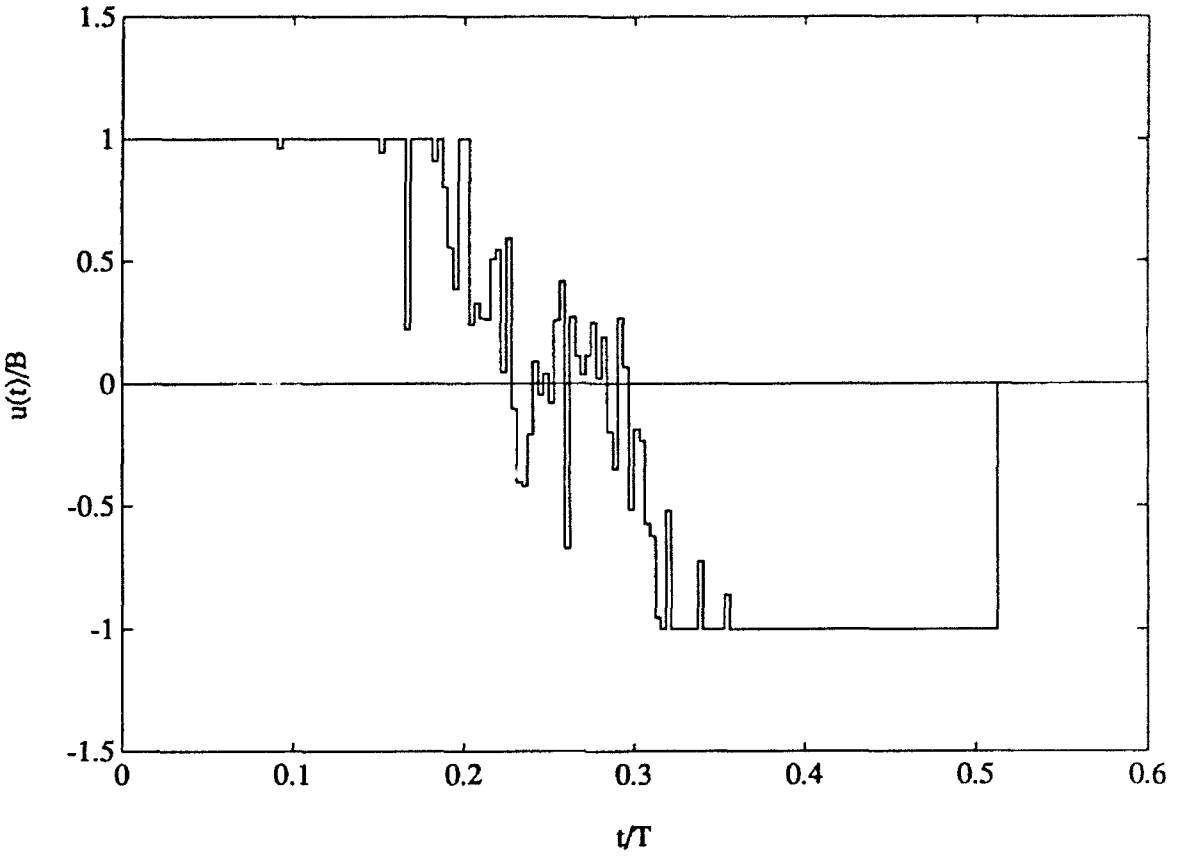

Figure 4.4: Control profile for maneuver

is taken into account. For comparison, if nonlinear behavior in only one mode is accounted for in correcting H, the residual energy is driven to 0.8% of mid-maneuver energy. If no correction is made for nonlinear behavior, but instead the original H matrices which represent linearization about the original rest state are used, the residual energy is driven to 20.2% of mid-maneuver energy even though the time step is halved three times in the solution process. This demonstrates the importance of correcting for nonlinear behavior in maneuvers this rapid. The minimum time control profile is shown in Fig. 4.4. The control inputs are equal to an upper or lower bound for most but not all of the control history, which would be expected for the exact minimum time profile.

Figure 4.5 shows the displacement of the beam during the rotational maneuver at intervals of $0.2t_f$. The dotted lines indicate the position of the Tisserand frame. The first anti-symmetric flexible mode dominates the flexible motion of the beam during the maneuver. However, at the end of the maneuver, the *third mode* dominates the flexible behavior of the beam, contributing as much as 74% of the final residual energy. This is because the nonlinear effects in only the first two

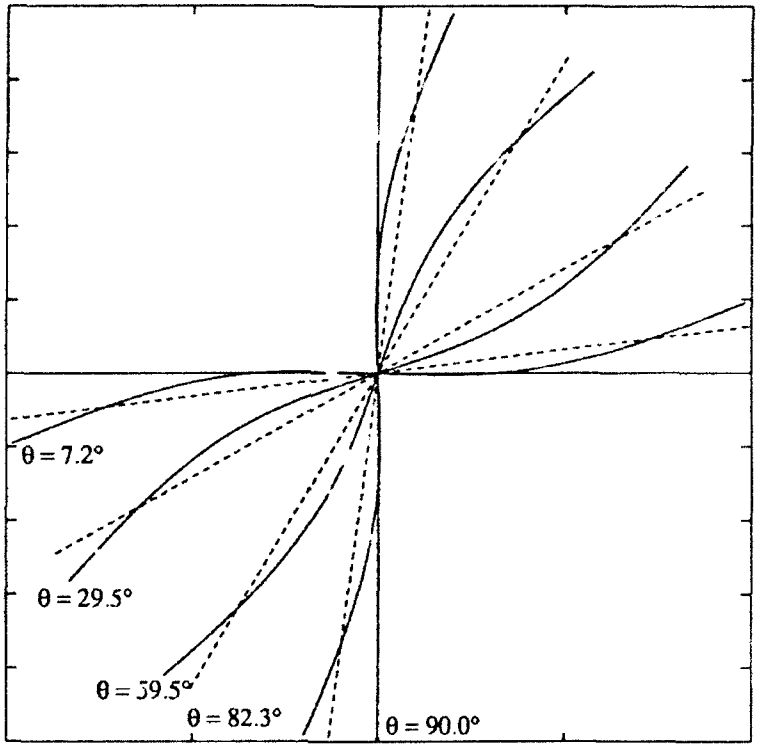

Figure 4.5: Deflected shape of the beam during the maneuver

modes have been considered in correcting the pulse response measurements.

Considering the low residual energy at the end of the maneuver and the fact that the algorithm used to solve the minimum time problems ensures that a control profile satisfying the specified constraints with fewer time steps does not exist, it can be concluded that a very accurate solution of the minimum time maneuver problem has been found.

4.4 Conclusions

A method for applying Pulse Response Based Control (PRBC) to maneuver problems involving nonlinear behavior associated with rapid large angle rotation is presented. This method obtains very accurate approximations of minimum time open loop control profiles without modal truncation or explicit modeling in linear behavior, but with explicit modeling of nonlinear behavior in those modes in which it is significant. The example of this chapter indicates that the number of modes that must be known accurately to account for nonlinear behavior can be expected to be very

small, even for an extremely rapid maneuver for which a minimum time control profile that ignores nonlinear effects results in very high levels of residual energy when applied to the nonlinear system. This means that modal identification requirements are likely to be very low when this method is used.

Chapter 5

Closed Loop Near Minimum Time Pulse Response Based Maneuver of Flexible Spacecraft

5.1 Introduction

In the last chapter, a method for obtaining open loop minimum time control profiles for maneuver of flexible structures, which takes linear behavior in all modes and nonlinear behavior in those few modes in which it is significant into account, was presented. The effectiveness of this method in accounting properly for the dynamics of the structure is evident in the low levels of residual energy obtained at the end of the maneuver. Although the amount of computation required for implementation of this method is quite small, especially in comparison with methods that solve a nonlinear two point boundary value problem, for example, it is quite possibly not small enough for real time implementation on a structure of realistic modal density. Another drawback is that the control profiles provided by the method of the last chapter are open loop profiles, and feedback control would obviously be desirable to enable compensation for disturbances during the maneuver, error in the pulse response data, unmodeled nonlinear behavior, etc.

These practical considerations motivate the work presented in this chapter. In recent years, minimum time control has often been approximated with a control consisting of an open loop component for the rigid body portion of the response and a feedback component for vibration suppression and fine terminal pointing.[4,5,8,29] The open loop component is typically bang-bang, possibly "smoothed" in an attempt to reduce excitation of vibration without explicit reference to the flexible response. Such an open loop component is based only on inertial properties and does

not take flexible behavior into account, except in the heuristic approach of smoothing to reduce excitation of unmodeled higher modes. This chapter presents a method for obtaining near minimum time profiles that account correctly for flexible behavior, rather than relying on smoothing. These profiles are not computed in real time, but are instead computed in advance, so the amount of computation time required is quite reasonable in an off-line context. The amount of real time computation necessary for obtaining near minimum time profiles for maneuver through an arbitrary angle, from the results that have been computed in advance, is negligible.

Although there is likely to be less need for feedback control when open loop control profiles take flexible behavior into account, the pulse response based control approach lends itself very naturally to feedback control because the outputs that should be observed over the course of a maneuver, including the effects of flexible behavior, are easily obtained with the same convolution approach used to obtain outputs at the end of the maneuver. Designing a feedback control to complement an open loop profile usually requires some compromise, because in minimum time profiles the control inputs are equal to their bounds much of the time and cannot be modified arbitrarily to produce a feedback component. A feedback control scheme for use in pulse response based control, which is guaranteed to be stable even in the presence of the input bounds that are in effect for the open loop control component, is developed in this chapter. Bounds on control inputs are commonly ignored in the design of a feedback control component, but this implies either that the bounds for the open loop control component are artificially low, or that saturation of the control inputs will prevent realization of the feedback component. In some cases, input bounds are selected rather arbitrarily and are motivated by the inaccuracy of actuators at high output levels, rather than by absolute limits on the forces or moments they can produce. This raises the question of whether it will be possible in these cases to realize a feedback component accurately enough for it to be of significant benefit.

It should be mentioned that another approach to the design of feedback control is to assign a subset of the control inputs to the open loop component and the remainder to a vibration suppression component of the control, so that input bounds are only considered for the first subset of the control inputs.[29] However, this approach does not result in minimum time maneuver with a given set of inputs, since some inputs cannot contribute to the rigid body portion of the control and the rest cannot be used in vibration suppression. Also, this approach, while simplifying the

design of the control somewhat, is likely to require more control hardware than a system in which each control input can be used for both parts of the control task.

The second section of this chapter presents the formulation of the dynamic response problem for an example system consisting of a rigid hub with four flexible appendages, and a torque actuator on the hub and force actuators at the ends of only two of the appendages. The third section presents a near minimum time PRBC method that requires negligible real-time computation and still results in virtually no residual vibration. The fourth section explains how a stable feedback control can be designed to complement a PRBC open loop control profile in maneuver problems. The fifth section presents a numerical example, and the final section contains a summary.

5.2 Minimum Time Maneuver of a Model System

The example system for this chapter is pictured in Figure 5.1, and consists of a rigid hub with four identical uniform flexible appendages that have identical discrete masses attached to their tips. This system has the same inertial and elastic properties as the experimental structure used for maneuver studies in Ref. 8. In this chapter, it is controlled by a torque $T(t)$ applied to the hub

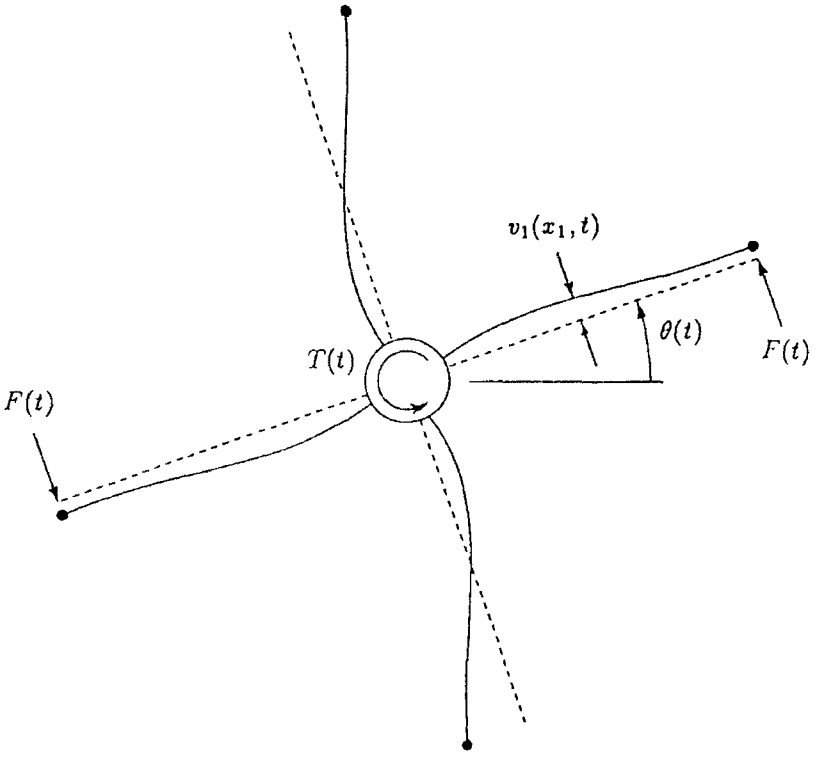

Figure 5.1: The model system

and two equal transverse forces $F(t)$ applied to the tip masses on the first and third appendages. Using force actuators on only two appendages makes the response more interesting, because flexible modes that involve the first and third appendages moving in opposition to the second and fourth appendages, as well as modes involving all appendages moving in unison, participate in the response. For this system, the instantaneous position vector of a point in the system is expressed as

$$\boldsymbol{R} = \boldsymbol{R}_G + \boldsymbol{r} + \boldsymbol{d}, \tag{5.1}$$

where $\boldsymbol{R}_G$ is expressed in terms of an inertial frame, and locates the instantaneous center of mass of the system and the origin of a Tisserand floating reference frame.[27] The vectors $\boldsymbol{r}$ and $\boldsymbol{d}$ are expressed in terms of the floating frame and are the position vector of the point relative to the origin in an undeformed position, and the elastic displacement, respectively. The location of the origin and the orientation of the reference frame are subject to the Tisserand constraints

$$\int_M (\boldsymbol{r} + \boldsymbol{d})\, dm = 0, \qquad \int_M (\boldsymbol{r} + \boldsymbol{d}) \times \dot{\boldsymbol{d}}\, dm = 0, \tag{5.2}$$

where M is the total mass of the system. Because of these constraints, in general motion the frame must rotate with angular velocity $\boldsymbol{\omega}$. The expression for the kinetic energy becomes

$$\begin{aligned} T &= \frac{1}{2} M \dot{\boldsymbol{R}}_G \cdot \dot{\boldsymbol{R}}_G + \frac{1}{2} \boldsymbol{\omega} \cdot \boldsymbol{\omega} \int_M (\boldsymbol{r} + \boldsymbol{d}) \cdot (\boldsymbol{r} + \boldsymbol{d})\, dm - \frac{1}{2} \int_M [\boldsymbol{\omega} \cdot (\boldsymbol{r} + \boldsymbol{d})]^2\, dm \\ &\quad + \frac{1}{2} \int_M \dot{\boldsymbol{d}} \cdot \dot{\boldsymbol{d}}\, dm + \boldsymbol{\omega} \cdot \int_M \boldsymbol{d} \times \dot{\boldsymbol{d}}\, dm. \end{aligned} \tag{5.3}$$

where an overdot represents differentiation with respect to time within the frame in which a vector is expressed. This chapter will be concerned with maneuver involving only planar rotation about the mass center, so that $\boldsymbol{R}_G$ will be set equal to zero and $\boldsymbol{\omega}$ equal to $\dot{\theta}\hat{\boldsymbol{k}}$, where $\hat{\boldsymbol{k}}$ is a unit vector normal to the plane of the motion. With a hub radius of r and a coordinate axis of x_i for the ith appendage, a point on the ith appendage in the undeformed position is located by the vector $r(x_i) = (r + x_i)\hat{\imath}_i$, where $\hat{\imath}_i$ is a unit vector along the x_i axis. Retaining up to quadratic terms in the transverse elastic displacement $v_i(x_i, t)$, the vector $\boldsymbol{d}$ for a point on the x_i axis is given by

$$d(x_i, t) \approx v_i(x_i, t)\hat{\jmath}_i - \frac{1}{2} \int_0^{x_i} v'(\xi_i, t)^2\, d\xi_i\, \hat{\imath}_i, \tag{5.4}$$

where a prime represents differentiation with respect to x_i. Neglecting rotatory inertia and shear deformation for the appendages, the kinetic and potential energies for the system become

$$T = \frac{1}{2} I_H (\dot{\theta}^2 + \dot{\theta}_H^2) + \frac{1}{2} \sum_{i=1}^{4} \left\{ \int_0^L m \left[\dot{v}_i^2 + \dot{\theta}^2 \Big((r + x_i)^2 + v_i^2 \right.\right.$$

$$- \left(r(L-x_i) + \frac{L^2 - x_i^2}{2}\right) v_i'(x_i,t)^2 \Big)\Big] dx_i + m_t\Big[\dot{v}_i^2(L,t) \tag{5.5}$$
$$+ \dot{\theta}^2\Big((r+L)^2 + v_i^2(L,t) - (r+L)\int_0^L v_i'(x_i,t)^2\, dx_i\Big)\Big]\Big\}$$

and

$$V = \frac{1}{2}\sum_{i=1}^{4}\int_0^L EI\left(v_i''(x_i,t)\right)^2 dx, \tag{5.6}$$

where I_H is the hub mass moment of inertia, L is the length of an appendage, m is the appendage mass per unit length, m_t refers to a tip mass, and EI is the flexural rigidity. The angle θ_H is the hub rotation relative to the floating frame, and is related kinematically to the appendage transverse displacements and slopes at $x_i = 0$ as expressed in the boundary conditions given below. With the given control inputs, the non-conservative virtual work, linearized in $v_i(x_i,t)$'s and their derivatives, is

$$\delta W_{nc} = T(t)(\delta\theta + \delta\theta_H) + F(t)\Big(2(r+L)\delta\theta + \delta v_1(L,t) + \delta v_3(L,t)\Big) \tag{5.7}$$

Applying the extended Hamilton's principle results in the ordinary differential equation

$$\left(I_H + \sum_{i=1}^{4}\int_0^L m(r+x_i)^2\, dx_i + 4m_t(r+L)^2\right)\ddot{\theta} = T(t) + 2(r+L)F(t) \tag{5.8}$$

and the partial differential equations

$$m\ddot{v}_i + EIv_i'''' - \dot{\theta}^2\left[\left\{\left[m\left(r(L-x_i) + \frac{L^2-x_i^2}{2}\right) + m_t(r+L)\right]v_i'\right\}' + mv_i\right] = 0, \quad i = 1,\ldots,4 \tag{5.9}$$

with boundary conditions

$$v_i(0,t) = \theta_H r,\ v_i'(0,t) = \theta_H,\ EIv_i''\Big|_{x_i=L} = 0, \tag{5.10}$$

and

$$EIv_i'''\Big|_{x_i=L} - m_t(\ddot{v}_i + \dot{\theta}^2(r+L)v_i')\Big|_{x_i=L} = \begin{cases} -F(t), & i = 1,3 \\ 0, & i = 2,4 \end{cases}. \tag{5.11}$$

Natural modes and frequencies for vibration about a stationary configuration can be obtained by setting $T(t)$ and $F(t)$ to zero, neglecting terms involving $\dot{\theta}^2$, and solving the differential eigenvalue problem resulting from separation of variables. Note that since translation of the hub is not considered, only those modes of the system for which the hub simply rotates or remains stationary will be included. These modes of vibration can then be used to discretize the problem, so that the transverse displacement of an appendage will be represented as

$$v_i(x_i,t) = \sum_{r=1}^{\infty}\phi_r(x_i)\eta_r(t). \tag{5.12}$$

This discretization results in the kinetic energy expression

$$T = \frac{1}{2}\left(I + \sum_{r=1}^{\infty}\sum_{s=1}^{\infty}(\delta_{rs} - k_{rs})\eta_r\eta_s\right)\dot{\theta}^2 + \frac{1}{2}\sum_{r=1}^{\infty}\dot{\eta}_r^2, \tag{5.13}$$

where I is the coefficient of $\ddot{\theta}$ in Eq. (5.8), δ_{rs} is the Kronecker delta, and the geometric stiffness coefficients k_{rs} are given by

$$k_{rs} \equiv \sum_{i=1}^{4}\int_0^L \left[m\left(r(L - x_i) + \frac{L^2 - x_i^2}{2}\right) + m_t(r + L)\right]\phi_r'(x_i)\phi_s'(x_i)\,dx_i \tag{5.14}$$

where ϕ_r is the rth eigenfunction for the system. It is assumed that modes are normalized with respect to the mass distribution. The potential energy takes the form

$$V = \frac{1}{2}\sum_{r=1}^{\infty}\omega_r^2\eta_r^2, \tag{5.15}$$

and the nonconservative virtual work becomes

$$\delta W_{nc} = (T(t) + 2F(t)(r + L))\,\delta\theta + \sum_{r=1}^{\infty} N_r(t)\delta\eta_r, \tag{5.16}$$

in which modal forces are given by

$$N_r(t) = T(t)\phi_r'\Big|_{x_1=0} + 2F(t)\phi_r\Big|_{x_1=L}, \quad r = 1, 2, \ldots \tag{5.17}$$

Then modal equations of motion become

$$\ddot{\eta}_r + \omega_r^2\eta_r + \dot{\theta}^2\sum_{r=1}^{\infty}(k_{rs} - \delta_{rs})\eta_s = N_r. \tag{5.18}$$

Minimum time maneuver profiles for this nonlinear system can be obtained by the approach outlined in the preceding chapter.

5.3 Near Minimum Time Maneuver Using PRBC

Obtaining minimum time control profiles requires considerably less computation when the PRBC approach is used than when other approaches that consider flexible response are used. However, if this computation must be done after the total desired slew angle is determined and before execution of the maneuver can begin, it is likely to substantially increase the time required to complete the maneuver. Because of this, a method for obtaining approximate minimum time control profiles with very little real time computation is needed.

The starting point for developing such a method is the result from the second chapter that, for linear undamped structures controlled by ideal inputs that are bounded in magnitude, it can be shown that given any minimum time rest-to-rest control profile, a new minimum time control profile can be constructed that is antisymmetric in time about the midpoint of the control interval. This means that there is always an antisymmetric minimum time control profile for this class of problems. For an antisymmetric control profile that drives the system to rest at the final time, all of the flexible modal displacements are zero at the midpoint of the control interval, although flexible modal velocities are nonzero at that time.[9]

This suggests an approach of separating the first and second halves of the control profile with a "coast" interval of the proper length so that the final rigid body displacement is equal to the desired value. To get an idea how much performance would be diminished by this, consider a rest-to-rest translation of a rigid mass by means of a force $F(t)$ subject to the bounds $-B \leq F(t) \leq B$. The minimum time control profile for accomplishing this is bang-bang. However, if a bang-off-bang profile is applied to the system such that the final state is the same, it is easily shown that the increase in the final time Δt_f is given by the equation

$$\frac{\Delta t_f}{t_{f_{MIN}}} = \frac{1}{2}\left(\frac{\Delta t_{OFF}}{t_{f_{MIN}}}\right)^2 - \frac{1}{8}\left(\frac{\Delta t_{OFF}}{t_{f_{MIN}}}\right)^4 + O\left(\frac{\Delta t_{OFF}}{t_{f_{MIN}}}\right)^6, \tag{5.19}$$

where $t_{f_{MIN}}$ is the time required for bang-bang control and Δt_{OFF} is the length of the "off" interval. From this equation, if Δt_{OFF} is as long as ten percent of the length of the minimum time control history, for example, t_f would only be increased by less than one-half of one percent. To the extent that the minimum time control profile for a flexible structure resembles the simple bang-bang profile, similar results can be expected. Fortunately, minimum time maneuver profiles for flexible spacecraft resemble bang-bang profiles very closely unless the maneuver is extremely rapid.

For flexible systems, there will be residual vibration at the end of a control profile constructed by simply separating the first and second halves of a minimum time antisymmetric control profile with a "off" interval. This is because there will be response in the flexible modes during the "off" interval, so the flexible mode states at the end of the interval will not be the same as at the beginning of the interval, and hence they will be incorrect at the end of the control profile. However, if flexible mode velocities, as well as displacements, are required to be zero at the end of the first half of the control profile, so that the system is in pure rigid body motion at the beginning

of the "off" interval, there will not be any response in flexible modes during this interval. Then it is easy to show that applying the reverse of the first half control profile at the end of the "off" interval will result in a final rigid body displacement with no residual vibration if the system is undamped and linear and control inputs are ideal.

A set of first halves and a matching set of second halves of maneuver profiles can be obtained, so that piecing matching halves together gives control profiles that will produce a set of final displacements spaced over the expected range of desired final displacements. Each first half drives the system from rest to pure rigid body velocity, with a rigid body displacement of half of a desired final displacement, in minimum time. Each matching second half drives the system from this state to rest as quickly as possible. It is straightforward to determine what outputs should be specified at the ends of first and second half control profiles so that PRBC can be used to obtain these profiles. If a final displacement $d_{desired}$ somewhat greater than the one resulting from joining these two halves together is desired, an "off" interval is inserted between them, whose length is obtained from the equation

$$d_{desired} = d_{half1} + d_{half2} + v_{half}\Delta t_{OFF}, \tag{5.20}$$

where d_{half1} and d_{half2} refer to changes in rigid body displacement over the two halves, and v_{half} refers to the rigid body velocity at the end of the first half. The computation required for determining Δt_{OFF} from this equation is negligible, so as soon as the desired final rigid body displacement is known, the pair of first and second halves that give the largest final displacement less than or equal to the desired one can be selected from the profiles that have been computed in advance, and the maneuver can begin almost immediately.

Note that control profiles constructed in this manner, even with an "off" interval of length zero, are not minimum time profiles because of the added constraint of zero flexible velocity at the midpoint of the maneuver. In fact, for structures that are damped or are subject to nonideal inputs or nonlinear effects, flexible modal displacements are also nonzero at the midpoint of a minimum time control profile. This means that for these systems the constraint of zero flexible displacement at mid-maneuver, which must be added to ensure that there will be no flexible response during the "off" interval, is another constraint that the minimum time solution does not satisfy. Another point on implementation of the method on these systems is that the changes in rigid body displacements

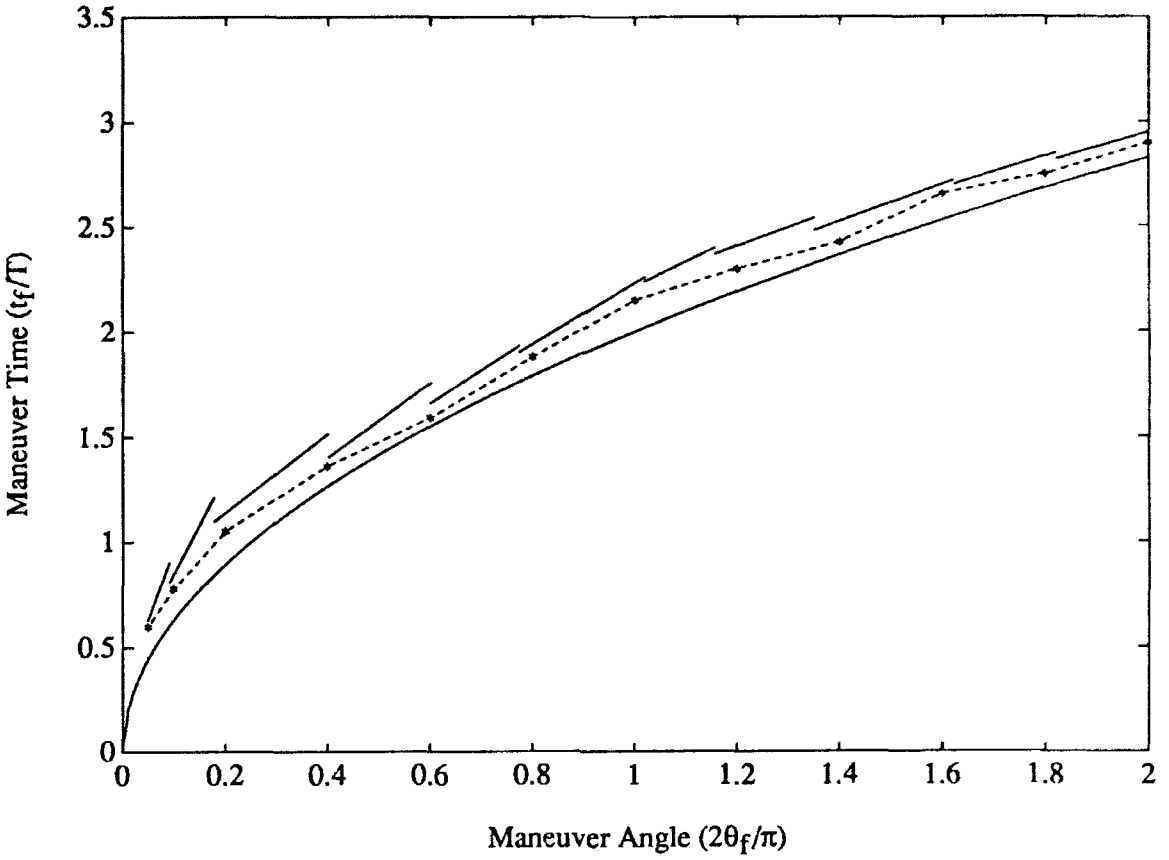

Figure 5.2: Maneuver time for rigid system (solid line), nonlinear flexible system (dashed line), and near minimum time method (line segments), for a very rapid maneuver

d_{half1} and d_{half2} will not necessarily be equal.

As an example, this approach has been applied to the model system described in the preceding section. Bounds on the torque and force inputs were selected so that the maximum moment on the system available from the torque input is equal to that available from the force inputs. These bounds were chosen so that a ninety degree rotation could be accomplished for an inertially identical rigid system in twice the period of the first flexible mode of the elastic system for a first case, and in one half of the period of the first flexible mode for a second case. This means that minimum time maneuvers are extremely rapid, especially for the second case, and the control profiles for the second case are quite different from a simple bang-bang profile. (For an example profile with these input bounds, as well as all of the properties of this system, see the fifth section of this chapter.)

Figures 5.2 and 5.3 are plots of the maneuver time, scaled by the period of the first flexible mode, vs. the final slew angle θ_f for the two cases. The solid line in each plot is the parabola

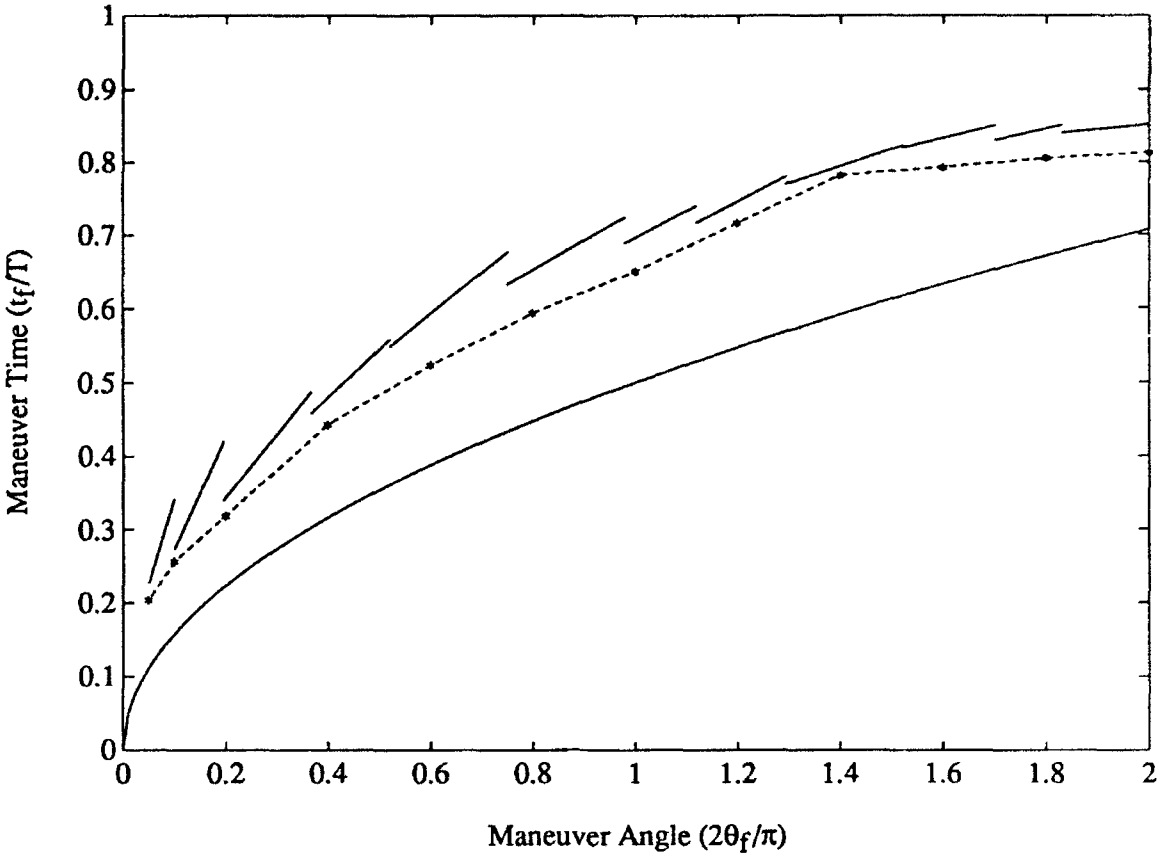

Figure 5.3: Maneuver time for rigid system (solid line), nonlinear flexible system (dashed line), and near minimum time method (line segments), for an extremely rapid maneuver

for minimum time control of an inertially identical rigid system, and the dashed line above this is a piecewise linear interpolation between points for which the minimum time control profile for the nonlinear flexible system was determined using PRBC, as explained in the preceding chapter. The line segments above this dashed line are obtained by the near minimum time approach of this section, where the leftmost point on each line segment corresponds to an "off" interval of length zero, and the final time increases linearly as the "off" interval is lengthened, according to Eq. (5.20). The leftmost point is not directly above the corresponding asterisk in many cases, because it is possible to bring the system to rest in the second half of the control profile with a smaller change in angular displacement than was obtained for the first half of the profile. This is a manifestation of the nonlinear rotational stiffening effect.

For both of these cases, the maneuvers are so rapid that they may not ever be representative of practical problems. However, they serve to illustrate the performance of the near minimum time

approach. For the first case, the time required to complete the maneuver is not much larger for the flexible system than for the corresponding rigid system, as shown by how close the dashed line is to the solid line, and the control profiles are nearly bang-bang. The maneuver times obtained using the near minimum time approach approximate the minimum time maneuver times very well. For the second case, the time required for the flexible maneuver is significantly larger than for the corresponding rigid system, and the minimum time control profiles are very different from bang-bang profiles. However, the near minimum time approximation still produces maneuver times very close to the minimum times for the flexible system. Of course, it is also significant that the near minimum time profiles result in essentially no residual vibration and require very little knowledge of the system.

5.4 Stable Feedback Control for PRBC

The same convolution approach that is used to compute outputs at the end of a maneuver in PRBC can be used to obtain reference outputs that should be observed over the course of a maneuver. If nonlinear effects are significant, corrections can be made by taking into account the response of a few modes as described earlier. Because outputs corresponding to the solution of the nonlinear flexible response problem can be obtained easily and with very little knowledge of system properties, PRBC lends itself to feedback control in a remarkable way. At the same time, there will be less need for feedback control when PRBC is used than when open-loop control is based on a rigid model of the spacecraft, since PRBC takes flexible and nonlinear behavior into account in the open-loop control component. This section presents a stable feedback control scheme that responds to the difference between outputs actually obtained over the course of a maneuver and those predicted using PRBC, and also satisfies the same bounds on control inputs that are specified for the open-loop control component.

For the model system described in the third section, the time derivative of the total system energy is evident from the nonconservative virtual work expression as simply

$$\dot{E} = T(\dot{\theta} + \dot{\theta}_H) + F\Big(2(r+L)\dot{\theta} + \dot{v}_1\Big|_{r_1=L} + \dot{v}_3\Big|_{r_3=L}\Big). \tag{5.21}$$

The actual response of the system and the control inputs can be expressed in terms of two components, of which the first corresponds to the reference open loop PRBC solution and the second

represents a deviation from this solution. These two components will be designated with subscripts "0" and "1", respectively, in this section. The second component of the response can be expected to be small, so that linearization of the response in θ_1 is justified. Recall that the response is already assumed to be linear in its flexible component, and that nonlinear terms in θ_0 are retained. When the $(\cdot)_0$ terms, which satisfy the equations of motion by themselves, are subtracted from the equations of motion, and higher-order terms are neglected, the rotation equation becomes

$$I\ddot{\theta}_1 = T_1 + 2(r+L)F_1 \tag{5.22}$$

and the modal equations of motion become

$$\ddot{\eta}_{r1} + \omega_r^2\eta_{r1} + \dot{\theta}_0^2\sum_s(k_{rs}-\delta_{rs})\eta_{s1} = T_1\phi_r'\Big|_{x_1=0} + 2F_1\phi_r\Big|_{x_1=L}, \quad r = 1,2,\ldots \tag{5.23}$$

An energy quantity associated with the deviation in the response, in which up to quadratic terms in $(\cdot)_1$ quantities are retained, is

$$E_1 \equiv \frac{1}{2}\left(I\dot{\theta}_1^2 + \sum_r(\dot{\eta}_{r1}^2 + \omega_r^2\eta_{r1}^2)\right). \tag{5.24}$$

The time derivative of E_1 is, upon substituting from the equations of motion,

$$\begin{aligned}
\dot{E}_1 &= I\dot{\theta}_1\ddot{\theta}_1 + \sum_r \dot{\eta}_{r1}(\ddot{\eta}_{r1} + \omega_r^2\eta_{r1}) \\
&= \dot{\theta}_1(T_1 + 2(r+L)F_1) + \sum_r \dot{\eta}_{r1}\left[(T_1\phi_r'\Big|_{x_1=0} + 2F_1\phi_r\Big|_{x_1=L} - \dot{\theta}_0^2\sum_s(k_{rs}-\delta_{rs})\eta_{s1}\right] \qquad (5.25)\\
&= T_1(\dot{\theta}_1 + \dot{\theta}_{H1}) + F_1\left(2(r+L)\dot{\theta}_1 + \dot{v}_{11}\Big|_{x_1=L} + \dot{v}_{31}\Big|_{x_3=L}\right) - \sum_r \dot{\eta}_{r1}\dot{\theta}_0^2\sum_s(k_{rs}-\delta_{rs})\eta_{s1}
\end{aligned}$$

Note that T_1 multiplies the total angular velocity of the hub, and F_1 multiplies the sum of the total transverse velocities of the ends of the first and third appendages, which will be equal according to the motion assumptions made in the derivation of the equations of motion. With this result for $\dot{E}_1$ in mind, the Lyapunov function

$$\begin{aligned}
U \equiv\ & \frac{1}{2}a_1\left[\left(I\dot{\theta}_1^2 + \sum_r(\dot{\eta}_{r1}^2 + \omega_r^2\eta_{r1}^2)\right) + \dot{\theta}_0^2\sum_r\sum_s(k_{rs}-\delta_{rs})\eta_{r1}\eta_{s1}\right] \qquad (5.26)\\
&+ \frac{1}{2}a_2(\theta_1 + \theta_{H1})^2 + \frac{1}{2}a_3(\dot{\theta}_1 + \dot{\theta}_{H1})^2
\end{aligned}$$

can be selected. Note that this function is a positive definite function of the difference from the reference solution if a_1 and a_2 are positive and a_3 is nonnegative. The fact that the term involving

$\dot{\theta}_0^2$ is nonnegative is evident from the physical argument that this term is equal to the dynamic potential of a system having no flexural rigidity but otherwise identical to the model system, if it is rotated with constant angular velocity $\dot{\theta}_0$. The time derivative of U is

$$\begin{aligned}\dot{U} &= a_1\Big(T_1(\dot{\theta}_1+\dot{\theta}_{H1})+F_1(2(r+L)\dot{\theta}_1+\dot{v}_{11}\Big|_{x_1=L}+\dot{v}_{31}\Big|_{x_3=L})\Big)+(\dot{\theta}_1+\dot{\theta}_{H1})\Big(a_2(\theta_1+\theta_{H1})\\ &\quad+a_3(\ddot{\theta}_1+\ddot{\theta}_{H1})\Big)+a_1\dot{\theta}_0\ddot{\theta}_0\sum_r\sum_s(k_{rs}-\delta_{rs})\eta_{r1}\eta_{s1}.\end{aligned}\tag{5.27}$$

If T_1 and F_1 are given by

$$T_1=-\frac{a_2}{a_1}(\theta_1+\theta_{H1})-\frac{a_3}{a_1}(\ddot{\theta}_1+\ddot{\theta}_{H1})-\frac{a_4}{a_1}(\dot{\theta}_1+\dot{\theta}_{H1})\tag{5.28}$$

and

$$F_1=-g_f(2(r+L)\dot{\theta}_1+\dot{v}_{11}\Big|_{x_1=L}+\dot{v}_{31}\Big|_{x_3=L}),\tag{5.29}$$

where a_4 and g_f are positive, then the time derivative of U becomes

$$\begin{aligned}\dot{U} &= -a_4(\dot{\theta}_1+\dot{\theta}_{H1})^2-g_fa_1\Big(2(r+L)\dot{\theta}_1+\dot{v}_{11}\Big|_{x_1=L}+\dot{v}_{31}\Big|_{x_3=L}\Big)^2\\ &\quad+a_1\dot{\theta}_0\ddot{\theta}_0\sum_r\sum_s(k_{rs}-\delta_{rs})\eta_{r1}\eta_{s1}.\end{aligned}\tag{5.30}$$

Since the double sum is nonnegative for the same reason that it is in Eq. (5.27), $\dot{U}$ is guaranteed to be nonpositive as long as the product $\dot{\theta}_0\ddot{\theta}_0$ is negative, which is ordinarily the case over most of the second half of the control history for rest-to-rest maneuvers. Note that this product involves only quantities from the open loop solution, so that it is easy to tell when $\dot{U}$ is guaranteed to be nonpositive once the open loop solution has been obtained. For guaranteed stability, the feedback component of the control can be employed only when $\dot{U}$ is guaranteed to be nonpositive, if desired. Of course, even when the term involving the product $\dot{\theta}_0\ddot{\theta}_0$ is positive, it will be dominated much of the time by the other negative terms in $\dot{U}$, so performance will likely be improved by employing feedback over all of the control history.

This feedback control law assumes that bounds on control inputs can be ignored in its design, which has been common practice in the design of feedback control for maneuver problems, as mentioned in the Introduction. This is inconsistent with requiring input bounds to be satisfied in the open loop component of the control. If it is recognized that the control inputs will be saturated over much of a minimum time control profile, it is evident that if a_2 and a_4 have finite values, it

will not always be possible to realize a T_1 that guarantees that $\dot{U} \leq 0$. A remedy for this is to use a positive semidefinite function $\tilde{U}$ of the difference from the reference solution, in which a_2 and a_3 are zero, until the end of the open loop control profile. The only component of the state of the system that is not represented in $\tilde{U}$ is the angular displacement of the reference frame θ_1. This indicates that a feedback control based on $\tilde{U}$ will not be effective in asymptotically driving the final angular displacement error to zero, although the residual energy will be asymptotically driven to zero. With this choice of $\tilde{U}$, T_1 and F_1 become direct velocity feedback on the difference from the reference solution, and considering saturation of the inputs, the actual control inputs can be written in terms of T_1 and F_1 as

$$T(t) = \begin{cases} -B_T, & \text{if } T_0 + T_1 < -B_T, \\ T_0 + T_1, & \text{if } -B_T \leq T_0 + T_1 \leq B_T, \\ B_T, & \text{if } T_0 + T_1 > B_T \end{cases} \tag{5.31}$$

and

$$F(t) = \begin{cases} -B_F, & \text{if } F_0 + F_1 < -B_F, \\ F_0 + F_1, & \text{if } -B_F \leq F_0 + F_1 \leq B_F, \\ B_F, & \text{if } F_0 + F_1 > B_F, \end{cases} \tag{5.32}$$

where B_T and B_F are bounds on the magnitudes of the torque and force inputs. The time derivative of $\tilde{U}$ is then similar to $\dot{U}$ above, and is easily shown to be nonpositive while $\dot{\theta}_0\ddot{\theta}_0 < 0$. When the end of the open loop control profile is reached, control input saturation is less of a threat, so a Lyapunov function with positive a_2 and a_3 can be used as a basis for the feedback control. Then any error in the angular displacement of the system will be driven to zero, so global asymptotic stability will be guaranteed for the overall control law.

When this feedback control is implemented with the near *minimum* time control approach of the preceding section, the outputs over the course of a maneuver corresponding to nonlinear flexible response can be computed in advance for each control profile. When this is done, a negligible amount of real-time computation will be required.

5.5 Numerical Example

In principle, if the pulse response measurements are obtained without measurement noise, the nonlinear behavior of the system is accurately represented, the open loop control profile is realized accurately, and there are no disturbances to the system during the course of the maneuver, then the feedback component described in the preceding section will be zero because the response

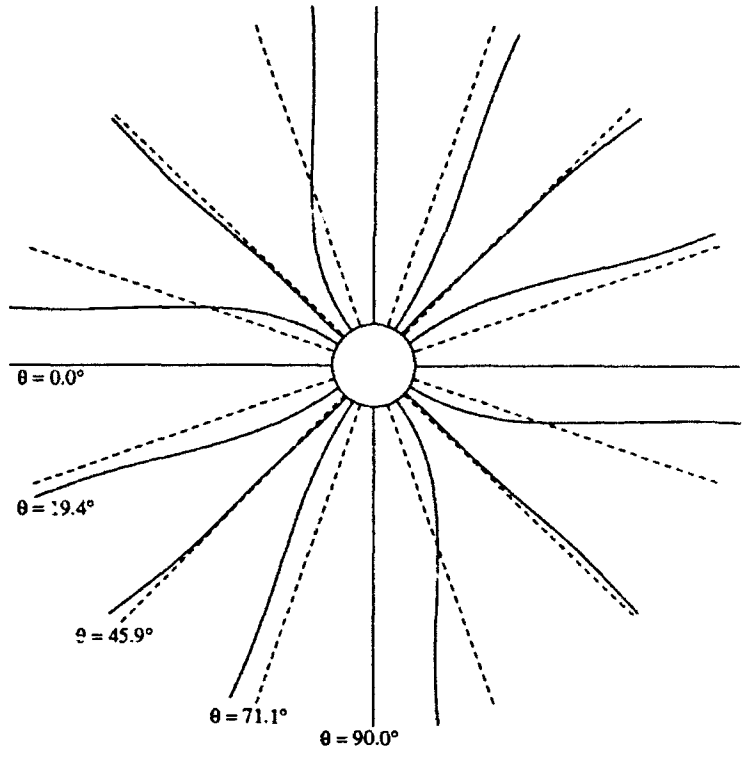

Figure 5.4: Controlled system response during maneuver

will agree exactly with the open loop prediction. Therefore a numerical example demonstrating the effectiveness of the feedback control could examine its performance in the presence of noise and disturbances of various types artificially introduced into the simulation. As an alternative to this, the numerical example presented here will address the important practical problem of how well the closed loop PRBC approach can execute an extremely rapid large angle maneuver with no knowledge of the system except the pulse response measurements and the overall undeformed

Table 5.1: System properties

System moment of inertia	2128 oz-s^2-in
Hub radius	5.547 in
Appendage length	45.523 in
Tip mass	0.15627 oz-s^2/in
Appendage Young's modulus	1.616e+8 oz-s^2/in
App. section mom. of inertia	0.000813 in^4
Appendage mass/length	0.003007 oz-s^2/in^2
Hub inertia	9.06 oz-s^2-in
Period of first flexible mode	1.3353 sec
Force bound	146.83 oz
Torque bound	1.4997e+4 oz-in

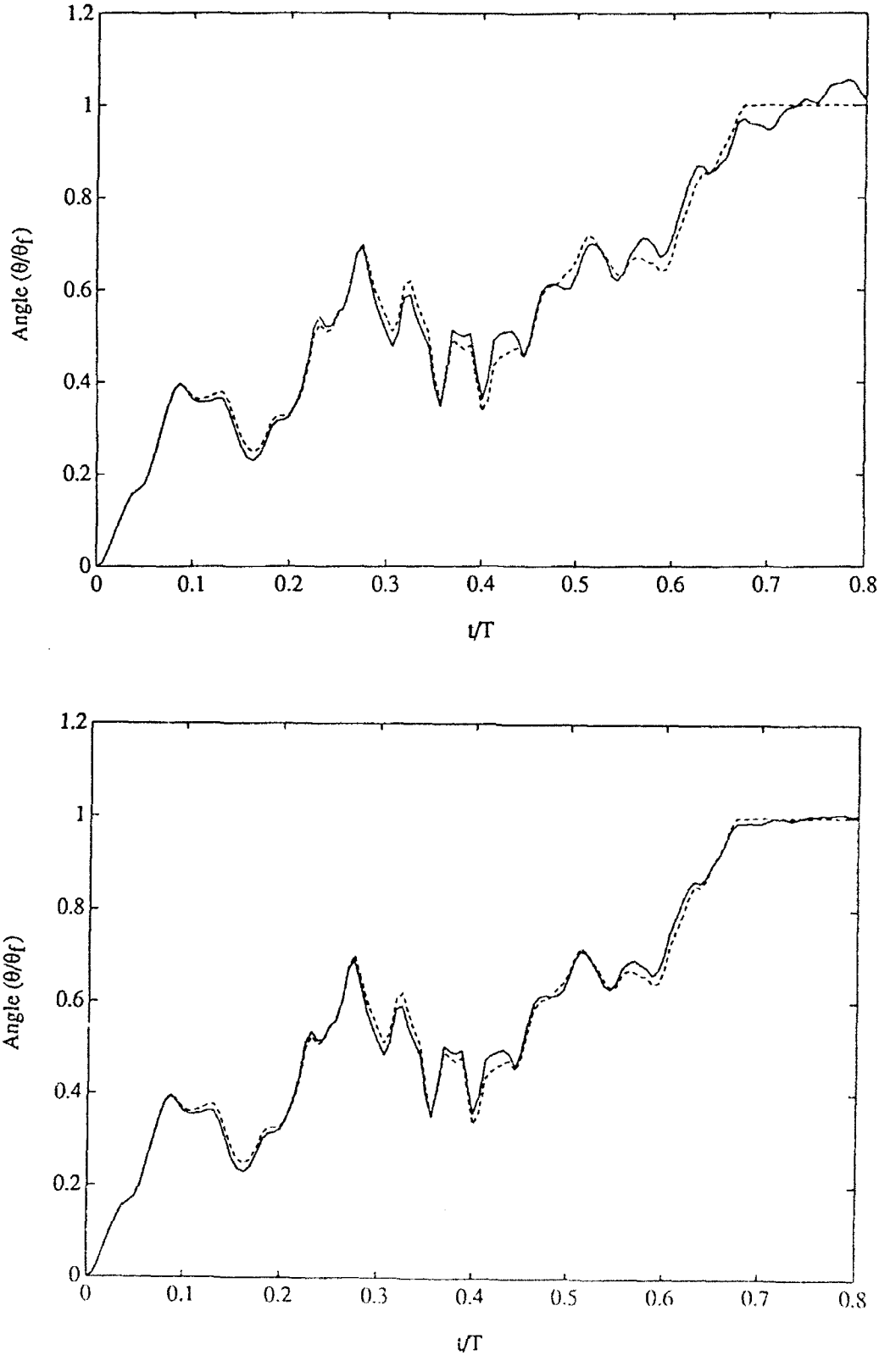

Figure 5.5: Hub angular displacement—linear open loop (dashed), nonlinear open loop (solid, upper), nonlinear closed loop (solid, lower)

mass moment of inertia about the rotation axis. This constraint on the explicit knowledge of the system precludes consideration of nonlinear effects in solving for the minimum time open loop profile because the lower modes of vibration are assumed to be unknown. The solution of the minimum time problem is therefore somewhat less costly. For simplicity, the open loop profiles will be minimum time rather than near minimum time profiles in this example.

For this example, the properties of the system are given in Table 5.1, and the bounds on the control inputs are chosen as described for the second case in the fourth section of this chapter. The force and torque bounds are chosen so that the moments that can be exerted by each type of control input are equal, and so that a ninety degree rotation could be accomplished on an inertially identical rigid system in one half of the period of the first flexible mode of the flexible system. A rest-to-rest rotation through ninety degrees is to be accomplished.

The gains for the feedback control are as follows. For this example, feedback at the tip masses over the course of the maneuver is found to contribute very little. Therefore, the only feedback before the end of the open loop control profiles is on the hub angular velocity, with a gain of 446.2 oz.-in.-sec./rad. After the end of the open loop profiles, the gains are equal to 429.6 oz.-in./rad. on the hub angular displacement, 573.7 oz.-in.-sec./rad. on the hub angular velocity, and 3.576 oz.-sec./in. on the tip velocity.

Figure 5.4 shows the response of the system to the closed loop control, at the beginning and end of the maneuver and at three intermediate times. It is evident from this figure that the first and third appendages, which have control forces applied at their ends, deflect less than the second and fourth appendages, which have no control forces and deflect considerably.

Figure 5.5 shows the total angular displacement of the hub over the course of the maneuver. The dashed line in each plot is the open loop response, which does not consider nonlinear effects. The solid line in the upper plot is the response of the nonlinear system without the feedback component of the control, and it is evident that nonlinear effects are responsible for significant error in the final state of the system. The solid line in the lower plot is the closed loop response, for which the error at the final time and afterward is significantly reduced.

Figure 5.6 shows the total angular velocity of the hub over the maneuver history, presented in the same manner as Figure 5.5. Again, it is clear that the feedback control is quite effective in keeping the difference from the linearized reference trajectory predicted by the pulse response

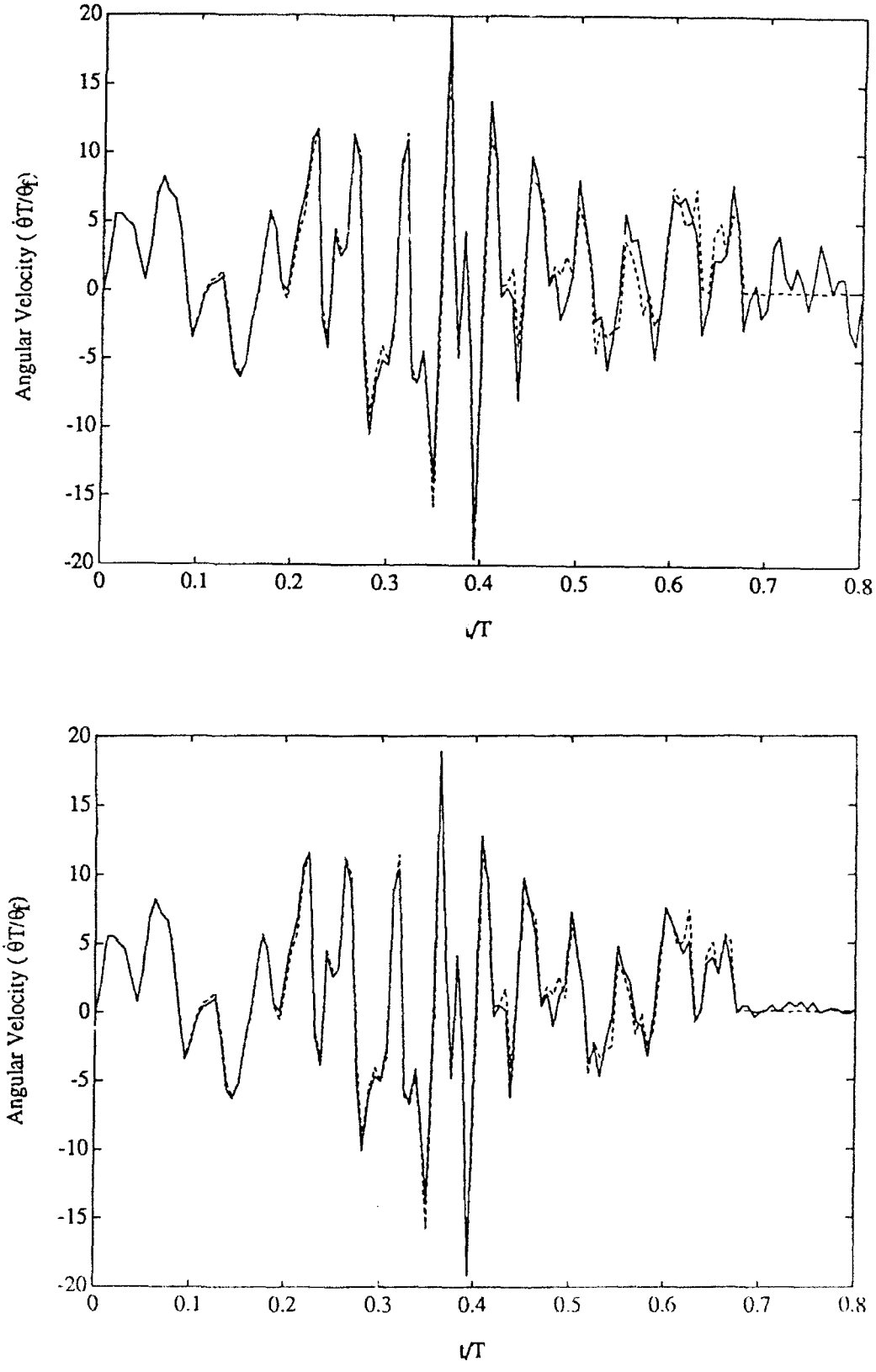

Figure 5.6: Hub angular velocity—linear open loop (dashed), nonlinear open loop (solid, upper), nonlinear closed loop (solid, lower)

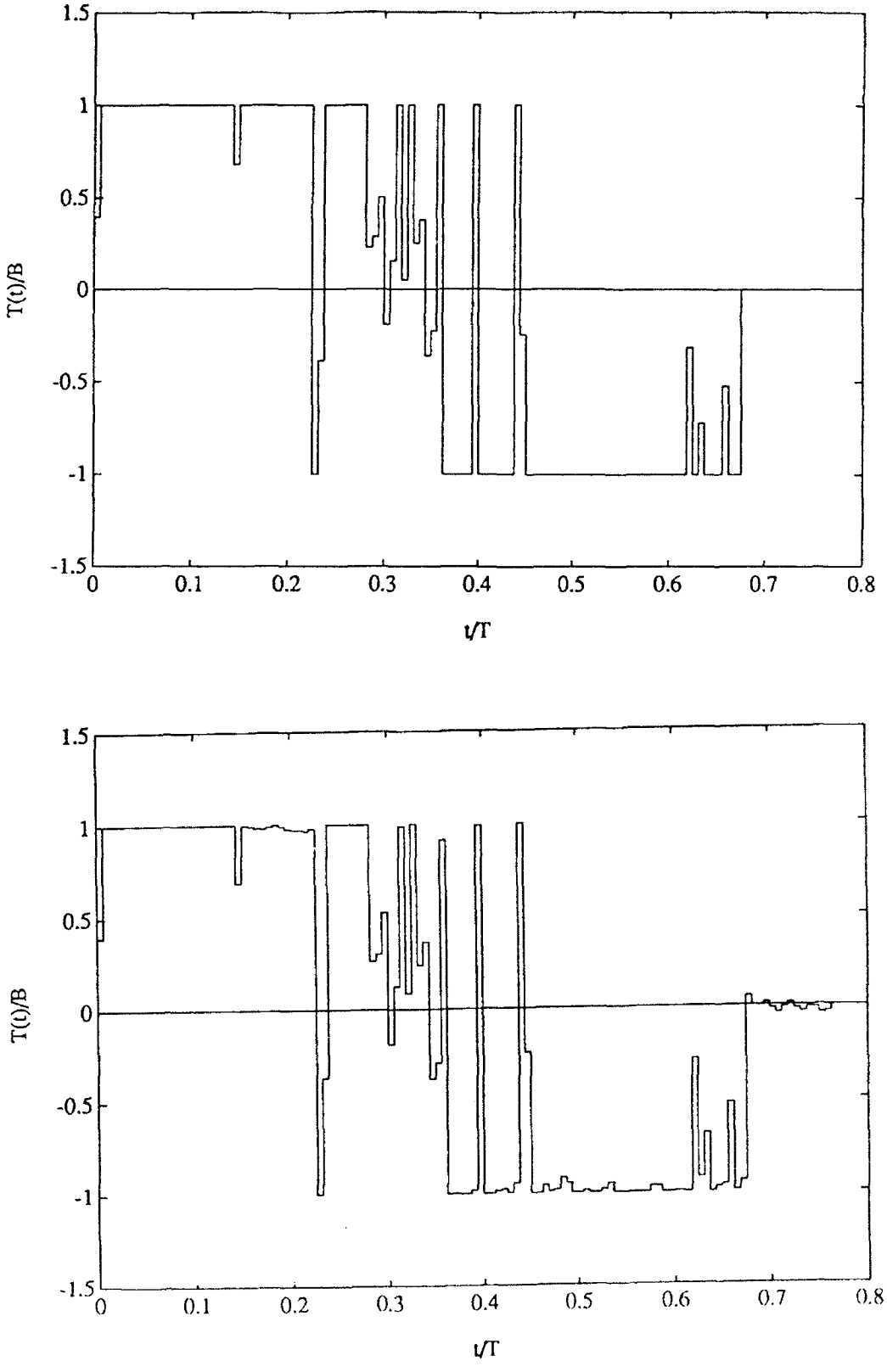

Figure 5.7: Torque profile– open loop (upper), closed loop (lower)

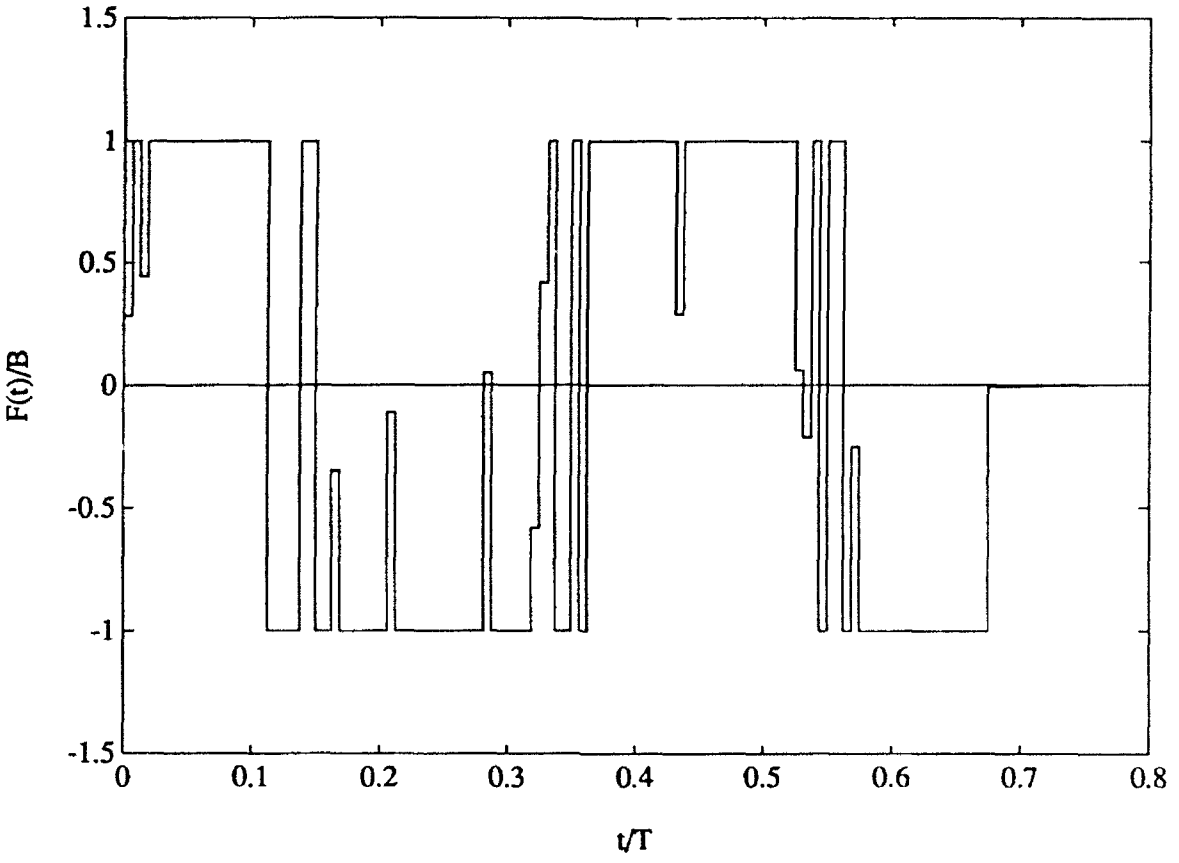

Figure 5.8: Force profile—closed loop

measurements small, and in driving the error in the state quickly to zero at the end of the maneuver.

Figure 5.7 shows the open loop and closed loop profiles for the torque input. The feedback component of the control is evident in the small departures from the bounds over much of the control history. Figure 5.8 shows the closed loop force input profile, which is identical to the open loop profile until the open loop control ends, at which point feedback in the force actuators is switched on. It is clear from the force profile that the minimum time profiles differ significantly from the bang-bang minimum time profile for a rigid system.

Figure 5.9 shows the open loop angular velocity of the Tisserand reference frame. It is evident from this figure that the product $\dot{\theta}_0\ddot{\theta}_0$ is nonpositive over approximately the last third of the open loop control history. This indicates that the time derivative of the function $\tilde{U}$ will be guaranteed to be nonpositive over a large portion of the control history even for rapid maneuver problems in which the control profiles are quite different from bang-bang rigid body maneuver profiles.

From this example, it is clear that the closed loop PRBC approach produces a very satisfactory

approximation of minimum time maneuver for a flexible spacecraft, even when knowledge of the system is minimal and nonlinear effects are significant, but are completely ignored in obtaining open loop control profiles When combined with the near minimum time method presented earlier in this chapter, this approach makes it possible to execute a very good approximation of minimum time maneuver virtually immediately.

5.6 Conclusions

This chapter presents a method for obtaining near minimum time PRBC profiles for maneuver of flexible spacecraft with virtually no real time computation. Also, a stable feedback control scheme for use with an open loop PRBC profile is presented which exploits the ease with which reference outputs corresponding to nonlinear flexible response to control profiles are available in PRBC. This scheme is stable in the presence of rotational stiffening effects, and even when saturation prevents realization of the feedback component of the control over much of the control history. A numerical

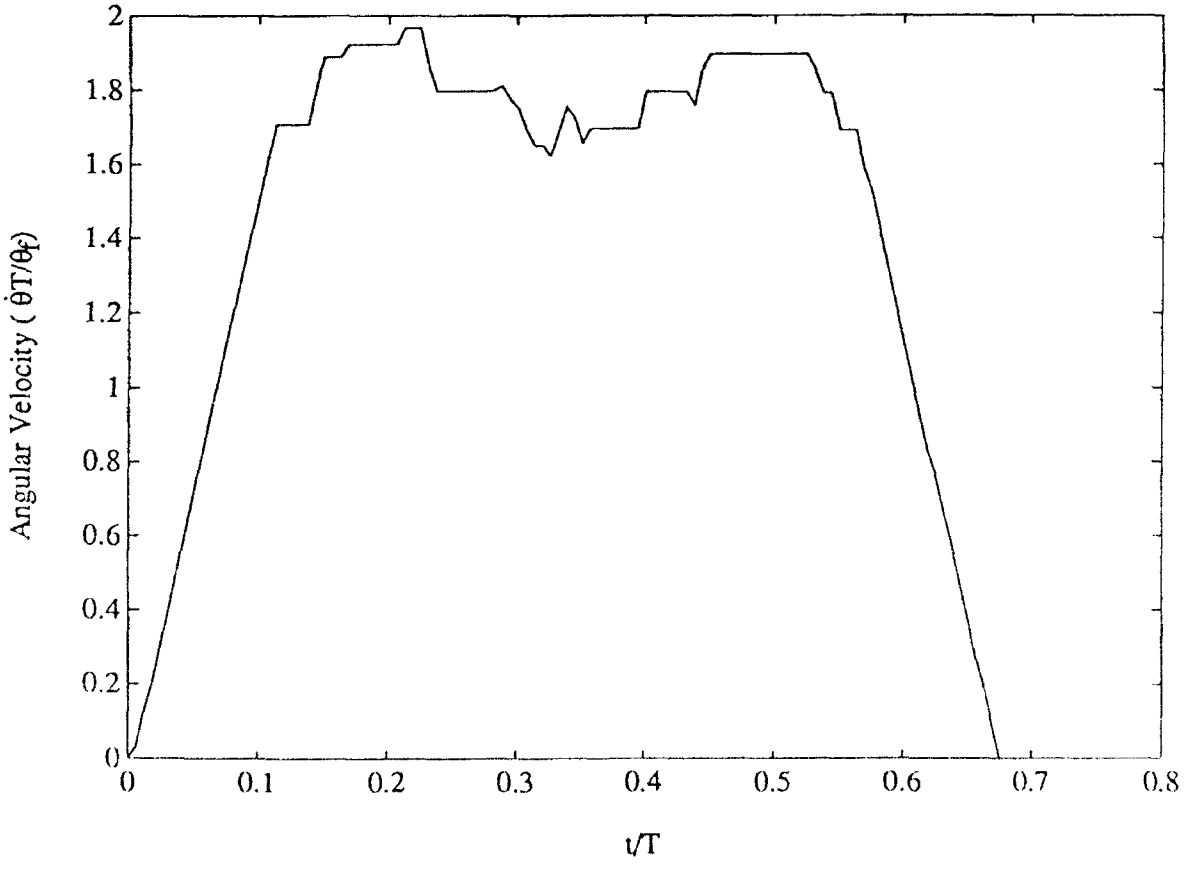

Figure 5.9: Open loop reference frame angular velocity profile

example demonstrates that the closed loop PRBC method presented in this chapter performs extremely well for a very rapid large angle maneuver, even when only the inertial properties of a spacecraft are known explicitly and nonlinear behavior is neglected completely in obtaining open loop minimum time control profiles.

Chapter 6

Summary and Conclusions

As discussed in the first chapter, before the work summarized in this report was begun, methods for obtaining control profiles for rapid maneuver of flexible spacecraft have either required an explicit modal or state space model of flexible behavior, or they have used an open loop control profile which does not take flexible behavior into account at all, and have relied on a Lyapunov-stable feedback component of the control which uses no explicit knowledge of flexible behavior to suppress the resulting vibration. The issue of how close the maneuver times obtained with these methods have been to the minimum maneuver time *possible with a given set of control inputs* had never been addressed with any real precision, because there was no practical way of obtaining minimum time solutions. In fact, the issue of how the well-known "Bang-Bang Principle" applies to minimum time maneuver of flexible structures was not well understood, since no exact solution of a minimum time control problem for a flexible system controlled by discrete bounded inputs had been obtained.

In this work, the first exact solution for a problem of this type was obtained, and this contributed considerable insight into the nature of the problem. The pulse response based control method was developed, initially for linear systems, and this method makes it possible to obtain excellent approximations of minimum time control profiles, knowing only the data from direct measurements of response to control input pulses and the gross inertial properties of the system. An additional attractive feature of the approach is that linear actuator dynamics can be very naturally and automatically taken into account. A special algorithm for solving the numerical optimization problem arising in this method was developed, which makes it possible to solve these minimum time control problems without a great deal of computation. Although the method and the algorithm have been intended for situations in which a good model of the system is unavailable, they can

be used easily to solve problems in which the controlled system is known and modeled well, as demonstrated in the various numerical examples presented here. This can be useful in the analysis of flexible spacecraft subject to rapid maneuver to determine strength requirements, for example. A preliminary investigation of the effects of measurement noise on accuracy of the final state was conducted. Also, numerical examples involving linear systems demonstrated that the pulse response based control method can easily obtain a minimum time exact solution which can be represented exactly in terms of the type of pulses used, and that it can obtain an excellent approximation in the more typical case in which the exact solution cannot be represented in terms of the pulses used.

The method was extended to nonlinear maneuver problems by explicitly modeling the deviation from linearity in those modes in which it is significant. It was found that the number of modes with significant nonlinear behavior is typically very small, so that identification requirements are low when this approach is taken. Also, modifications to the algorithm to accomodate nonlinear problems are straightforward, and the amount of computation required to solve a nonlinear maneuver problem is not much greater than the amount required for the corresponding linearized problem.

Another approach for addressing nonlinear behavior is to ignore it in obtaining an open loop component of the control profile, and use feedback control to drive the deviation from linear response to zero over the course of the maneuver. The pulse response based control method lends itself very naturally to implementation of feedback control because the outputs that are expected over the course of a maneuver are readily available through convolution, so that feedback can respond to the deviation from these expected outputs. A feedback control strategy that is stable even in the presence of nonlinear rotational stiffening effects and the control input bounds that are in effect for the open loop component was developed. The numerical example of the fifth chapter demonstrates that even for an extremely rapid maneuver, ignoring nonlinear behavior while obtaining the open loop component and using feedback control gives very satisfactory results. Of course, feedback control is attractive for dealing with deviations from the expected response arising from disturbances, error in the pulse response data due to measurement noise, and other sources. Because virtually all linear flexible behavior, and as much nonlinear behavior as knowledge of the system will allow, can be taken into account in the open loop control component, the feedback control component can be expected to be much smaller for pulse response based control than for methods in which the open loop component is simply bang-bang or smoothed bang-bang.

Another important extension for the method makes it possible to obtain near minimum time control profiles with virtually no real time computation. First and second halves of control profiles are computed in advance, and then the length of a coast interval is computed once a total desired slew angle is known, so that a near minimum time control profile can be assembled virtually immediately. Even for extremely rapid maneuver, it was found that the maneuver times obtained in this manner approximate minimum maneuver times very well.

The pulse response based control method has been demonstrated to be effective in the solution of extremely rapid maneuver problems. Previous methods either explicitly or tacitly assume that the control profiles will be small perturbations of bang-bang or smoothed bang-bang profiles, and as the examples presented here have shown, as maneuver gets more rapid this assumption is less and less valid. It is unlikely that the approximate minimum time solutions obtained in this report using pulse response based control could have been obtained using any other existing method with the same assurance of accuracy. In these examples, this assurance came from the fact that time step sizes were quite small and a control profile with fewer time steps resulting in the desired final state was shown not to exist. Accuracy of the final state was evident in the extremely low residual energy at the end of each maneuver. Even if this capability for extremely rapid maneuver is not needed in the near future, the pulse response based control approach offers new capabilities for solving minimum time maneuver problems with minimal explicit knowledge of the system being controlled, and with assurance that the profiles obtained approximate the exact minimum time profiles very accurately.

References

1. Turner, J. D. and Junkins, J. L., "Optimal Large-Angle Single-Axis Rotational Maneuvers of Flexible Spacecraft," *Journal of Guidance and Control*, Vol. 3, No. 6, 1980, pp. 578-585.

2. Turner, J. D. and Chun, H. M., "Optimal Distributed Control of a Flexible Spacecraft During a Large-Angle Maneuver," *Journal of Guidance, Control and Dynamics*, Vol. 7, No. 3, 1984, pp. 257-264.

3. Meirovitch, L. and Quinn, R. D., "Maneuvering and Vibration Control of Flexible Spacecraft," *Journal of the Astronautical Sciences*, Vol. 35, No. 3, 1987, pp. 301-328.

4. Chun, H. M., Turner, J. D. and Juang, J.-N., "Frequency-Shaped Large-Angle Maneuvers," AIAA 25th Aerospace Sciences Meeting, Reno, Nevada, Paper No. AIAA-87-0714, 1987.

5. Chun, H. M., Turner, J. D. and Juang, J.-N., "A Frequency-Shaped Programmed-Motion Approach for Flexible Spacecraft Maneuvers," AIAA Dynamics Specialists Conference, Monterey, California, Paper No. AIAA-87-0926-CP, 1987.

6. Meirovitch, L. and Sharony, Y., "Optimal Vibration Control of a Flexible Spacecraft During a Minimum-Time Maneuver," *Proceedings of the Sixth VPI&SU/AIAA Symposium on Dynamics and Control of Large Structures*, Blacksburg, Virginia, 1987, pp. 579-601.

7. Ben-Asher, J., Burns, J. A. and Cliff, E. M., "Time Optimal Slewing of Flexible Spacecraft," *Proceedings of the 26th Conference on Decision and Control*, Los Angeles, California, 1987, pp. 524-528.

8. Junkins, J. L., Rahman, Z. H. and Bang, H. "Near-Minimum Time Control of Distributed Parameter Systems: Analytical and Experimental Results," *J. of Guidance, Control and Dynamics*, Vol. 14, No. 2, 1991, pp. 406-415.

9. Bennighof, J. K. and Boucher, R. L., "Exact Minimum-Time Control of a Distributed System Using a Traveling Wave Formulation," *J. of Optimization Theory and Applications*, Vol. 73, No. 1, 1992, pp. 149-167.

10. Bennighof, J. K., Chang, S.-H., and Subramaniam, M., "Minimum Time Pulse Response Based Control of Flexible Structures," 32nd AIAA/ASME/ASCE/AHS/ASC Structures, Structural Dynamics and Materials Conference, Baltimore, April 1991, pp. 2900-2910. To appear, *J. of Guidance, Control and Dynamics.*

11. Bennighof, J. K. and Subramaniam, M., "Minimum Time Maneuver of Structures Using Pulse Response Based Control," AIAA Dynamics Specialists Conference, Dallas, April 1992, pp. 326-333. In review, *J. of Guidance, Control and Dynamics.*

12. Bennighof, J. K. and Chang, S.-H., "Closed Loop Near Minimum Time Pulse Response Based Control of Flexible Spacecraft," AIAA Guidance, Navigation and Control Conference, Hilton Head Island, August 1992, pp. 705-716.

13. LaSalle, J. P., "The Time Optimal Control Problem," *Contributions to the Theory of Nonlinear Oscillations*, Edited by L. Cesari, J. P. LaSalle, and S. Lefschetz, Princeton University Press, Princeton, New Jersey, Vol. 5, 1960, pp. 1-24.

14. Egorov, I. V., "Optimal Control in Banach Space," *Doklady Akademii nauk SSSR*, Vol. 150, 1963, pp. 241-244, (in Russian).

15. Fattorini, H. O., "Time-Optimal Control of Solutions of Operational Differential Equations," *SIAM Journal of Control*, Vol. 2, No. 1, 1964, pp. 54-59.

16. Friedman, A., "Optimal Control in Banach Spaces," *Journal of Mathematical Analysis and Applications*, Vol. 19, No. 1, 1967, pp. 35-55.

17. Balakrishnan, A. V., "Optimal Control Problems in Banach Spaces," *SIAM Journal of Control*, Vol. 3, No. 1, 1965, pp. 152-180.

18. Thompson, R. C., Junkins, J. L., and Vadali, S. R., "Near-Minimum Time Open-Loop Slewing of Flexible Vehicles," *Journal of Guidance, Control and Dynamics*, Vol. 12, No. 1, 1989, pp. 82-88.

19. Baruh, H., and Silverberg, L. M., "Maneuver of Distributed Spacecraft," AIAA Guidance and Control Conference, Seattle, Washington, 1984.

20. Lions, J. L., "Exact Controllability, Stabilization and Perturbations for Distributed Systems," *SIAM Review*, Vol. 30, No. 1, 1988, pp. 1-68.

21. von Flotow, A. H., "Traveling Wave Control for Large Spacecraft Structures," *Journal of Guidance, Control, and Dynamics*, Vol. 9, No. 4, 1986, pp. 462-468.

22. Meirovitch, L., *Analytical Methods in Vibrations*, Macmillan, New York, New York, 1967.

23. Bennighof, J. K., and Boucher, R. L., "An Investigation of the Time Required for Control of Structures," *Journal of Guidance, Control and Dynamics*, Vol. 12, No. 6, 1989, pp. 851-857.

24. Singh, G., Kabamba, P. T., and McClamroch, N. H., " Planar, Time-Optimal, Rest-to-Rest Slewing Maneuvers of Flexible Spacecraft," *Journal of Guidance, Control, and Dynamics*, Vol. 12, No. 1, 1989, pp. 71-81.

25. Juang, J.-N. and Pappa, R. S., "An Eigensystem Realization Algorithm for Modal Parameter Identification and Model Reduction," *Journal of Guidance, Control and Dynamics*, Vol. 8, No. 5, 1985, pp. 620-627.

26. Best, M. J. and Ritter, K., *Linear Programming: Active Set Analysis and Computer Programs*, Prentice-Hall, Englewood Cliffs, New Jersey, 1985.

27. Canavin, J. R. and Likins, P. W., "Floating Reference Frames for Flexible Spacecraft," *Journal of Spacecraft*, Vol. 14, No. 12, 1977, pp. 724-732.

28. Kinariwala, B. K., "Analysis of Time Varying Networks," *IRE Inter. Conv. Record*, Pt. 4, 1961, pp. 268-276.

29. Sharony, Y. and Meirovitch, L., "Accomodation of Kinematic Disturbances During Minimum-Time Maneuvers of Flexible Spacecraft," *J. of Guidance, Control and Dynamics*, Vol. 14, No. 2, 1991, pp. 268-277.